A REVIEW ON SUPERCAPACITOR & ITS APPLICATION

by

MD. MAHBUBUR RAHMAN (122426)
MD. ABDULLAH AL JOHA (122430)
SHADMAN AHSAN (122431)

A Thesis Submitted to the Academic Faculty in Partial Fulfillment of the Requirements for the Degree of

BACHELOR OF SCIENCE IN ELECTRICAL AND ELECTRONIC ENGINEERING

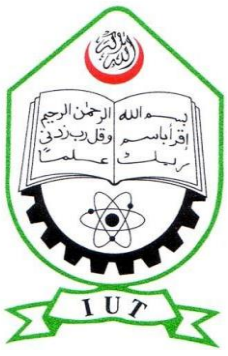

Department of Electrical and Electronic Engineering
Islamic University of Technology (IUT)
Gazipur, Bangladesh

November 2016

DECLARATION OF CANDIDATE

It is hereby declared that the work reported in the B.Sc. thesis entitled "**A REVIEW ON SUPERCAPACITOR & ITS APPLICATION**" submitted at **Islamic University of Technology (IUT),** Board Bazar, Gazipur, Bangladesh, is an authentic record of our work carried out under the supervision of **Associate Professor Dr. Syed Iftekhar Ali**. We have not submitted this work elsewhere for any other degree or diploma.

Submitted By

……	……	……
Md. Mahbubur Rahman	**Md. Abdullah Al Joha**	**Shadman Ahsan**
Student No:122426	Student No:122430	Student No:122431
Academic Year: 2015-2016	Academic Year: 2015-2016	Academic Year: 2015-2016

Approved by

……..
Dr. Md. Ashraful Hoque
Professor and Departmental Head
Department of Electrical and Electronic Engineering,
Islamic University of Technology (IUT),
Boardbazar, Gazipur-1704
Date:

Supervised By

……..
Dr. Syed Iftekhar Ali
Associate Professor
Department of Electrical and Electronic Engineering,
Islamic University of Technology (IUT),

Table of Contents

List of Tables

List of Figures

List of Acronyms

CNT	Carbon Nano Tube
SC	Supercapacitor
EDLC	Electric Double Layer Capacitor
SWCNT	Single Walled Carbon Nano Tube
DWCNT	Double Walled Carbon Nano Tube
MWCNT	Multi Walled Carbon Nano Tube
LSG	Laser Scribed Graphene
PVA	Polyvinyl Alcohol
SMPS	Switch-Mode Power Supply
SEM	Scanning Electron Microscopy
PG	Porous Graphene
CVD	Chemical Vapor Deposition
GA	Graphene Aerogels
GF	Grapheme Fiber
PVDF	Poly Vinyli Dine Fluoride

Acknowledgements

We would like to convey our deepest gratitude to our thesis supervisor, Dr. Syed Iftekhar Ali, who is the backbone of this whole thesis work. He is a figure of motivation that lead us to complete our work with satisfactory result. A true mentor and friend, whose guidance made us seek knowledge and finally managed to achieve the desired outcome.

Abstract

Capacitors are commonly used in electronic resonance circuits; however, capacitors have not been used for storing large amounts of electrical energy in electrical circuits. Also they are not known to be long lasting. Thus appears the need of supercapacitor with variety of electrodes, offering high power density, fast charging & elongated life-cycle. Highly conducting and porous carbon nanotube (CNT) networks are popular as the sole electron conducting material in supercapacitors. The high conductivity of CNT networks and the high surface area allow the replacement of both the metallic current collector and the active material that forms one side of the electrochemical double layer. The combination of both functions in one single layer leads to lightweight charge storage devices that can be manufactured using simple and cheap room temperature methods. In case of solid-state supercapacitor, device fabrication is done by a simple vacuum thermal evaporation method, which allows not only a multilayer stacking structure to further enhance the capacitance, but also permits the supercapacitor to be easily incorporated with other electronic devices, showing interesting characteristics for both fundamental study and practical applications. supercapacitors are being used to increase the efficiency of hybrid electric vehicles in several ways. Aging of a capacitor is a topic to be concerned about. The voltage difference in cells and temperature tend to shorten the life span. Methods are being developed to tackle this problem. Until recently, supercapacitors were relegated to fairly mundane applications such as memory protection and internal battery backup, but in the last few years the application space has broadened significantly into hybrid vehicles, smartphones, and energy harvesting. New technologies on the horizon promise to bring supercapacitors into full competition with rechargeable batteries.

Chapter 1

Introduction

1.1 OBJECTIVE

The function of a normal capacitor and super-capacitor are the same. The difference is in the structure of the electrode and dielectric.

In ordinary capacitors, electrons are moved from one electrode and deposited on the other, and charge is separated by a solid dielectric between the electrodes.

In supercapacitors, also known as Electric double-layer capacitors, instead of a solid dielectric, the two electrodes are separated by a liquid electrolyte rich in ions. When a voltage is applied to a supercapacitor, these solvated ions form a double-layer of ions at each electrode (separated by the non-conductive solvent) in what's known as the electrical double layer effect. The layer of solvent between the double-layers acts as an extremely thin dielectric (typically only molecules thick), and thanks to the porous structure of the electrodes, these double-layers have an extremely high surface area.

This quality ensures, a capacitor with a huge capacitance (due to the high surface area), but also a very low breakdown voltage rating (due to the thinness of the double layer). Supercapacitors can be found having capacitances in the hundreds to thousands of Farads, but with voltage ratings of only a few volts. In high-voltage applications, supercapacitors have to be stacked in series to obtain the desired voltage ratings.

Another trait, probably the most important one, is that the supercapacitor has a long life span. So in the mega-structures, supercapacitors are gradually being introduced. For the betterment of an electrical system, the time has come to take the study on supercapacitor even further.

1.2 OVERVIEW

The book contains the basic idea of a supercapacitor, followed by its classification according to different electodes and its field of applicaton. Emphasis is given on carbon nano-tube as electrode material for its high surface area and increased porosity. Formation of electrodes are shown along with their synthesis method. Detailed discussion is present on aging mechanism of supercapacitor which involves many circuit implementations. The end portion contains various type of application of supercapacitor from small scale to large ones.

Chapter 2

SUPERCAPACITOR & ITS CLASSIFICATION

2.1 SUPERCAPACITOR

Supercapacitor is also known as ultracapacitor, pseudocapacitor or electric double-layer capacitor (EDLC). It is a high-capacity electrochemical capacitor with capacitance values much higher than other capacitors. It is the combination of electrolytic capacitors and rechargeable batteries. It has higher life span than normal capacitor.

2.2 ADVANTAGES OF SUPERCAPACITOR

Supercapacitor has virtually unlimited cycle life. It has high specific power. It can be charged in seconds. So simple charging. Low temperature charging performance is shown by it. It enhances battery's performance & extends the longevity of the battery. Overcharge does not create any problem to supercapacitor. Here no end of charge termination is required. Thus it is overall safe.

2.3 CLASSIFICATION OF SUPERCAPACITOR

Supercapacitors are mainly classified into three types. They are-

1. Double layer capacitor
2. Pseudocapacitors
3. Hybrid capacitors

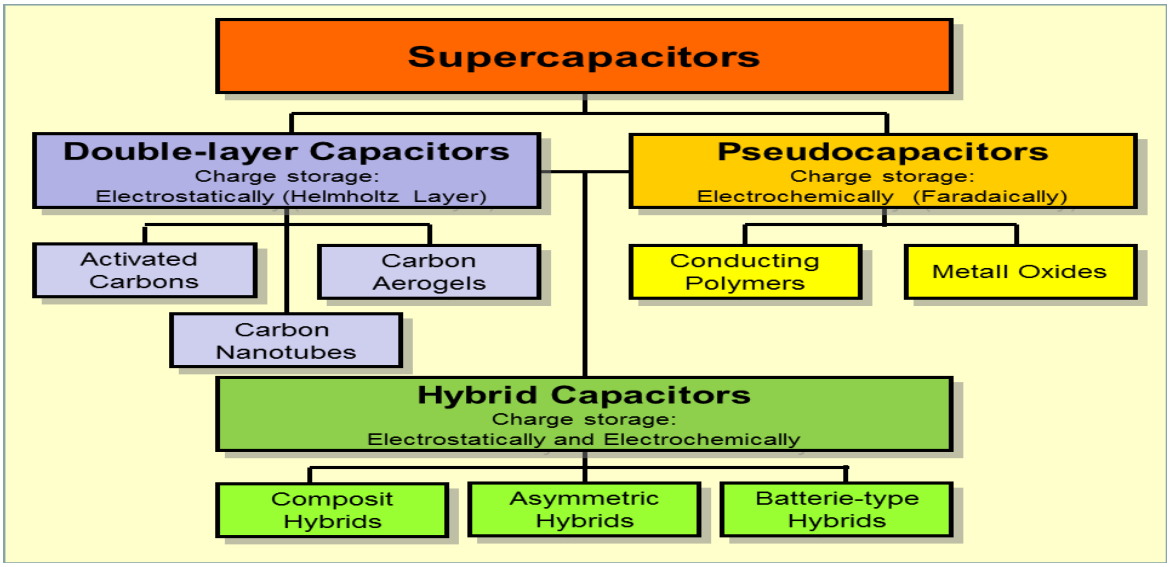

Figure 2.1: Classification of supercapacitor

2.3.1 ELECTRIC DOUBLE LAYER CAPACITOR

Compared to the commonly used rechargeable batteries, Electric Double Layer Capacitor (EDLC), which is capable to be charged discharged with high current, is an energy storage device which has excellent charge-discharge cycle life. In the recent years, with energy issues (reduction of oil consumption, consumer electric power, CO_2 emission, and effective use of new energy) being focused, using EDLC on more and more new applications is considered. Installation of EDLC in hybrid or fuel-cell vehicle is also considered.

Basic Mechanism of ELDC

Conventional capacitors have a dielectric sandwiched between two electrodes. When voltage is applied, dipoles are oriented, and thus electric charge is stored. Electric double layer capacitors have electric charges oriented at the boundary of electrolyte and electrodes which is called the "electric double layer."

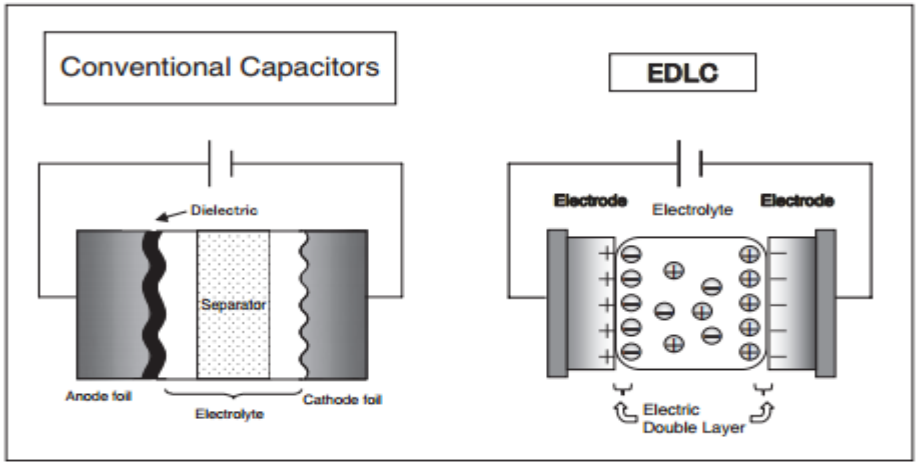

Figure 2.2: Mechanism of ELDC

Characteristics

Unlike rechargeable batteries, EDLC does not use chemical reactions and it stores energy solely by physical movement of ion to the surface of activated carbon. That gives EDLC features as following;

・With low degradation, it withstands multimillion charge-discharge cycles.

・With the high power density, rapid (high current) charge-discharge is possible.

・With a high charge-discharge efficiency, the output efficiency of over 95% with a power density 1kW/kg is achieved.

・Environment-friendly without containing heavy metals.

・High in safety at irregular occasions, and will be not destroyed even by short circuiting.

Structure

The basic structure of a cylindrical type EDLC is shown in (Figure 2.3-b) and cylindrical type ELDC is shown in (Figure 2.3-a). Basic structure is, aluminum foils with electrode pasted on the surface wound into a roll. Using activated carbon for the electrode utilizing its very large surface area, and with the original high-density electrode manufacturing technology, both high capacitance and low resistance is achieved.

Figure 2.3(a): cylindrical type EDLC

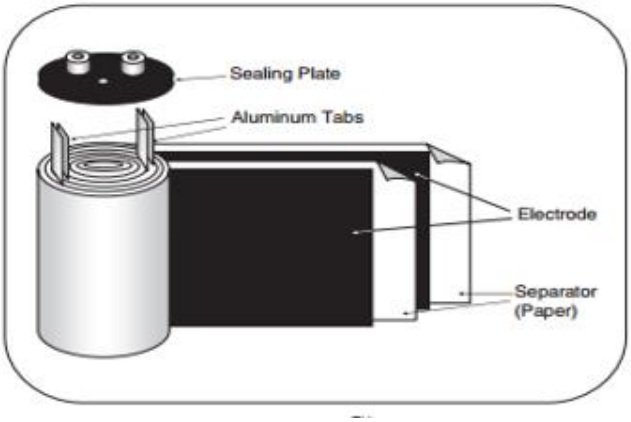

Figure 2.3 (b): basic structure

ELECTRODE TYPE OF ELDC

Based on which type of electrode is used ELDC is classified into 3 types. They are-

1. Activated Carbon
2. Carbon Aerogel
3. Carbon Nanotube

Activated Carbon

Activated carbon, also called activated charcoal, is a form of carbon processed to have small, low-volume pores that increase the surface area available for adsorption or chemical reactions. Activated is sometimes substituted with active. Due to its high degree of micro porosity, just one gram of activated carbon has a surface area in excess of 3,000 m^2 (32,000 sq ft),[1]as determined by gas adsorption. An activation level sufficient for useful application may be attained solely from high surface area; however, further chemical treatment often enhances adsorption properties. Activated carbon is usually derived from charcoal and is sometimes utilized as biochar. Those derived from coal and coke are referred as activated coal and activated coke respectively.

Figure 2.4: Activated Charcoal

Carbon Aerogel

Aerogel is a synthetic porous ultralight material derived from a gel, in which the liquid component of the gel has been replaced with a gas.[2] The result is a solid with extremely low density and low thermal conductivity. Nicknames include frozen smoke,[3] solid smoke, solid air, or blue smoke owing to its translucent nature and the way light scatters in the material. It feels like fragile expanded polystyrene to the touch. Aerogels can be made from a variety of chemical compounds.[4]

Aerogel was first created by Samuel Stephens Kistler in 1931, as a result of a bet with Charles Learned over who could replace the liquid in "jellies" with gas without causing shrinkage.[5] [6]
Aerogels are produced by extracting the liquid component of a gel through supercritical drying. This allows the liquid to be slowly dried off without causing the solid matrix in the gel to collapse from capillary action, as would happen with conventional evaporation. The first aerogels were produced from silica gels. Kistler's later work involved aerogels based on alumina, chromium and tin dioxide. Carbon aerogels were first developed in the late 1980s.
Aerogel does not have a designated material with set chemical formula but the term is used to group all the material with a certain geometric structure.[7]

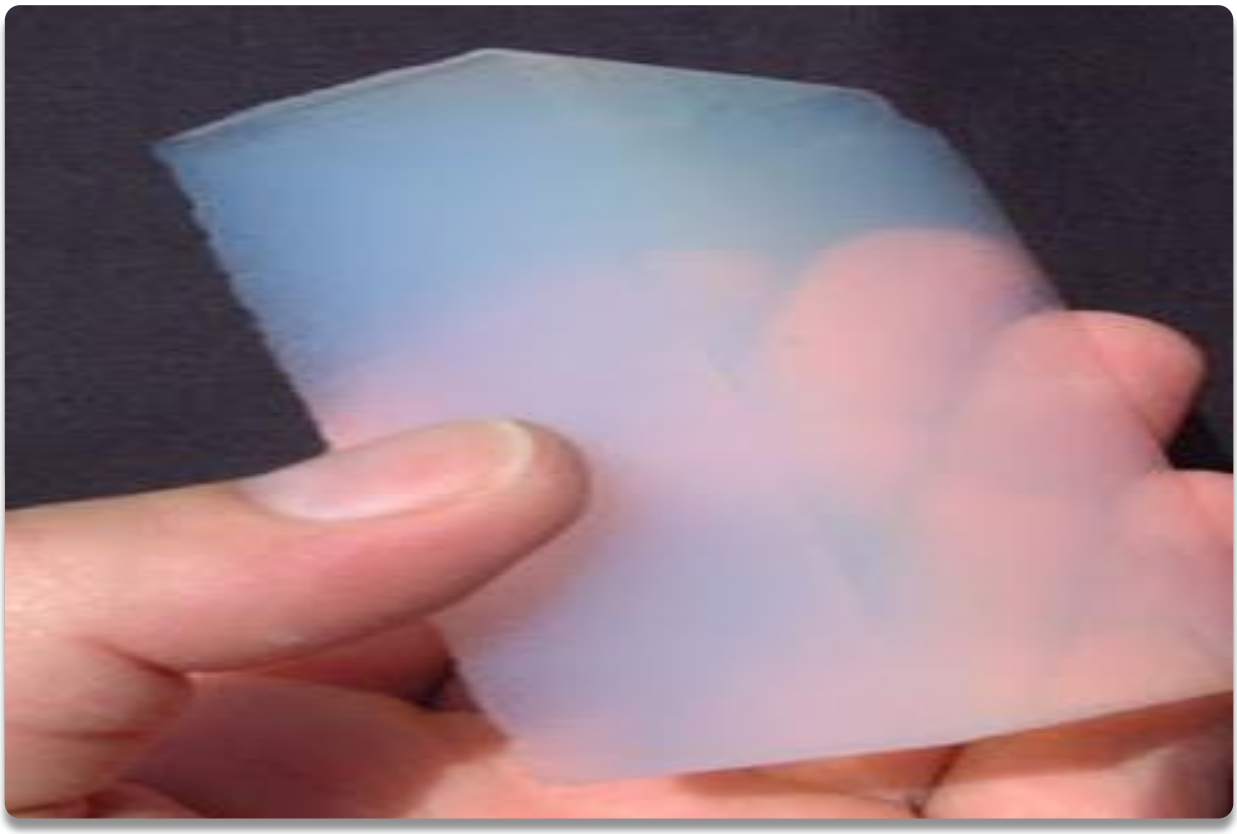

Figure 2.5: Carbon Aerogel

Figure 2.6: Supercapacitor using carbon aerogel

Carbon Nanotube

It is a miniature cylindrical carbon structure that has hexagonal graphite molecules attached at the edges. It is 1/50,000th the width of a human hair. It is strongest and stiffest material (>300 X Steal).It has low density, lightweight and made with semiconductor.

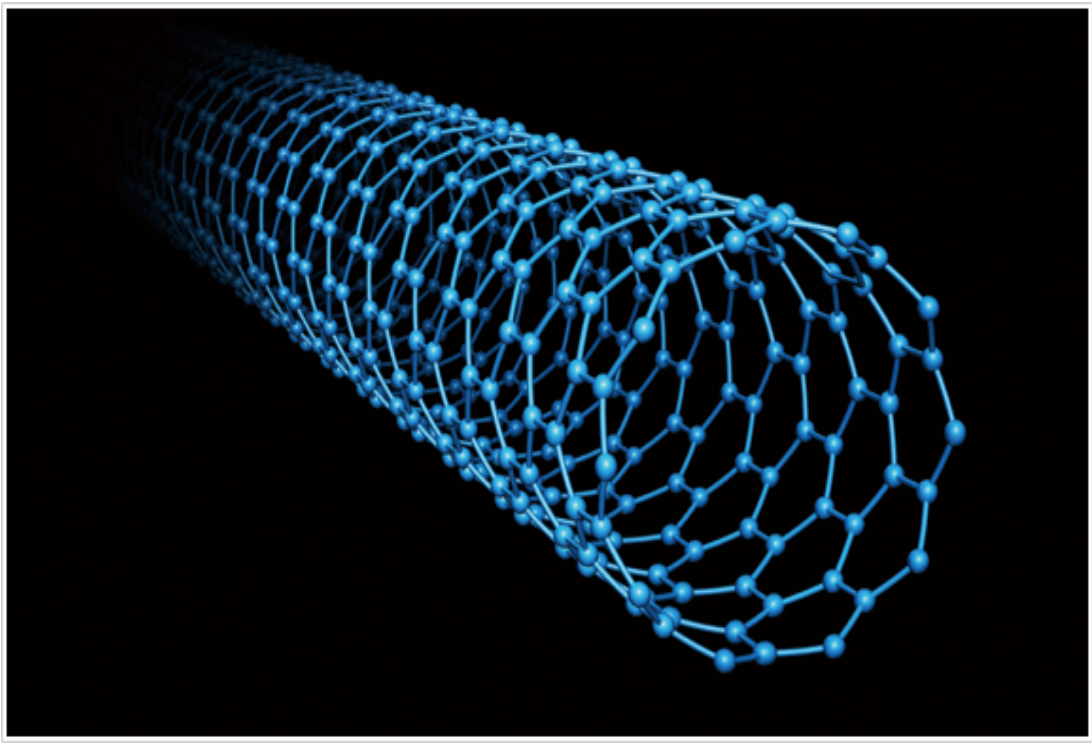

Figure 2.7: Carbon Nanotube

Classification of CNT'S

CNT's are classified into 3 types. They are-

1. Single walled carbon nanotube
2. Double walled carbon nanotube
3. Multi walled carbon nanotube

Single Walled Carbon Nanotube (SWNTs, SWCNTSs)

Most single-walled nanotubes (SWNT) have a diameter of close to 1 nanometer, with a tube length that can be many millions of times longer. The structure of a SWNT can be conceptualized by wrapping a one-atom-thick layer of graphite called graphene into a seamless cylinder.

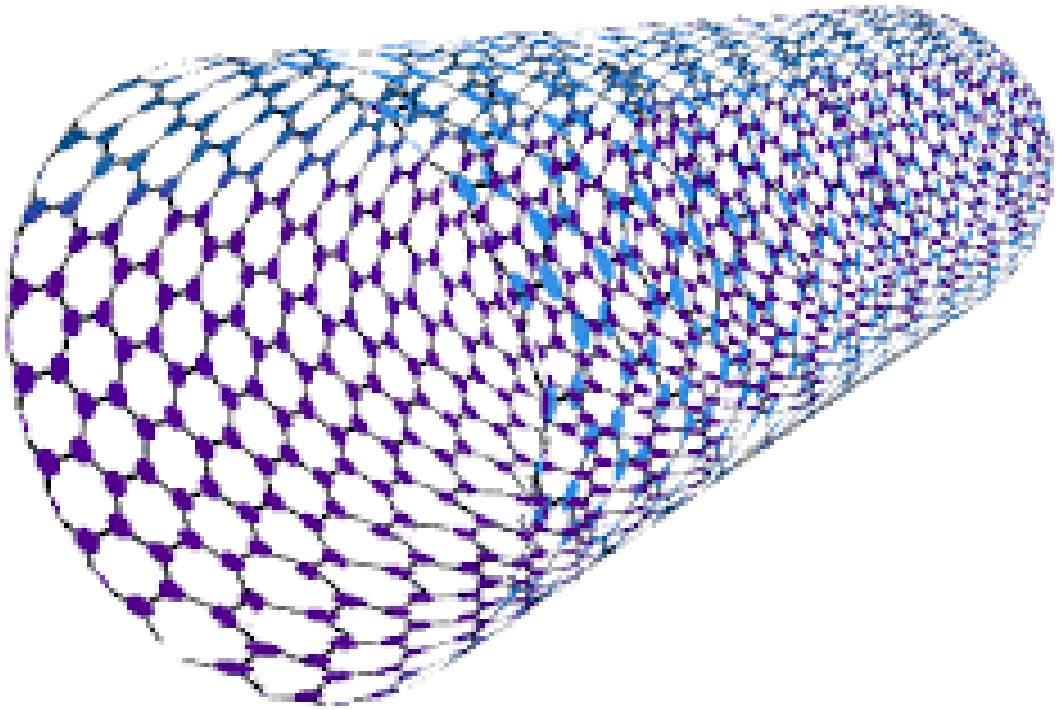

Figure 2.8: Single-walled nanotubes

Double Walled Nanotube (DWNT)

Double-walled carbon nanotubes are coaxial nanostructures composed of exactly two single-walled carbon nanotubes, one nested in another.

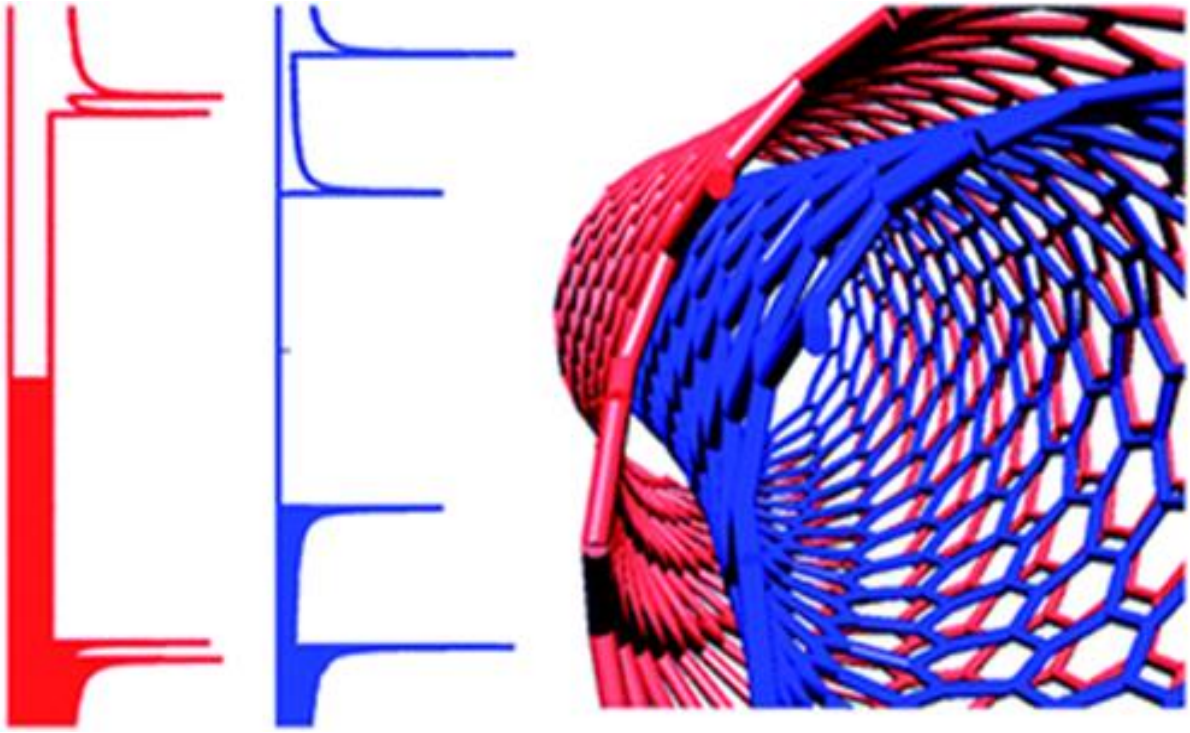

Figure 2.9: Double walled CNT

Multi Walled Nanotube (MWNTs)

Multi-walled nanotubes (MWNTs) consist of multiple rolled layers (concentric tubes) of graphene.

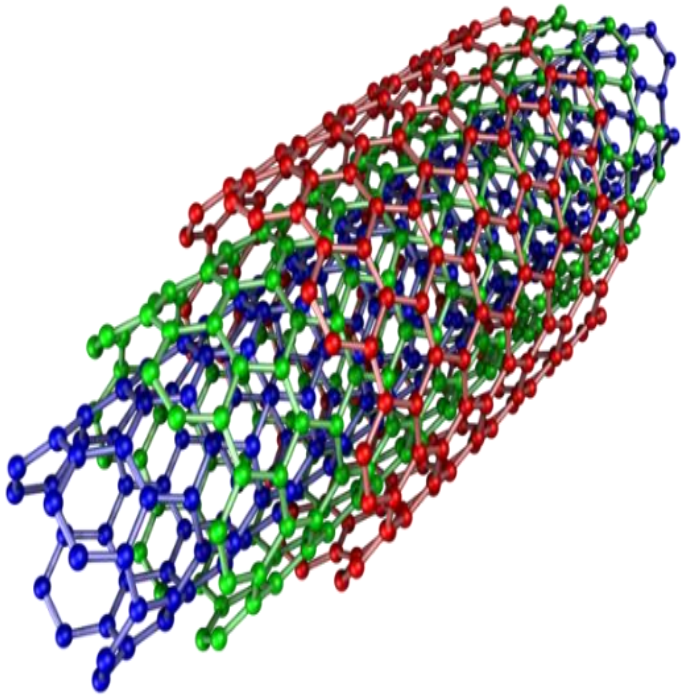

Figure 2.10: Multi Walled Nanotube

2.3.2 PSEUDOCAPACITOR

Pseudocapacitors store electrical energy fanatically by electron charge transfer between electrode and electrolyte. This is accomplished through electrosorption, reduction-oxidation reactions (redox reactions), and intercalation processes, termed pseudocapacitance.[8] [9] [10]

A pseudocapacitor is part of an electrochemical capacitor, and forms together with an electric double-layer capacitor (EDLC) to create a supercapacitor. Pseudocapacitance and double-layer capacitance add up to a common inseparable capacitance value of a supercapacitor. However, they can be effective with very different parts of the total capacitance value depending on the design of the electrodes. A pseudocapacitance may be higher by a factor of 100 as a double-layer capacitance with the same electrode surface.

A pseudocapacitor has a chemical reaction at the electrode, unlike EDLCs where the electrical charge storage is stored electrostatically with no interaction between the electrode and the ions. Pseudocapacitance is accompanied by an electron charge transfer between electrolyte and electrode coming from a de-solvated and adsorbed ion. One electron per charge unit is involved. The adsorbed ion has no chemical reaction with the atoms of the electrode (no chemical bonds arise[11]) since only a charge-transfer take place. An example is a redox reaction where the ion is O_2+ and during charging, one electrode hosts a reduction reaction and the other an oxidation reaction. Under discharge the reactions are reversed.

Unlike batteries, in faradaic electron charge-transfer ions simply cling to the atomic structure of an electrode. This faradaic energy storage with only fast redox reactions makes charging and discharging much faster than batteries.

Electrochemical pseudocapacitors use metal oxide or conductive polymer electrodes with a high amount of electrochemical pseudocapacitance. The amount of electric charge stored in a pseudocapacitance is linearly proportional to the applied voltage. The unit of pseudocapacitance is farad.

Examples of Pseudocapacitor

Brezesinki et al. showed that mesoporous films of α-MoO_3 have improved charge storage due to lithium ions inserting into the gaps of α-MoO_3. They claim this intercalation pseudocapacitance takes place on the same timescale as redox pseudocapacitance and gives better charge-storage capacity without changing kinetics in mesoporous MoO_3. This approach is promising for batteries with rapid charging ability, comparable to that of lithium batteries,[12] and are promising for efficient energy materials.

Other groups have used vanadium oxide thin films on carbon nanotubes for pseudocapacitors. Kim et al. electrochemically deposited amorphous $V_2O_5 \cdot xH_2O$ onto a carbon nanotube film. The three-dimensional structure of the carbon nanotubes substrate facilitates high specific lithium-ion capacitance and shows three times higher capacitance than vanadium oxide deposited on a typical Pt substrate.[13] These studies demonstrate the capability of deposited oxides to effectively store charge in pseudocapacitors.

Conducting polymers, such as polypyrrole (PPy) and poly(3,4-ethylenedioxythiophene) (PEDOT), have tunable electronic conductivity and can achieve high doping levels with the proper countering. A high-performing conducting polymer pseudocapacitor has high cycling stability after undergoing charge/discharge cycles. Successful approaches include embedding the redox polymer in a host phase (e.g. titanium carbide) for stability and depositing a carbonaceous shell onto the conducting polymer electrode. These techniques improve cyclability and stability of the pseudocapacitor device.

Materials

Electrodes' ability to produce pseudocapacitance strongly depends on the electrode materials' chemical affinity to the ions adsorbed on the electrode surface as well as on the electrode pore structure and dimension. Materials exhibiting redox behavior for use as pseudocapacitor electrodes are transition-metal oxides inserted by doping in the conductive electrode material such as active carbon, as well as conducting polymers such as polyaniline or derivatives of polythiophene covering the electrode material.

Transition Metal Oxides/Sulfides

These materials provide high pseudocapacitance and were thoroughly studied by Conway. Many oxides of transition metals like ruthenium (RuO_2), iridium (IrO_2), iron (Fe_3O_4), manganese (MnO_2) or sulfides such as titanium sulfide (TiS_2) or their combinations generate faradaic electron–transferring reactions with low conducting resistance.[14]

Ruthenium dioxide (RuO_2), in combination with sulfuric acid (H_2SO_4) electrolyte provides one of the best examples of pseudocapacitance, with a charge/discharge over a window of about 1.2 V per electrode. Furthermore, the reversibility on these transition metal electrodes is excellent, with a cycle life of more than several hundred-thousand cycles. Pseudocapacitance originates from a coupled, reversible redox reaction with several oxidation steps with overlapping potential. The electrons mostly come from the electrode's valence orbitals. The electron transfer reaction is very fast and can be accompanied with high currents.

The electron transfer reaction takes place according to:

$$RuO_2 + xH^+ + xe^- \leftrightarrow RuO_{2-x}(OH)_x \text{ where } 0 \leq x \leq 2$$ [15]

During charge and discharge, H+ (protons) are incorporated into or removed from the RuO2 crystal lattice, which generates storage of electrical energy without chemical transformation. The OH groups are deposited as a molecular layer on the electrode surface and remain in the region of the Helmholtz layer. Since the measurable voltage from the redox reaction is proportional to the charged state, the reaction behaves like a capacitor rather than a battery, whose voltage is largely independent of the state of charge.

Conducting Polymers

Another type of material with a high amount of pseudocapacitance is electron-conducting polymers. Conductive polymer such as polyaniline, polythiophene, polypyrrole and polyacetylene have a lower reversibility of the redox processes involving faradaic charge transfer than transition metal oxides, and suffer from a limited stability during cycling.[16] Such electrodes employ electrochemical doping or dedoping of the polymers with anions and cataions. Highest capacitance and power density are achieved with a n/p-type polymer configuration, with one negatively charged (n-doped) and one positively charged (p-doped) electrode.

2.2 HYBRID CAPACITOR

They are composed of both double-layer capacitors and pseudocapacitor. They can store charge in both electrostatically and electrochemically. They are further classified as below-

1. Composite Hybrids
2. Battery-type Hybrids
3. Asymmetric Hybrids

2.2.2 COMPOSITE ELECTRODES

Composite electrodes for hybrid-type supercapacitors are constructed from carbon-based material with incorporated or deposited pseudocapacitive active materials like metal oxides

and conducting polymers. As of 2013 most research for supercapacitors explores composite electrodes.

CNTs give a backbone for a homogeneous distribution of metal oxide or electrically conducting polymers (ECPs), producing good pseudocapacitance and good double-layer capacitance. These electrodes achieve higher capacitances than either pure carbon or pure metal oxide or polymer-based electrodes. This is attributed to the accessibility of the nanotubes' tangled mat structure, which allows a uniform coating of pseudocapacitive materials and three-dimensional charge distribution. The process to anchor pseudocapacitve materials usually use hydrothermal process, however, recent researcher, Li et al., from University of Delaware found facile and scalable approach to precipitate MnO2 on SWNTs film to make organic-electrolyte based supercapacitor.[17]

Another way to enhance CNT electrodes is by doping with a pseudocapacitive dopant as in lithium-ion capacitors. In this case the relatively small lithium atoms intercalate between the layers of carbon.[18] The anode is made of lithium-doped carbon, which enables lower negative potential with a cathode made of activated carbon. This results in a larger voltage of 3.8-4 V that prevents electrolyte oxidation. As of 2007 they had achieved capacitance of 550 F/g.[19] and reach an specific energy up to 14 Wh/kg (50.4 kJ/kg).

2.2.3 BATTERY TYPE ELECTRODE

Rechargeable battery electrodes influenced the development of electrodes for new hybrid-type supercapacitor electrodes as for lithium-ion capacitors.[20] Together with a carbon EDLC electrode in an asymmetric construction offers this configuration higher specific energy than typical supercapacitors with higher specific power, longer cycle life and faster charging and recharging times than batteries

2.2.4 ASYMMETRIC ELECTRODES (PSEUDO/EDLC)

Recently some asymmetric hybrid supercapacitors were developed in which the positive electrode were based on a real pseudocapacitive metal oxide electrode (not a composite electrode), and the negative electrode on an EDLC activated carbon electrode.
An advantage of this type of supercapacitors is their higher voltage and correspondingly their higher specific energy (up to 10-20 Wh/kg (36-72 kJ/kg)).[21]
As far as known no commercial offered supercapacitors with such kind of asymmetric electrodes are on the market.

Chapter 3

SUPERCAPACITOR FROM CNTs, OXIDE COMPOSITE & POLYMERS

3.1 SUPERCAPACITOR FROM CNTs

In 1997, Niu et al.[22] first suggested that CNTs could be used in supercapacitors. The MWCNTs were functionalized in nitric acid with functional groups introduced on the surface. These functionalized MWCNTs had a specific area of 430 m^2/g, a gravimetric capacitance of 102 F/g and an energy density of 0.5 W·h/kg obtained at 1 Hz on a single-cell device, using 38 wt% sulfuric acid as the electrolyte. Although 90% of the catalyst residue was removed, the remaining catalyst in the MWCNTs (mainly within the inner of the tubes) would affect the performance of the supercapacitor. The pseudocapacitance could be induced by the functional groups and the remaining catalyst. Therefore, both of the Faradaic and non-Faradaic processes were involved in the CNTs-based supercapacitor.

The redox response observed on the cyclic voltammetric (CV) plot of the SWCNT-based electrodes also indicated that the pseudocapacitance was really occurred to the CNT-based capacitor due to the functional groups and impurities.[23] However, it was demonstrated that the performance of the purified SWCNT, where the catalyst (Fe) was removed by thermal oxidization followed by immersion in HCl, was not as great as expected because of the formation of amorphous carbon by the thermal oxidization.[24] It is difficult to totally remove the catalyst from the catalyst-assisted CNTs and keep the graphitization at the same time, and then the effect of the catalyst is always there. To simplify the discussion, we firstly focus on the structural properties of CNTs, such as diameter, length, and pore size, which play an important role on the EDLC, and discuss the catalyst's and functional groups' effects later.

3.1.1 EFFECTS OF STRUCTURE

The amount of electrical charge accumulated due to electrostatic attraction in EDLC depends on the area of the electrode/electrolyte interface that can be accessed by the charge carriers. The higher surface area of the electrode material could leads to higher capacitance if the area can be fully accessed by the charge carriers. However, the higher surface area does not always result in higher capacitance because the capacitance also depends on the pore size, the size distribution and conductivity. Higher capacitance can be achieved by optimizing all of the related factors. For example, the vertically aligned CNTs with the diameter of about 25 nm and a specific area of 69.5 m^2/g had a specific capacitance of 14.1 F/g and showed excellent rate capability, which were better than those of entangled CNTs due to the larger pore size, more regular pore structure and more conductive paths.[25]

The effects of structures and diameters of CNTs, and macrotexture and elemental composition of the materials on the capacitance were systematically investigated by Frackowiak et al.[26] Table 1 shows the capacitance increases with the increase in the specific surface area. The smallest value is obtained in CNTs with closed tips and graphitized carbon layers, where the mesoporous volume for the diffusion of ions and the active surface for the formation of the electrical double layer are very limited in this material. The nanotubes with numerous edge planes, either due to herringbone morphology (A900Co/Si) or due to amorphous carbon coating (A700Co/Si), are the most efficient for the collection of charges. Quite moderate performance is given by straight and rigid nanotubes of large diameter (P800Al) despite a relatively high specific surface area. However, taking into account the diameter of the central canal, it is too large in comparison with the size of the solvated ions. On the other hand, this particular behavior could be also due to a very hydrophobic character of these tubes, as suggested by the very small value of oxygen content (Table 1)

Table 2.1: Particular behavior due to a very hydrophobic character

Type of nanotubes	A700Co/Si	A900Co/Si	A600Co/NaY	P800/Al
*V*meso (cm^3STP/g)	435	381	269	643
*S*BET (m^2/g)	411	396	128	311
Oxygen (mass%)	10.8	4.6	0.8	<0.3
Capacitance (F/g)	80	62	4	36

Figure 3.1: Particular behavior due to a very hydrophobic character

Anodic aluminum oxide (AAO) template-based MWCNTs is particularly suitable for the investigation into the size effect on supercapacitance due to the uniform diameter and length.[27] Jung et al. produced AAO-based CNTs with a diameter of 50 nm and a specific surface area of 360 m^2/g using the AAO template with a diameter and length of 90 nm and 100 μm, respectively, and catalyst Co. The CNTs with the template was directly used as the electrode without removing the alumina. The specific capacitance of the template-based CNT electrodes was around 50 F/g. The enhancement of the capacitance is due to the uniformity of the template-based CNTs comparing with the non-uniform CNTs. Ahn et al. found that the capacitance of the CNTs with smaller diameter (33 nm) is larger than that of with larger diameter (200 nm) due to the larger surface area in smaller diameter CNTs.

3.1.2 EFFECTS OF HEATING

Heating is one of important ways to improve the graphitization of CNTs and remove the amorphous carbon. The effects of heating on the capacitance depend on the heating temperature and the quality of the as-grown CNTs. The capacitance of as-received SWCNTs (Rice) was about 40 F/g and reduced to 18 F/g after heating treatment at 1,650 °C probably due to the more perfect graphitization of the tubes. However, Li et al.[28] found that the specific capacitance was increased by the oxidization up to 650 °C due to the enhanced specific surface area and dispersity. But the capacitance decreased with further increasing the temperature due to reduced surface area. At the same time, the heat treatment led to the reduction in the equivalent series resistance, resulting in the enhancement of the power density because of the improvement on graphitization.

Figure 3.2(a,b) shows the Brunauer-Emmett-Teller (BET; N_2) specific surface area and average pore diameter of as-grown CNTs as a function of heat-treatment temperature (carried out for 30 min).[29 30] With increasing temperature, the specific surface area increases, whereas the average pore diameter decreases and saturates at high temperature. The raw sample shows a peak at 150 Å and has less distribution in the smaller pore diameter near 20 Å. With increasing heat-treatment temperature, the number of smaller pore diameters increases and reaches the maximum at 1,000 °C, whereas the number of pore diameters ranging from 50 ± 250 Å decreases. Figure 3.3 shows the specific capacitance as a function of charging time and current, the CV curves, and impedance plots. A maximum specific capacitance of 180 F/g and a measured power density of 20 kW/kg for the heat-treated SWCNTs were obtained. The increased capacitance was well explained by the enhancement of the specific surface area and the abundant pore distributions at lower pore sizes.

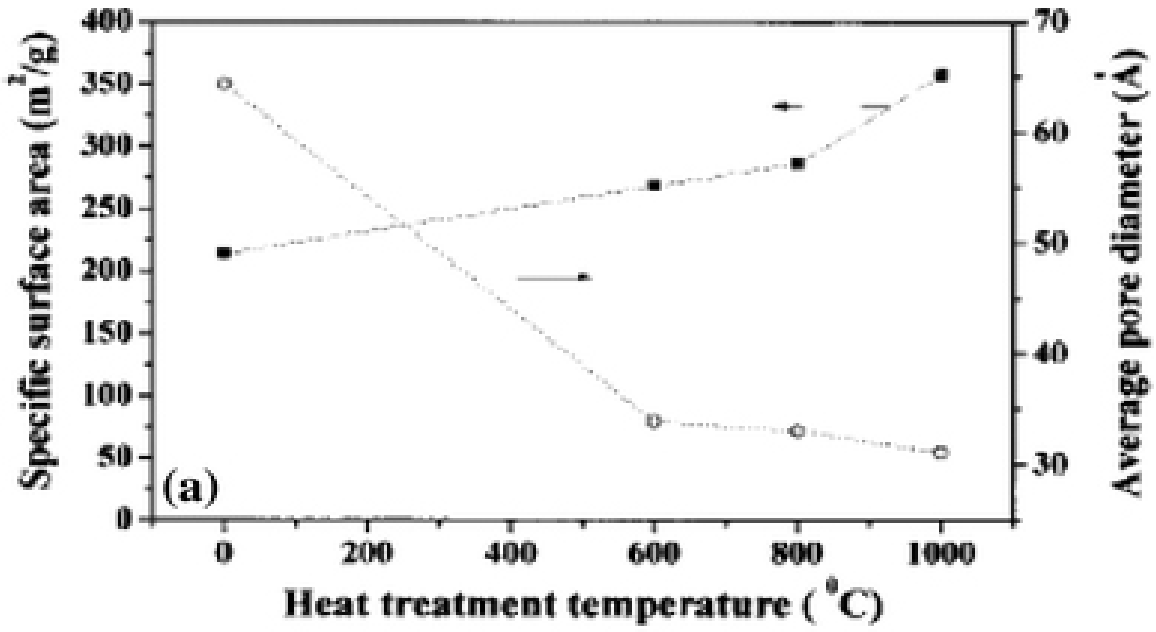

Figure 3.2(a): The BET (N_2) specific surface areas and the average pore diameters of the CNT electrode as a function of heat-treatment temperature

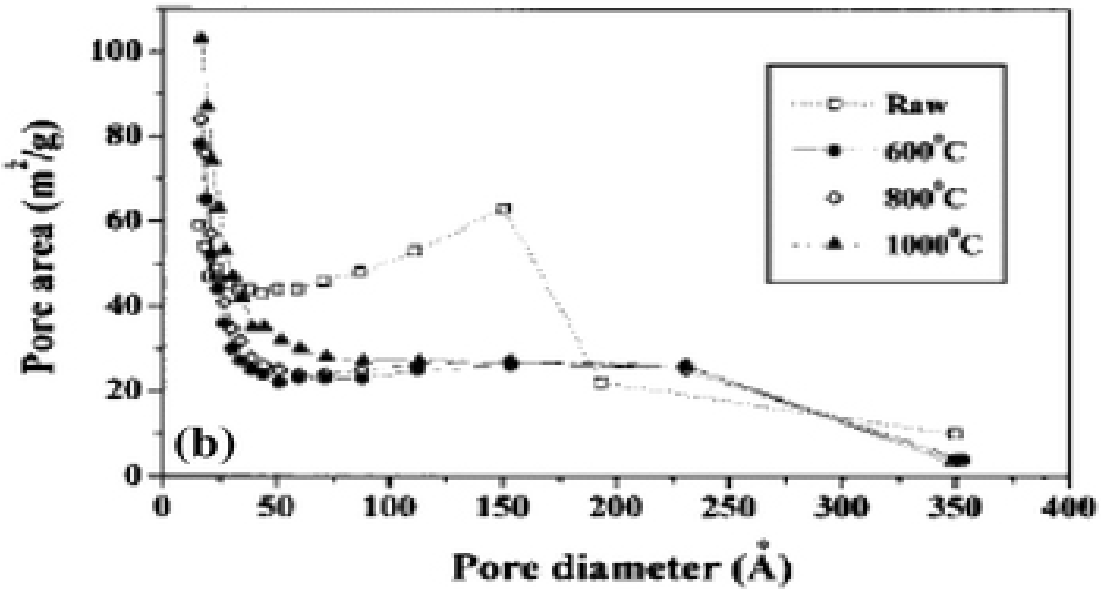

Figure 3.2(**b**): The pore size distribution of the CNT electrodes.

The following figures show electrochemical properties of the supercapacitor using the CNT electrodes.

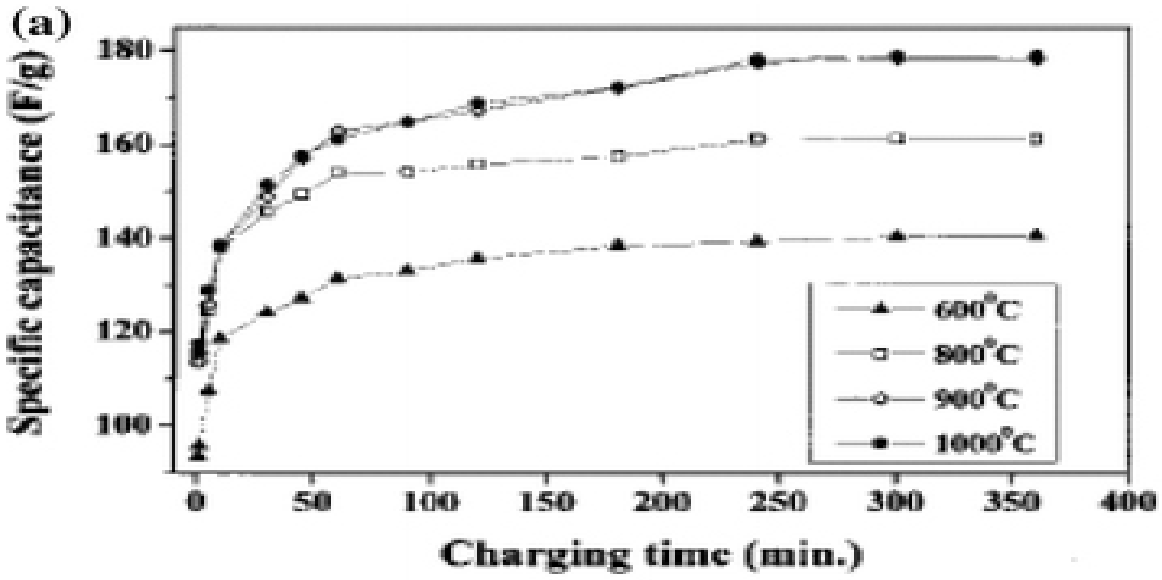

Fig 3.3 (**a**): The specific capacitances of the heat-treated electrodes at various temperatures as a function of the charging time at a charging voltage of 0.9 V, where the capacitance was measured at a discharging current of 1 mA/cm^2.

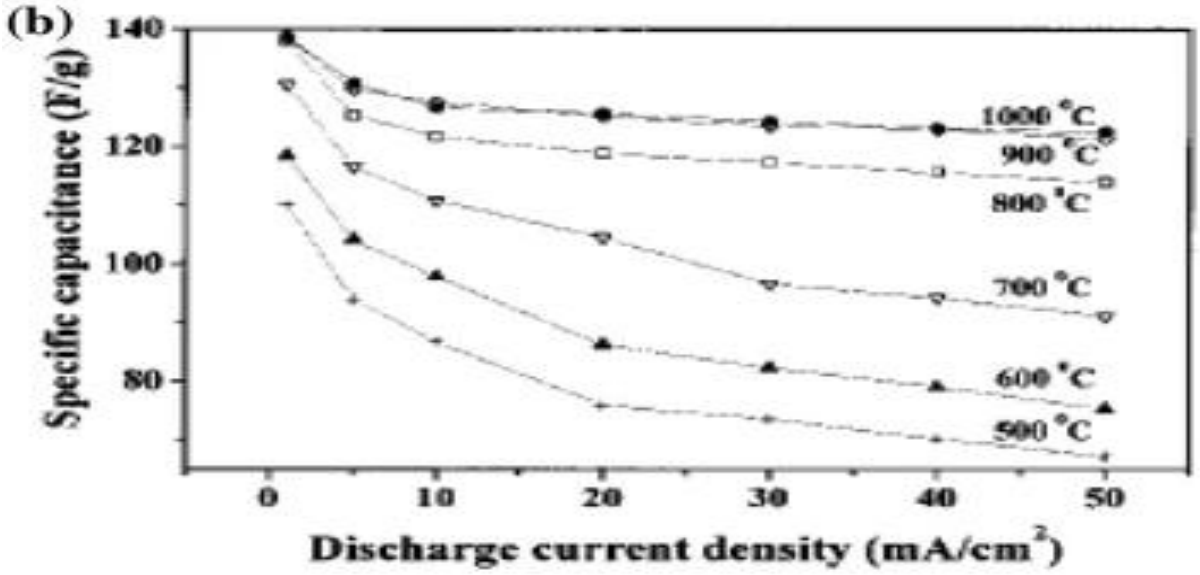

Fig 3.3 (**b**): The specific capacitances of the heat-treated electrodes at various temperatures as a function of the discharging current density at a charging voltage of 0.9 V for 10 min.

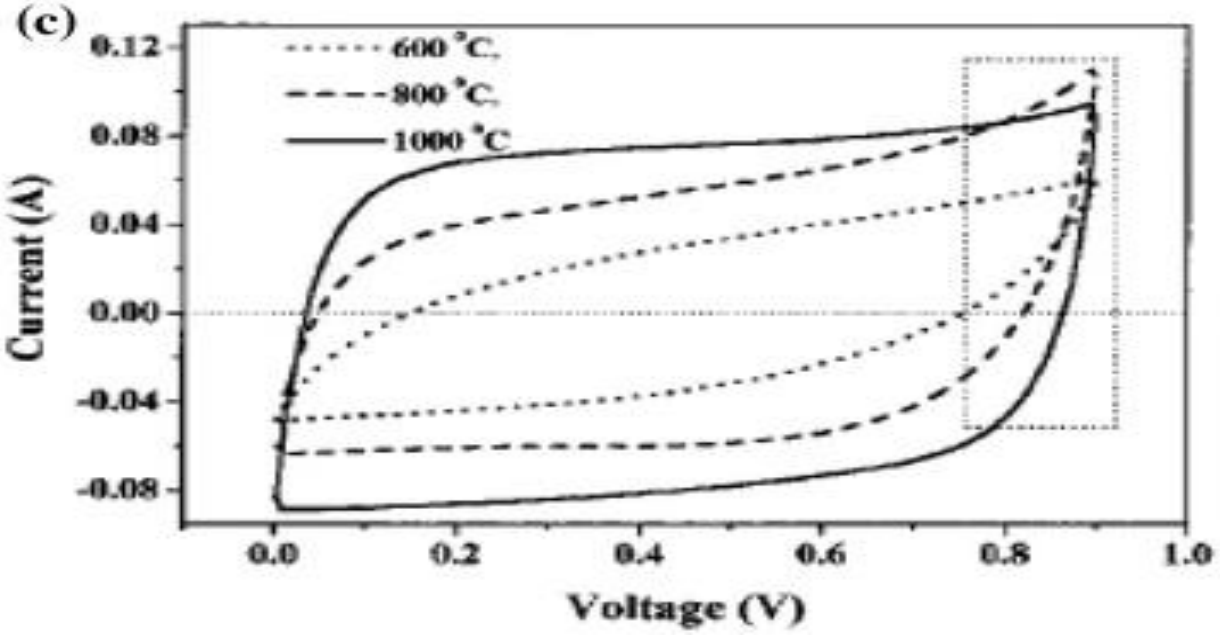

Fig 3.3 (**c**): The cyclic voltammetric (*CV*) behaviors (sweep rate, 100 mV/s) for the CNT electrodes at various heat-treatment temperatures.

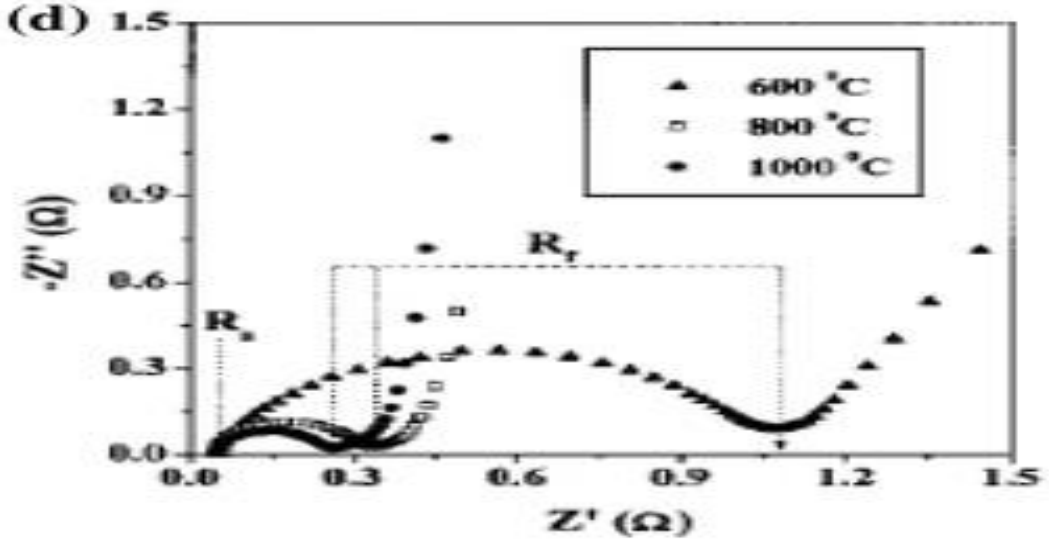

Fig 3.3 (**d**): The complex-plane impedance plots for the CNT electrodes for various heat-treatment temperatures at an ac-voltage amplitude of 5 mV, Z″: imaginary impedance, Z′: real impedance.

3.1.3 EFFECTS OF FUNCTIONALIZATION

Capacitance of CNT-based supercapacitor can also be enhanced by chemical activation,[31 32 33] functionalization,[34 35 36] and heat and surface treatment.[37 38] The value of specific capacitance increased significantly after strong oxidation in nitride acid due to the increase of the functional groups on the CNT's surface. Enhanced values of capacitance were observed after activation: in some cases, it increased almost seven times, because the microporosity of pure MWCNTs can be highly developed using chemical KOH activation.[39] The activated material still possessed a nanotubular morphology with many defects on the outer walls that gave a significant increase in micropore volume, while keeping a noticeable mesoporosity. The electrochemical treatment of CNTs provides an effective and controllable method for changing the pore size distribution (PSD) of SWCNTs.[40]

In particular, a remarkable volume of the small mesopores in the 3.0–5.0 nm diameter range was increased. The SWCNTs treated for 24 h at 1.5 V have a higher specific surface area (109.4 m^2/g) and larger volume of small mesopores (0.048 cm^3/g in 3.0–5.0 nm diameter range), compared with the as-grown SWCNTs (46.8 m^2/g and 0.026 cm^3/g, respectively). The specific capacitance was increased three-fold after electrochemical treatment. The electric double-layer capacitance, depending on the surface functional groups, can be dramatically changed, from a large increase to complete disappearance. The introduction of surface carboxyl groups created a 3.2 times larger capacitance due to the increased hydrophilicity of MWCNTs in an aqueous electrolyte.

In contrast, the introduction of alkyl groups resulted in a marked decrease in capacitance. Notably, the complete disappearance of capacitance for samples functionalized with longer alkyl groups, indicating the perfect block of proton access to the carbon nanotubes' surfaces by extreme hydrophobicity. The specific capacitance can also be enhanced by fluorine functionalization with heat treatment.[41] The fluorination of SWCNT walls transformed the nonpolar SWCNTs to the polar ones by forming dipole layers on the walls, resulting in high solubility in deionized water. Fluorinated samples gave lower capacitance than the raw samples before heat treatment due to the increase in the micropore area and the decrease in the average pore diameter.

However, after heat treatment, the specific capacitance of the fluorinated samples became higher than those of the raw samples because of the additional redox reaction due to the residual oxygen gases present on the surface of the electrodes. The reduction of ERS was attributed to the improvement in conductivity because of the carrier induced by the functionalization. Pyrrole treated-functionalized SWCNTs have high values of capacitance (350 F/g), power density (4.8 kW/kg), and energy density (3.3 kJ/kg). The high capacitance can also be obtained by the plasma surface treatment with NH_3 due to the enhancement of the total surface area and wettability of the MWCNTs.[42]

3.1.4 EFFECTS OF SHAPE ENGINEERING

Shape engineering of CNTs can also greatly improve the capacitance and power density. When compared with activated carbon cells, the high-densely packed and aligned SWCNTs showed higher capacitance, less capacitance drop at high-power operation, and better performance for thick electrodes. Figure 3.4 shows that the SWCNTs are high-densely packed after the engineering.

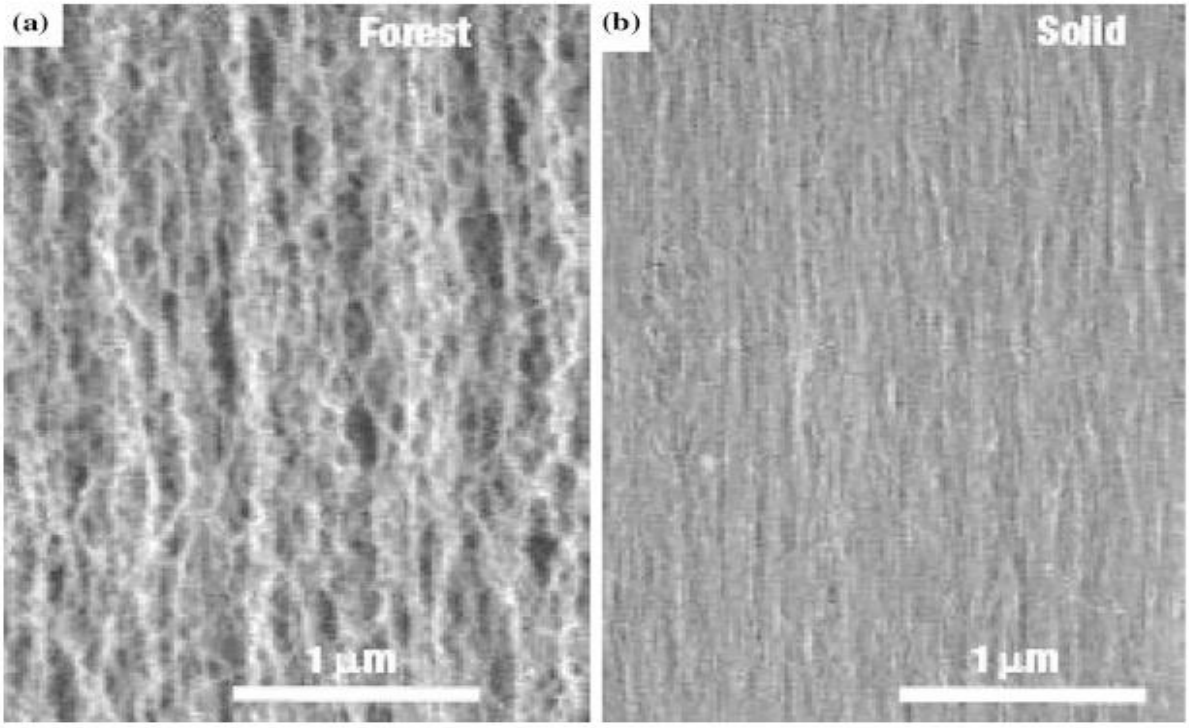

Figure 3.4: SEM images of (**a**) the as-grown forest and (**b**) shape-engineered SWCNTs.

Cyclic voltammograms of the solid sheet and forest cells were very similar, meaning the two materials have nearly the same capacitance per weight. The capacitance of the SWCNT solid EDLC was larger than that of forest cell. The energy density was estimated to be 69.4 W h/kg. Ion diffusivity plays a key factor to realize compact supercapacitors with high energy density and high power density. Because the electrolyte ions must diffuse through the pores of interstitial regions within the SWCNT packing structure, ion accessibility is limited in the inner region of the solids on the relevant timescale. Superior electrochemical properties of SWCNT solid cells originate from the aligned pore structures compared with activated carbon due to the fast and easy ion diffusivity.[43]

3.2 SUPERCAPACITOR FROM CNTs & OXIDE COMPOSITE

A hybrid electrode consisting of CNTs and oxide incorporates a Nano tubular backbone coated by an active phase with pseudocapacitive properties, which fully utilize the advantages of the pseudocapacitance and EDLC. The open mesoporous network formed by the entanglement of nanotubes may allow the ions to diffuse easily to the active surface of the composite components and to lower the equivalent series resistance (R_s) and consequently increase the power density.

3.2.1 RUTHENIUM OXIDE & CNTs COMPOSITE

Ruthenium oxide (RuO_2) has been proved to be one of important materials in oxide supercapacitors. The electrostatic charge storage as well as pseudofaradaic reactions of RuO_2 nanoparticles can be affected by the surface functionality of CNTs due to the increased hydrophilicity. Such hydrophilicity enables easy access of the solvated ions to the electrode/electrolyte interface, which increases faradaic reaction site number of RuO_2 nanoparticles and leads to higher capacitance. The specific capacitance of RuO_2/pristine CNT nanocomposites based on the combined mass was about 70 F/g
(RuO_2: 13 wt% loading).

However, the specific capacitance of RuO_2/hydrophilic CNT (nitric acid treated) nanocomposites based on the combined mass was about 120 F/g (RuO_2: 13 wt% loading). Kim et al.[44] reported that a three-dimensional CNT film substrate with RuO_2 showed both a very high specific capacitance of 1,170 F/g and a high-rate capability. To enhance its pseudocapacitance, ruthenium oxide must be formed with a hydrated amorphous and porous structure and a small size, because this structure provides a large surface area and forms conduction paths for protons to easily access even the inner part of the RuO_2.

The highly dispersed RuO_2 nanoparticles can be obtained on carboxylated carbon nanotubes by preventing agglomeration among RuO_2 nanoparticles through bond formation between the RuO_2 and the surface carboxyl groups of the carbon nanotubes or by treating the CNTs in a concentrated H_2SO_4/HNO_3 (3:1 volume ratio) mixture at 70 °C. The highly dispersed RuO_2 nanoparticles on carbon nanotubes show an increased capacitance, because the protons are able to access the inner part of RuO_2 with the decrease in size, and its utilization is increased. The high dispersion of RuO_2 is therefore a key factor to increase the capacitance of nanocomposite electrode materials for supercapacitors. A prominently enhanced capacitive performance was also observed in well-dispersed RuO_2 nanoparticles (NPs) on nitrogen-containing carbon nanotubes.[45]

The function of nitrogen amalgamation is to create preferential sites on CNTs with lower interfacial energy for attachment of RuO_2 nanoparticles (Figure 3.5). This crucial phenomenon leads to a significant improvement in the overall specific capacitance up to the measured scan rate of 2,000 mV/s, indicating that superior electrochemical performances for supercapacitor applications can be achieved with RuO_2–CNT-based electrodes using nitrogen incorporation technique. However, the commercialization of RuO_2/CNTs composite is very difficult because of the high cost and high toxicity of RuO_2.

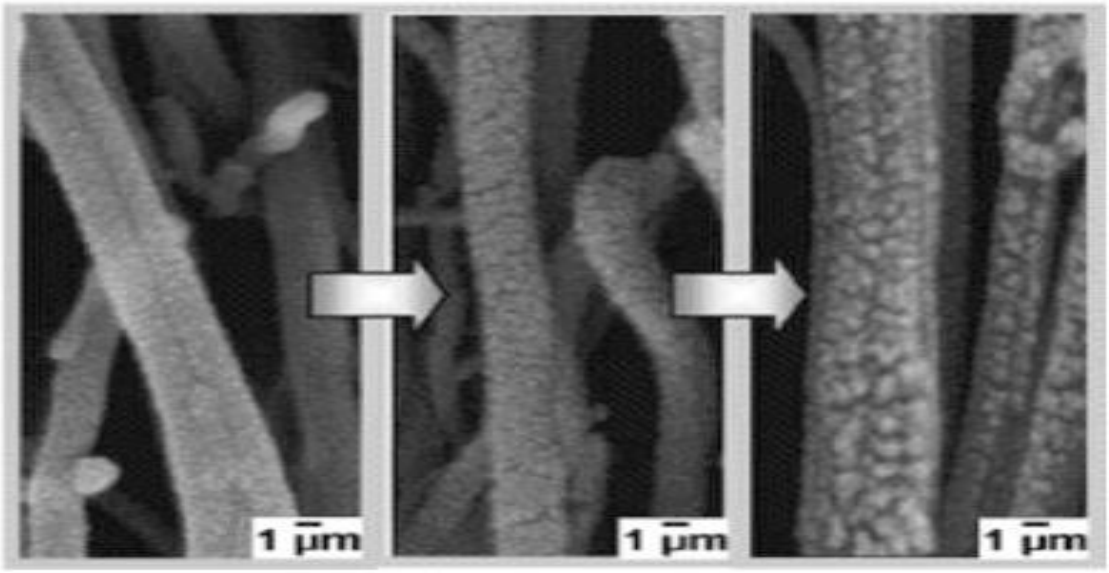

Fig 3.5: Evolutionary SEM images of one single N-containing CNT capturing RuO_2 NPs under distinct coating quantity.

3.2.2 Co_3O_4 AND CNTS COMPOSITE

Co_3O_4 is also an important transition-metal oxide and has great application in heterogeneous catalysts, anode materials in Li-ion rechargeable batteries, solid-state sensors, solar energy absorbers, ceramic pigments, and electrochromic devices.[46] Shan et al.[47] reported a novel type of multi-walled carbon nanotubes (MWCNTs)/Co_3O_4 composite electrode for supercapacitors. The electrode was prepared through a facile and effective method, which combined the acid treatment of MWCNTs and in situ decomposition of $Co(NO_3)_2$ in *n*-hexanol solution at 140 °C. The MWCNTs/Co_3O_4 composites show high capacitor property, and their best specific capacitance is up to 200 F/g, which is significantly greater than that of pure MWCNTs (90 F/g).

3.2.3 MANGANISE OXIDE AND CNTS COMPOSITE

Manganese oxide is one of the most promising pseudocapacitor electrode materials with respect to both its specific capacitance and cost effectiveness. CNT is effective for increasing the capacitance and improving the electrochemical properties of the a-$MnO_2 \cdot nH_2O$ electrodes and a very promising material as a conductive additive for capacitor or battery electrodes. The performance of real capacitors based on manganese oxide is limited by the two irreversible reactions Mn(IV)–Mn(II) and Mn(IV)–Mn(VII), which potentially depend on the electrolyte pH. In particular, with real capacitors, the electrolyte usually leads to the dissolution of the negative electrode.

The CNTs can help in preserving the electrodes integrity during cycling. The long cycle performance at a high charge–discharge current of 2 A/g for the a-MnO_2/SWCNTs composites was obtained.[48] All the composites with different SWCNT loads showed excellent cycling capability, even at the high current of 2 A/g, with the MnO_2 and 20 wt% SWCNT composite showing the best combination of efficiency of 75% and specific capacitance of 110 F/g after 750 cycles. The initial specific capacitance of the MnO_2/CNTs nanocomposite (CNTs coated with uniform birnessite-type MnO_2) in an organic electrolyte at a large current density of 1 A/g was 250 F/g, indicating excellent electrochemical utilization of the MnO_2because the addition of CNTs as a conducting agent improved the high-rate capability of the nanocomposite considerably.[49]

An in situ coating technique was used to prepare the MnO_2/MWCNT composite, where the nanosized ε-MnO_2 uniform layer (6.2 nm in thickness) covered the surface of the MWCNT and the original structure of the pristine MWCNT was retained during the coating process. The specific capacitance of the composite electrode reached 250.5 F/g, which was significantly higher than that of a pure MWCNT electrode.[50]

3.2.4 $Ni(OH)_2$ AND CNT COMPOSITE

$Ni(OH)_2$ is often used in the hybrid supercapacitor with carbon (using KOH solution as electrolyte). The positive electrode materials $Ni(OH)_2$ converts to NiOOH with the formation of proton and electron during the charge process. The rate capability of $Ni(OH)_2$ is associated with the proton diffusion in $Ni(OH)_2$ framework. The $Ni(OH)_2$ / CNTs composite provided a shorter diffusion path for proton diffusion and larger reaction surface areas, as well as reduces the electrode resistance due to the high electronic conductivity of CNTs. Wang et al. reported that the CNTs can reduce the aggregation of $Ni(OH)_2$ nanoparticles, inducing a good distribution of the nanosized $Ni(OH)_2$ particles on the cross-linked, netlike structure CNTs.

The rate capability and utilization of $Ni(OH)_2$ were greatly improved, and the composite electrode resistance was reduced. A specific energy density of 32 Wh/kg at a specific power density of 1,500 W/kg was obtained in the hybrid supercapacitor. The capacitance can be further improved by heating the $Ni(OH)_2$/CNTs composite at 300 °C because of the formation of an extremely NiO_x thin layer on CNT film. The specific capacitance decreased with the increase in NiO_x in the composite if the NiO_x percentage was above 8.9 wt%. A specific capacitance of 1,701 F/g was reported for 8.9 wt% NiO_x/CNT electrode.

3.2.5 OTHER OXIDES AND CNTS COMPOSITES

The Ni–Co oxides/CNT composite electrode, prepared by adding and thermally decomposing nickel and cobalt nitrates directly onto the surface of carbon nanotube/graphite electrode, has excellent charge–discharge cycle stability (0.2% loss of the specific capacitance at the 1,000th charge–discharge cycles) and good charge–discharge properties at high current density.[51] The specific capacitance of the composite increases significantly with a decrease in Ni/Co molar ratio when cobalt content is below 50% (in molar ratio) and then decreases rapidly when cobalt content is in the range between 50 and 100%.

A maximum value of the specific capacitance (569 F/g) was obtained at Ni/Co molar ratio = 1:1. Also, the specific capacitance of the nickel–cobalt oxides/CNT (Ni/Co = 1:1) electrode is much larger than the simple sum of the specific capacitances of the nickel oxide/CNT and cobalt oxide/CNT electrodes. Su et al.[52] reported a self-hybrid composite electrode composing of MWCNT and Co–Al-layered double hydroxides. The CV curves approached rectangle shapes, and the charge and discharge curves were basically symmetrical. Compared to MWCNTs supercapacitor, this new supercapacitor has good long-term stability, larger maximum power (6,400 W/kg) and energy density (13.2 Wh/kg), and a higher specific capacitance of 15.2 F/g even after 1,000 cycles at a large current of 2 A/g.

The capacitance of V_2O_5/CNTs composite is also larger than those of pure V_2O_5 and CNTs.[53] The addition of SnO_2 to the V_2O_5/CNTs can further increase the capacitance, because SnO_2 can improve the electronic properties of V_2O_5. The $LiNi_{0.8}Co_{0.2}O_2$/MWCNT (5–15 nm in diameter) composite capacitor has a specific capacitance and energy density of 270 F/g and 317 Wh/kg, respectively.[54] The MWCNTs substantially improves the electrochemical performance of the $LiNi_{0.8}Co_{0.2}O_2$-based capacitor because of the combination of increased conductivity, proper pore distributions, good mechanical properties, and electrolyte accessibility.

A chromium oxide/SWCNT-based electrodes shows exceptionally quick charge propagation due to the overall physical and textural properties of SWCNT. Nanosized chromium oxide particles finely dispersed at nanoscale in the SWCNT make possible the enhanced charging rate of the electrical double layer and allow fast faradaic reactions. Chromium-containing species present as CrO_3 inside SWCNTs as well as in the form of CrO_2Cl_2 (possibly along with

CrO_3 too) between SWCNTs within bundles supply redox reactions due to access by the electrolyte in spite of its encapsulated (and intercalated) location because of the numerous side openings created all along the SWCNT defective walls during the filling step.

Reddy et al. compared the electrochemical properties of RuO_2/MWCNT, TiO_2/MWCNT, and SnO_2/MWCNT monocrystalline composites for supercapacitor electrodes. The average specific capacitances measured using the three electrochemical techniques of the pure MWCNT, RuO_2/MWCNT, TiO_2/MWCNT, and SnO_2/MWCNT nanocomposite electrodes are 67, 138, 160, and 93 F/g, respectively. The enhancement of the specific capacitance of metal oxide dispersed MWCNT from pure MWCNT is due to the progressive redox reactions occurring at the surface and bulk of transition metal oxides through faradaic charge transfer due to the modification of the surface morphology of MWCNT by the Nano crystal line RuO_2, TiO_2, and SnO_2.

3.3 SUPERCAPACITOR FROM CNTs & POLYMER COMPOSITE

Electronically conducting polymers are promising supercapacitor materials for two main reasons: (1) high specific capacitance because the charge process involves the entire mass and (2) high conductivity in charged state, leading to low ESR and high power density. The main drawback using polymer in supercapacitor is the cycling stability because of typical shrinkage, breaking, and cracks appearing in subsequent cycles. It has been already proved that composites based on CNTs and conducting polymers, such as polypyrrole and polyaniline, are very interesting electrode materials, because the entangled mesoporous network of nanotubes in the composite can adapt to the volume change. That allows the shrinkage to be avoided, and hence a more stable capacitance with cycling to be obtained

3.3.1 POLYMAR AND CNTS HYBRID COMPOSITE

Lota et al. reported a novel composite material prepared from a homogenous mixture of polymer poly(3,4-ethylenedioxythiophene; PEDOT) and CNTs or by chemical or electrochemical polymerization of EDOT directly on CNTs. The optimal proportions of the composite are 20–30% of CNTs and 70–80% of PEDOT. Among the three methods used for the composites preparation, the electrochemical method gave the best capacitance results (150 F/g). And such material had a good cycling performance with a high stability in all the electrolytes. Another quite important advantage of this composite is its significant volumetric energy because of the high density of PEDOT. Due to the open mesoporous network of nanotubes, the easily accessible electrode/electrolyte interface allows quick charge propagation

in the composite material and an efficient reversible storage of energy in PEDOT during subsequent charging/discharging cycles.

The capacitance values for the composites [20 wt% of CNTs and 80 wt% of conducting polymers (ECP), such as polyaniline (PANI) and polypyrrole (PPy)] strongly depend on the cell construction.[55] In the case of three electrode cells, extremely high values could be found from 250 to 1100 F/g; however, in the two-electrode cell, much smaller specific capacitance values of 190 F/g for PPy/CNTs and 360 F/g for PANI/CNTs had been measured. It highlights the fact that only two-electrode cells allow a good estimation of materials performance in electrochemical capacitors.

The CNTs/PPy film shows excellent charge storage and transfer capabilities, attributed to the high surface area, conductivity, and electrolyte accessibility of the nanoporous structure.[56] The aligned CNTs/PPy composite film had an exciting combination of exceptional charge storage capacities as large as 2.25 F/cm^2 and improved device response times relative to pure PPy films. The superior performance of the composite relative to their component materials is attributed to the combination of electrolyte accessibility, reduced diffusion distances, and improved conductivity in the redox-pseudocapacitive composite structure.

An et al.[57] demonstrated that the SWCNT/PPy (1/1 in weight) nanocomposite electrode shows much higher specific capacitance than pure PPy and as-grown SWCNT electrodes, due to the uniformly coated PPy on the SWNTs. A maximum specific capacitance of 265 F/g from the SWNTs/PPy nanocomposite electrode containing 15 wt% of the conducting agent was obtained. The addition of conducting agent into the SWCNT-PPy nanocomposite electrode gives rise to an increase in the specific capacitance by reducing the internal resistance of the supercapacitor.

The specific capacitance of PANI/SWCNT composite electrode increased as the amount of the deposited PANI onto SWCNTs increases up to 73 wt%, where the PANI was wrapped around SWCNT.[58] Beyond 73 wt%, the additional PANI was deposited either in the mesopores between SWCNTs or in the form of film over the surface, which caused drop in the capacitance. The trend of the capacitance as a function of the PANI weight was opposite to that of specific resistivity.

The highest specific capacitance, specific power, and specific energy values of 485 F/g, 228Wh/kg and 2,250 W/kg were observed for 73 wt% PANI deposited onto SWCNTs. And the PANI/SWCNT composites showed long cyclic stability. Figure 3.6 shows the specific capacitance of PANI/SWCNT composite films electrodes as a function of discharge current density. The SWCNT/PANI composite film shows a higher specific capacitance, because the presence of SWCNT in the growth solution could promote the rate of aniline polymerization and result in a smooth, uniform, and highly porous composite film with a higher doping degree and lower defect density compared to the rough spherical grain-based pure PANI film. A MWCNT/PANI composite synthesized by an in situ chemical oxidative polymerization method showed much higher specific capacitance (328 F/g) because MWCNT made the

composites had more active sites for faradiac reaction.[59] Similarly, the highest specific capacitance value of 224 F/g was obtained for the MWCNT/PANI composite materials containing MWCNTs of 0.8 wt%. The same composite (MWCNT/PANI) synthesized by microwave-assisted polymerization was a core–shell structure with PANI layers (50–70 nm), which has an enhanced specific capacitance of 322 F/g with a specific energy density of 22 W h/kg.[60]

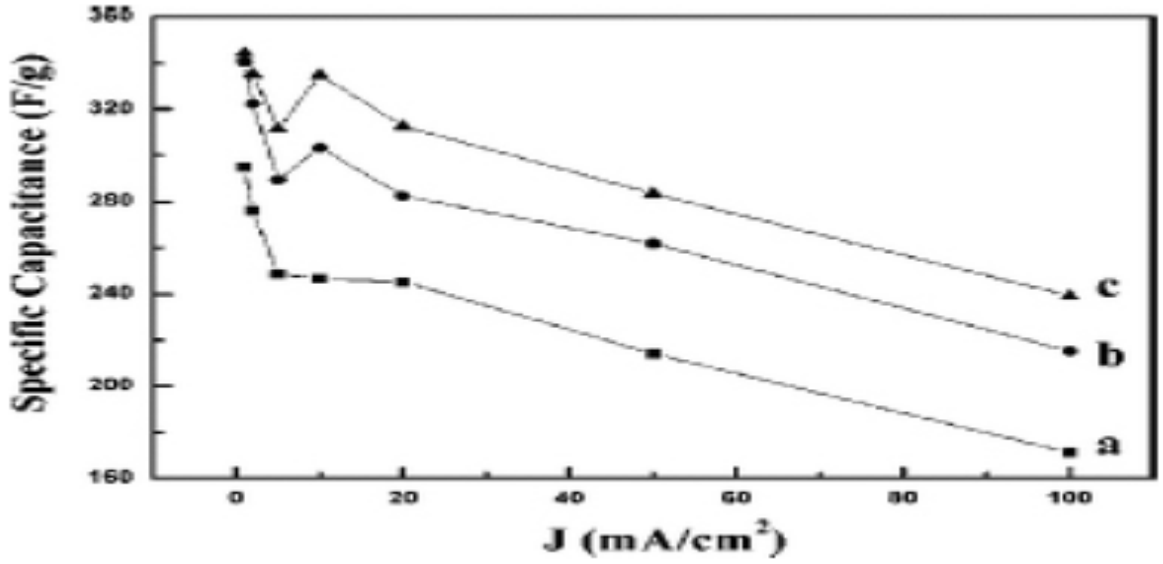

Figure 3.6: Specific capacitances of the SWNT/PANI composite film prepared from the growth solutions with (**a**) 0, (**b**) 4, and (**c**) 8 wt% SWCNT as a function of current density.

The CNTs/PAN composite with a ratio of 30/70 between CNT and PAN pyrolysized from a CNT/PAN blends for 180 min gave a high capacitance (100 F/g) although its specific surface area (157 m^2/g) is not the highest compared with the 50/50 CNT/PAN composite (233 m^2/g, 57 F/g).[61] This suggested that the content of PAN must be high enough not only to favor a large gas evolution, which develops porosity, but also to obtain the highest amount of residual nitrogen in the negative and positive ranges of potential, respectively, which contributed more to the pseudofaradiac charge transfer reactions.

3.3.2 POLYMAR AND CNTS TARNARY COMPOSITE

Single wall carbon nanotubes in the ternary composite, PAN/SAN/SWCNTs, acted as a compatabilizer for polyacrylonitrile (PAN)/styreneeacrylonitrile (SAN) copolymer blends, which was used to develop porosity control in the carbonized PAN/SAN/SWCNT composites with an average pore size in the range of 3–13 nm. Extremely high electrical double-layer capacity in the range of 83–205 mF/cm^2 was observed in the ternary composites.

3.3.3 DNA AND CNTS COMPOSITES

DNA is a good candidate for improved electrical conductivity for electrochemical devices with CNTs, because DNA has electrical characteristics similar to those of semiconducting diodes. In addition, DNA can more effectively coat, separate, and solubilize CNTs than other surfactants because of the large surface area of its phosphate backbone, which interacts with water, and there are many bases in DNA that can bind to CNTs. Therefore, DNA wrapping can debundle CNTs in high concentration CNT dispersions. Recently, Shin et al. reported the DNA-wrapped SWCNT hydrid fibers for supercapacitor electrode materials. The DNA–SWNT hybrid fibers were obtained using the wet-spinning method reported previously. The capacitance of the DNA-wrapped SWCNT fibers was 60 F/g (in a phosphate buffered saline solution), larger than that of pure SWCNT mat (30 F/g) due to the improved electrical conductivity, high CNT surface area and enhanced mechanical stability due to the π–π interaction between the DNA and the CNT sidewall.

Chapter 4

ELECTRODE CONSTRUCTION & SYNTHESIS METHOD

4.1 CONSTRUCTION OF ELECTRODE WITH CNT

Suspension of CNT was filtered by a filter membrane. For example 0.1 mg CNTS/ml in 1% aqueous solution of sodium dodecyl sulfate as surfactant can be filtered, which provides the pore size of 20 nm. A simple filter flask and moderate vacuum can be used in this regard. The CNTs that remain in the filter form an entangled network. This needs to be washed and dried. After that, the CNT network is peeled off. Films can treated in Ar gas at 600 degree celsius. The freestanding CNT networks are ready to be used as electrodes. The film thickness for instance can be 20 um and the conductivity is 10^3 S/cm. The capacitance is measured in the configuration of two electrodes. The device can be constructed in the following way:

Two CNT network strips taken and fixed separately with double-sided scotch tape to a substrate made of polyethylenetherephthalate (PET). The parts that overlap from the substrate are glued together with a nitrocellulose membrane which works as a separator in between. The top part is left opened and it is filled in with electrolyte (1M H_2SO_4). This provides both, the support for CNT network and encapsulant for the electrolyte. Cyclovoltammetry and galvanostatic charge/discharge experiments can be used to determine the capacitance of the CNT electrode.

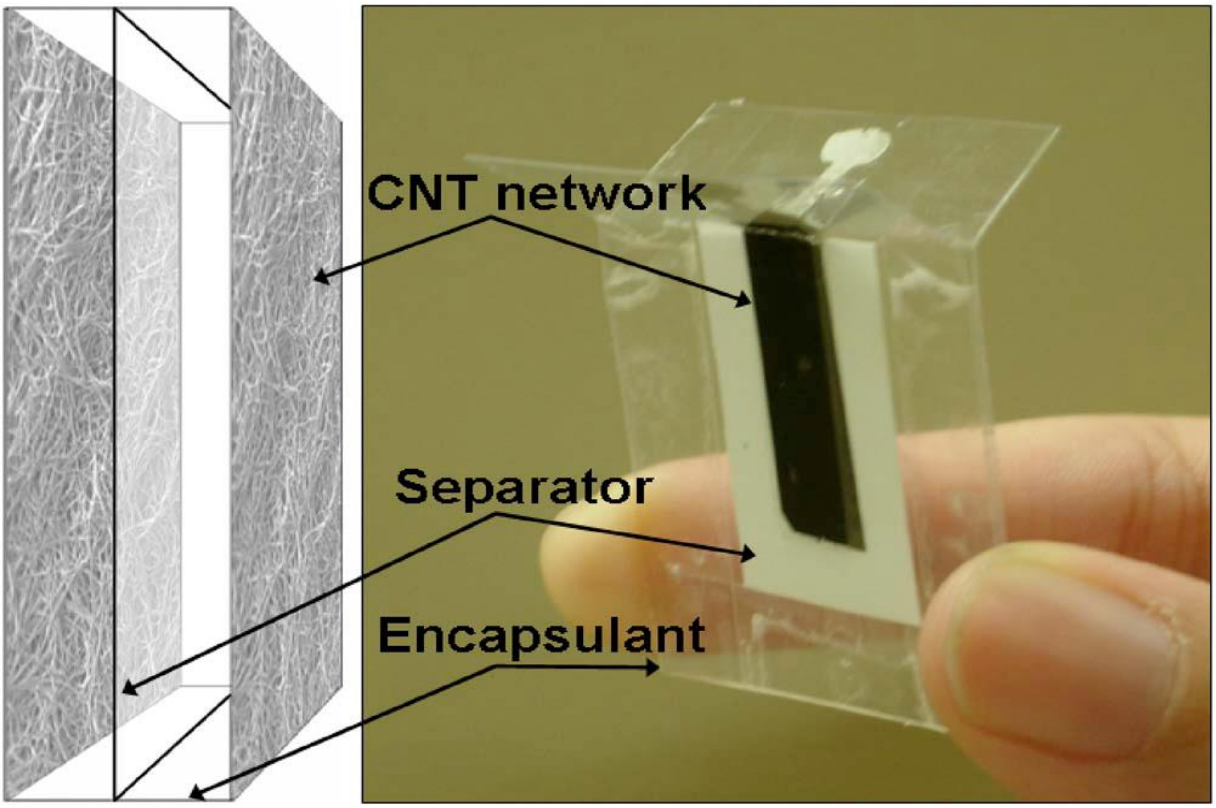

Figure 4.1: Setting up supercapacitor using CNT network

A Cyclovoltammogramm of the device is presented in Fig 4.2. The CV shows typical CV of a dense CNT network. The peak is spotted at 0.35 V, can be attributed to oxygen containing functional groups which contributes as pseudocapacitance to the overall capacitance.[62] In general, functional groups, impurities, and an unoptimized conductivity lead to the difference to an ideal box-shape CV of a supercapacitor without internal resistance (dotted line).[63] From the CV, we calculated the specific capacitance *c* of our device according to $c = i / v$, where *v* is the scan rate (20 mV/s) and *i* the corresponding current of the voltage applied. This way, we found the specific capacitance of our device to be 44 F/g at 1 V. This is in very good agreement to previously published results,[64] [65] [66] [67]even though these studies had used metallic current collectors or mixed CNTs with *a*-C. In Figure the result of a galvanostatic charge/discharge at 1 mA is presented.

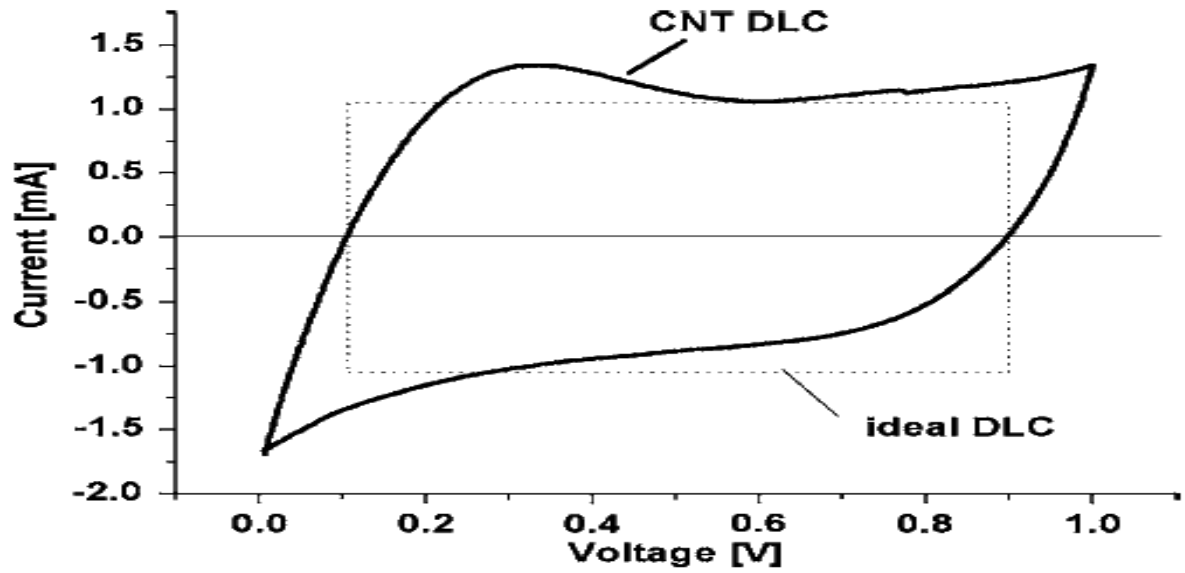

Figure 4.2: Voltage vs current

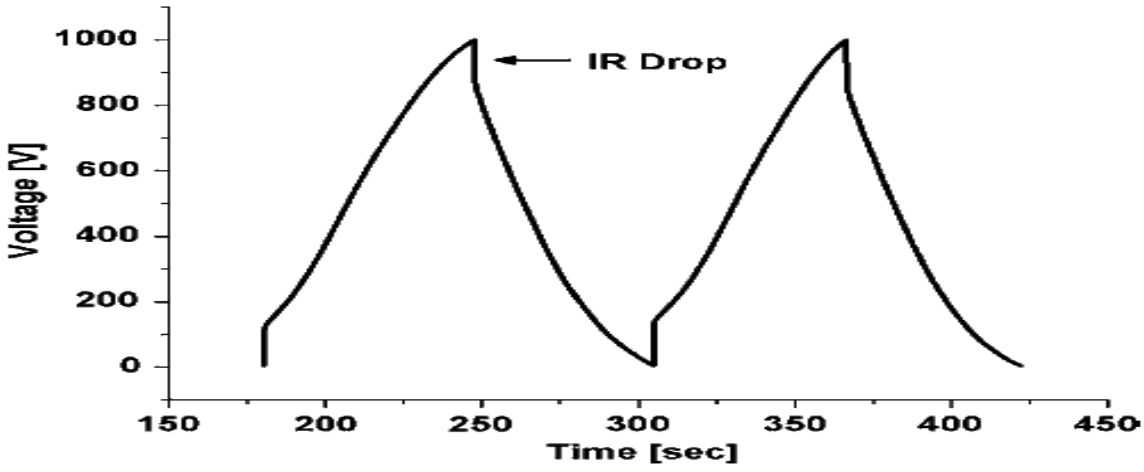

Figure 4.3: Voltage vs time

4.2 CNT SYNTHESIS METHOD

1) High-pressure carbon monoxide disproportionation
2) Arc discharge method
3) Laser ablation.
4) Chemical vapor deposition method

There are some other methods used as well, but the method involving carbon monoxide is not used nowadays.
A question may be asked, why this synthesis method is important to supercapacitor. The performance of the SC depends on the purity of the electrode. Thus comes the need of synthesis.

4.2.1 ARC DISCHARGE METHOD

Arc discharge was the first recognized technique for producing MWNTs[68] and SWNTs.[69 70] The arc discharge technique generally involves the use of two high-purity graphite electrodes as the anode and the cathode. The electrodes were vaporized by the passage of a DC current (~100 A) through the two high-purity graphite separated (~ 1–2 mm) in 400 mbar of Helium atmosphere. Experimental set up of arc discharge apparatus was shown in Figure 1. After arc discharging for a period of time, a carbon rod is built up at the cathode. This method can mostly produce MWNTs but can also produce SWNT with the addition of metal catalyst such as Fe, Co, Ni, Y or Mo, on either the anode or the cathode. The quantity and quality such as lengths, diameters, purity and etc. of the nanotubes obtained depend on various parameters such as the metal concentration, inert gas pressure, type of gas, plasma arc, temperature, the current and system geometry.

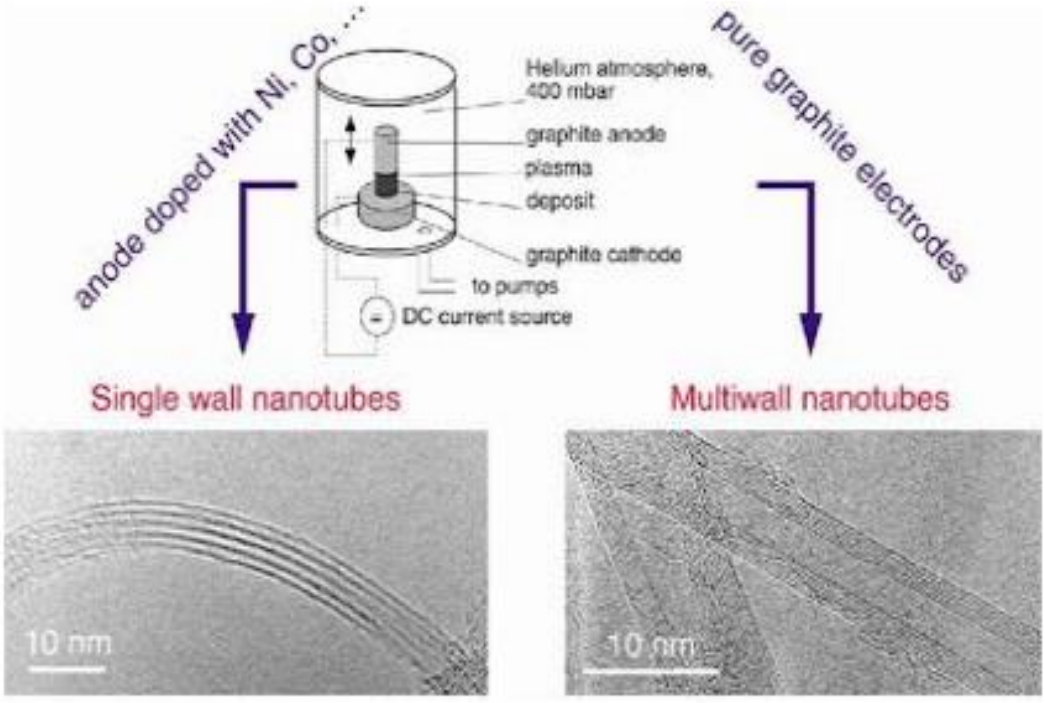

Figure 4.4: Arc Discharge Method

4.2.2 CHEMICAL VAPOR DEPOSITION

Chemical vapor deposition of hydrocarbons over a metal catalyst is a classical method that has been used to produce various carbon materials such as carbon fibers and filaments for over twenty years. Also produces graphene from methane. Large amounts of CNTs can be formed by catalytic CVD of acetylene over cobalt and iron catalysts supported on silica or zeolite. The carbon deposition activity seems to relate to the cobalt content of the catalyst, whereas the CNTs' selectivity seems to be a function of the pH in catalyst preparation. Fullerenes and bundles of single walled nanotubes were also found among the multi walled nanotubes produced on the carbon/zeolite catalyst. Some researchers are experimenting with the formation of CNTs from ethylene. Supported catalysts such as iron, cobalt, and nickel, containing either a single metal or a mixture of metals, seem to induce the growth of isolated single walled nanotubes or single walled nanotubes bundles in the ethylene atmosphere. The production of single walled nanotubes, as well as double-walled CNTs, on molybdenum and molybdenum-iron alloy catalysts has also been demonstrated. CVD of carbon within the pores of a thin alumina template with or without a Nickel catalyst has been achieved. Ethylene was used with reaction temperatures of 545°C for Nickel-catalyzed CVD, and 900°C for an uncatalyzed process.

The resultant carbon nanostructures have open ends, with no caps. Methane has also been used as a carbon source. In particular it has been used to obtain 'nanotube chips' containing isolated single walled nanotubes at controlled locations. High yields of single walled nanotubes have been obtained by catalytic decomposition of a H_2/CH_4 mixture over well-dispersed metal particles such as Cobalt, Nickel, and Iron on magnesium oxide at 1000°C. It has been reported that the synthesis of composite powders containing well-dispersed CNTs can be achieved by selective reduction in a H_2/CH_4 atmosphere of oxide solid solutions between a non-reducible oxide such as Al_2O_3 or $MgAl_2O_3$ and one or more transition metal oxides. The reduction produces very small transition metal particles at a temperature of usually >800°C. The decomposition of CH_4 over the freshly formed nanoparticles prevents their further growth, and thus results in a very high proportion of single walled nanotubes and fewer multi walled nanotubes.

Some common steps of making pure graphene out of methane using CVD:

1) Pressures ranging from 1 to 1500 Pa in a chamber.
2) Hydrogen gas and inert gases such as argon are flowed into the system.
3) Standard quartz tubing are used in CVD of graphene.

After several stage of heating and cooling, upto 97-99% pure graphene is achieved.

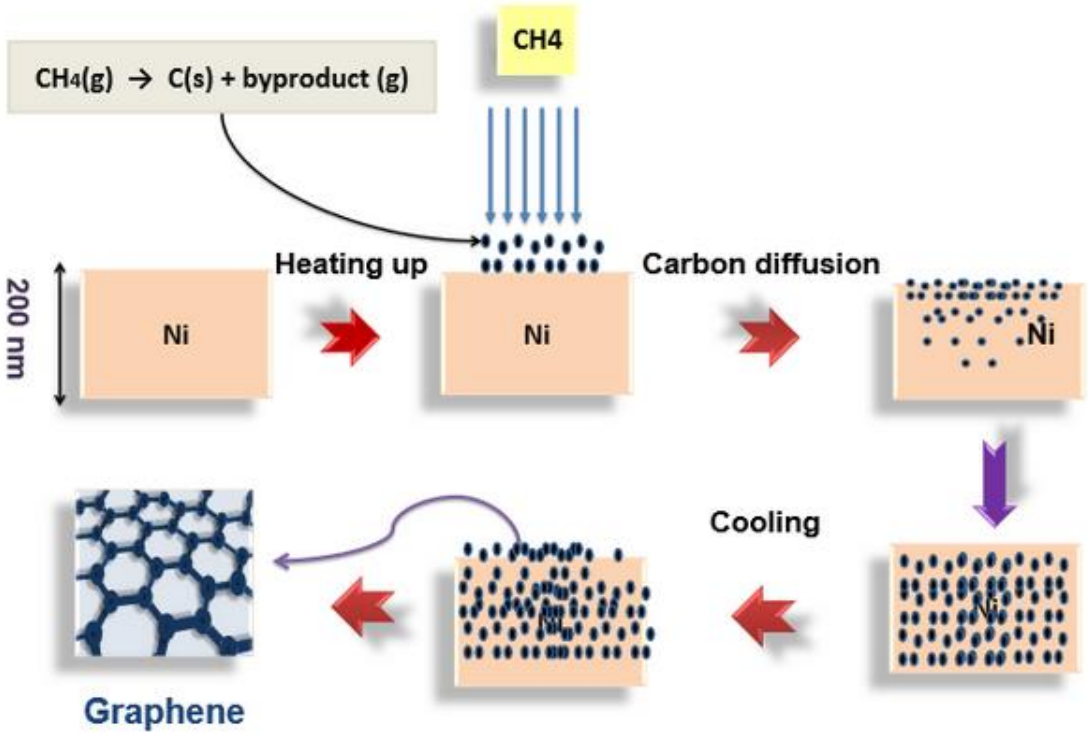

Figure 4.5: Flow diagram of making graphene from CVD

4.2.3 LASER ABLATION

In 1996 CNTs were first synthesized using a dual-pulsed laser and achieved yields of >70wt% purity. Samples were prepared by laser vaporization of graphite rods with a 50:50 catalyst mixture of Cobalt and nickel at 1200°C in flowing argon, followed by heat treatment in a vacuum at 1000°C to remove the C60 and other fullerenes. The initial laser vaporization pulse was followed by a second pulse, to vaporize the target more uniformly. The use of two successive laser pulses minimizes the amount of carbon deposited as soot. The second laser pulse breaks up the larger particles ablated by the first one, and feeds them into the growing nanotube structure.

The material produced by this method appears as a mat of "ropes", 10-20nm in diameter and up to 100µm or more in length. Each rope is found to consist primarily of a bundle of single walled nanotubes, aligned along a common axis. By varying the growth temperature, the catalyst composition, and other process parameters, the average nanotube diameter and size distribution can be varied. Arc-discharge and laser vaporization are currently the principal methods for obtaining small quantities of high quality CNTs. However, both methods suffer from drawbacks. The first is that both methods involve evaporating the carbon source, so it has been unclear how to scale up production to the industrial level using these approaches. The second issue relates to the fact that vaporization methods grow CNTs in highly tangled forms, mixed with unwanted forms of carbon and/or metal species. The CNTs thus produced are

difficult to purify, manipulate, and assemble for building nanotube-device architectures for practical applications.

4.2.4 OTHER METHODS

CNTs can also be produced by ball milling, diffusion flame synthesis, electrolysis, use of solar energy, heat treatment of a polymer, and low-temperature solid pyrolysis.

Chapter 5

FREQUENCY RESPONSE OF SUPERCAPACITOR MADE WITH SWNT

Supercapacitors are energy storage devices with high power density due to their fast charge propagation.[71 72 73 74 75 76 77 78 79] Single-walled carbon nanotubes (SWNTs) are predicted to be a suitable candidate for the electrode of supercapacitors because of their high accessible surface area, low electric resistance, low mass density, high stability, and the network structure of entangling with each other. It is reported that the frequency "knee" of carbon nanotube supercapacitors was around 100Hz, which suggests that most of their stored energy is accessible at frequencies below 100Hz. This is unprecedented for this type of devices because the highest reported knee frequency in other capacitors is 6Hz and the knee frequency for most commercially available supercapacitors, including those specially designed for high power applications, is <1Hz. A better frequency response means a better power performance. In particular, for low frequency electrical filtering device application, the demand of frequency response performance of supercapacitors is high. Therefore, to find suitable materials which own good frequency response is important. In this study, impedance characterization of SWNTs was investigated, from which the frequency response of the SWNT electrodes in supercapacitors was analyzed. The knee frequency around 631Hz for the electrochemically oxidized SWNT supercapacitor was achieved due to the introduction of nanosized mesopores and oxygen-containing groups.

he SWNTs used in this study were synthesized by a hydrogen arc discharge method, in which graphite was the carbon feedstock, hydrogen and argon gases were used as buffer gas, a mixture of Ni, Co, and Fe powders as catalyst, and FeS as growth promoter. The purity of the as-prepared SWNTs was estimated to be over 40wt% based on transmission electron microscopic observations and thermogravitric analysis results.

Typically, 10–80mg of SWNTs was placed between two sheets of nickel foam in a cylindrical steel mold and a pellet with 8mm diameter was formed by pressing the carbon material and nickel foam under 2MPa. Supercapacitor was assembled in a cell with two identical pellets separated by a nylon cloth in 6*M* KOH aqueous solution at room temperature and atmospheric pressure. Some of the SWNT electrodes were at first electrochemically oxidized in 6*M* KOH aqueous solution at the voltage of 1.5V for 36h. These will be called as electrochemically oxidized SWNT electrode below.

The impedance measurements were made at a dc bias of 0Vwith a 10mV amplitude sinusoidal signal over the frequency range of 100 kHz–0.01Hz using a Solartron model 1260 frequency response analyzer with a Solartron model 1287 potentiostat/galvanostat.

The complex-plane impedance plots of the as-prepared SWNT and electrochemically oxidized SWNT supercapacitors are shown in Figure 5.1

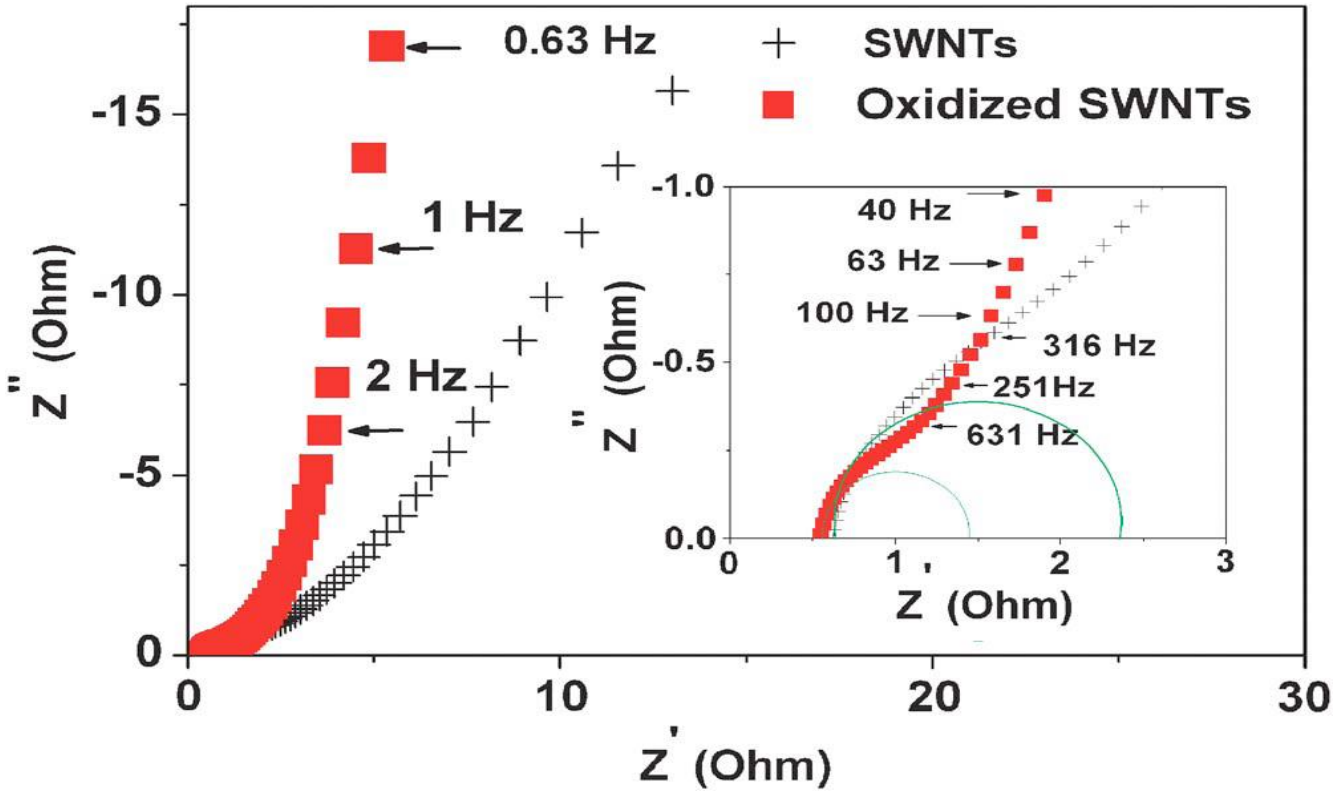

Figure 5.1: Complex-plane impedance of a single cell supercapacitor fabricated with the as-prepared and electrochemically oxidized SWNTs.

The impedance spectrum in the high frequency range being fitted exhibits semicircles but straight lines in the low frequency range, as shown in Figure 5.1. An electrode-solution system, especially those porous materials, as in supercapacitors, has complex combinations of *C* and *R* components. The interfacial impedance of a supercapacitor is associated with a double-layer capacitance *Cdl*, a pseudocapacitance *Cp*, a Faradaic charge-transfer resistance *Rf* and the sum of the electrolyte resistance, the electrode resistance, and the contact resistance between the electrode and the current collector *Rs*. The presence of semicircles of SWNT supercapacitors is attributed to the Faradic reaction of oxygen-containing functional groups at the electrode surface. From the value of *Rs* (the point impedance curve intersects the *Z′* axis at high frequency range), the equivalent series resistance of the electrochemically oxidized SWNT and the as-prepared SWNT supercapacitor can be obtained as 0.54 and 0.62Ω, respectively. The electrolyte resistance and the contact resistance are identical in both SWNT supercapacitors. Therefore, a decrease of *Rs* indicates a decrease of the SWNT electrode resistance in electrochemically oxidized SWNT capacitor.

In the complex-plane impedance plots, SWNT supercapacitors differ somewhat from those of conventional capacitors at the low frequency range. The ideal capacitor exhibits a vertical line, while the plot of SWNT supercapacitors starts with a 45° impedance line and approaching an almost vertical line at low frequencies. It is due to the diffusion process on the porous surface of SWNTs. It is consistent with the porous nature of the electrodes when saturated with electrolyte. The 45° region (Warburg region) is a consequence of the distributed resistance/capacitance in a porous electrode. At higher frequency, the resistance as well as the capacitance of a porous electrode decreases because only part of the active porous layer is accessible at high frequency. The knee frequency for the electrochemically oxidized SWNT supercapacitor was found around 631Hz from Figure 5.1, much higher than those of the as-prepared one (around 316Hz). Figure 5.2 shows a Bode angle plot of the as-prepared SWNT supercapacitor and electrochemically oxidized SWNT supercapacitor. For frequency of up to 1Hz, the phase angle of the electrochemically oxidized SWNT supercapacitor is close to −90°, while it is −50° for the as-prepared one.

This suggests that the electrochemically oxidized SWNT supercapacitor functions like an ideal capacitor and better than the as-prepared one. Such improved frequency response performance is mainly achieved by the introduction of nanosized mesopores and oxygen-containing groups, favouring the access of electrolyte to the surface of SWNT. After electrochemical oxidation treatment, parts of the tips and sidewall of SWNTs were etched and the amount of small mesopores was increased. It is considered that the small mesopores serve as channels for electrolytes and can be readily accessed in the charge/discharge process. On the other hand, oxygen-containing groups can form during the electrochemical oxidation process, which are confirmed by x-ray photoemission spectroscopy (XPS) data, as shown in Figure 5.3(a). A strong peak of O 1*s* has been observed for electrochemically oxidized SWNTs, indicating a high surface oxygen concentration.[80 81]

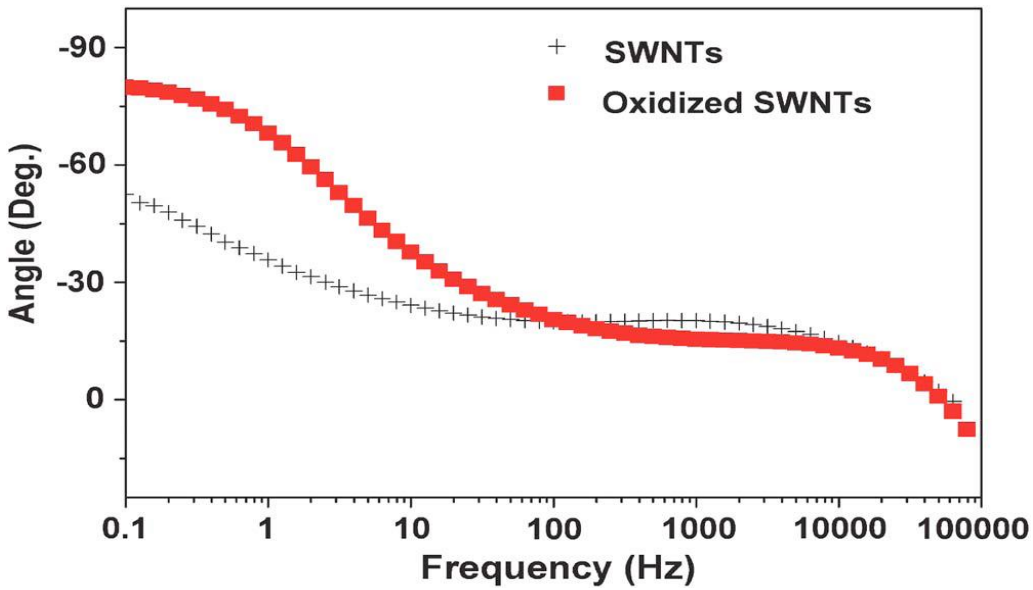

Figure 5.2: Bode angle plot of a single cell supercapacitor fabricated with the as-prepared and electrochemically oxidized SWNTs.

Table-1 summarizes the elemental composition detected by XPS and the oxygen/carbon (O⁄C) ration. Obviously, electrochemically oxidized SWNTs show higher O⁄C ration of ~70.9%, indicating that the surfaces were severely oxidized during the electrochemical oxidation process. Figure 5.3(b) shows O1*s* XPS analysis results of the electrochemically oxidized SWNT. To identify the O 1*s* XPS results, a curve-fitting procedure was employed. Dots shown in Figure 5.3(b) correspond to XPS experimental data and bold solid lines are the fitting curves for the experimental data. C-O and C=O groups on electrochemically oxidized SWNT surfaces were identified. Moreover, the detection of oxygen-containing functional groups in oxidized SWNTs is in agreement with other reports. The increased oxygen-containing groups can enhance the wettability of carbon materials in aqueous electrolyte, which is important to maximize the access of the electrolyte to the surface of carbon.

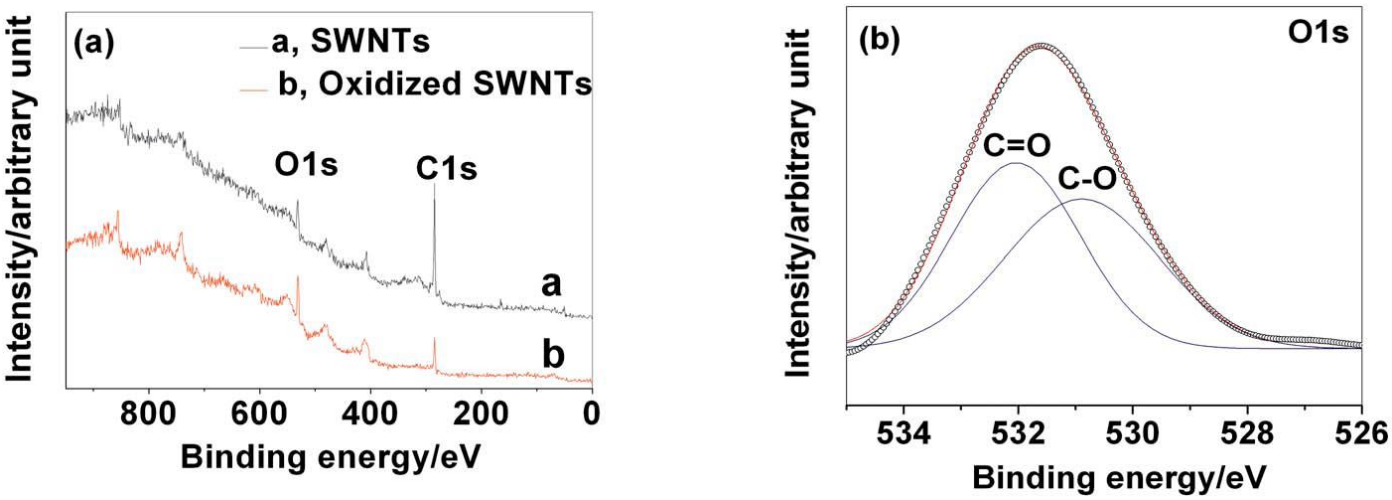

Figure 5.3: XPS survey scan of as-prepared and electrochemically oxidized SWNTs (a). O 1*s* peaks of electrochemically oxidized SWNTs (b).

Table-5.1: Elemental composition of as-prepared and electrochemically oxidized SWNT

SWNTs	C 1*s*, at. %	O 1*s*, at. %	O/C ration, %
Nonoxidized	87.2	12.8	14.7
Oxidized	58.5	41.5	70.9

Elemental composition of as-prepared and electrochemically oxidized SWNT surfaces detected by XPS.

Not only own good frequency response of the electrochemically oxidized SWNT supercapacitors makes it suitable for the application of strict frequency demand but also high specific capacitance for the introduction of nanosized mesopores and oxygen-containing groups. The effect of electrochemical oxidation on the capacitance of SWNT capacitors is shown in Figure 5.4(a). The specific capacitance was measured in galvanostatic experiments

using an Arbin BT-2000 system with the discharge current density of 50mA⁄g. The capacitance was obtained from the formula $C=(I\times\Delta t)/\Delta v$, where I is the constant discharging current, Δt is the discharging time measured from 0.6to0.4V (60%–40% of the peak voltage), and Δv is the voltage change at a constant current discharge. From the discharge curves in Figure 5.4(a), the specific capacitance of 113F⁄g was obtained for the electrochemically oxidized SWNT supercapacitor only compared to 20F⁄g for the as-prepared SWNT supercapacitor. Figure 5.4(b) shows the cycling performance of the electrochemically oxidized and the as-prepared SWNT supercapacitor. Both capacitors have good cycling performance and almost no capacitance decrease was observed after 300cycles

.

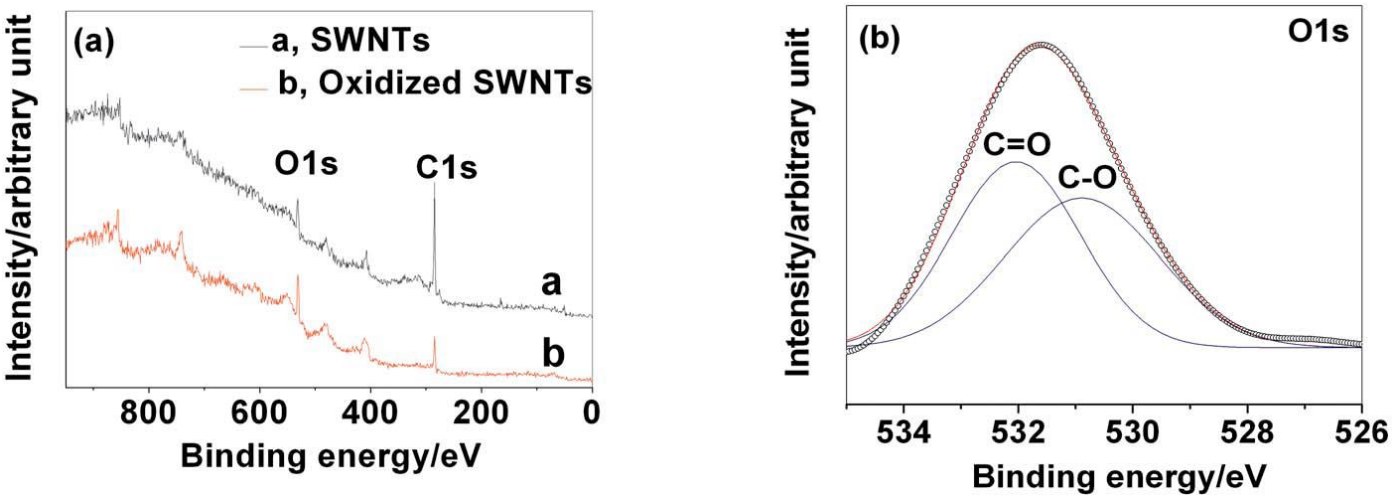

Figure 5.4: Galvanostatic discharge curves (a) and cycling performance (b) of a single cell supercapacitor fabricated with the as-prepared and electrochemically oxidized SWNTs.

Impedance analysis is employed in case of frequency response characteristics of supercapacitors utilizing SWNTs as an electrode material. It is found that the knee frequency is around 631Hz for the electrochemically oxidized SWNT supercapacitor, much higher than those of the as-prepared one (around 316Hz) and the common activated carbon supercapacitor (<1Hz). The good frequency response performance is due to the introduction of nanosized mesopores and oxygen-containing groups. The former serves as effective channels for electrolytes in the charge/discharge process and the latter can improve the wettability of SWNT electrode to maximize the access of the electrolyte to the SWNT surface. Moreover, the electrochemically oxidized SWNT supercapacitor has a specific capacitance of 113F⁄g, which is much higher than the specific capacitance (20F⁄g) of the as-prepared SWNT. From the results, it is expected that the electrochemically oxidized SWNTs will be good electrode material in supercapacitor application.

Chapter 6

EFFECTS OF AGING

Due to the decomposition voltage of the organic electrolyte of approximately 3 V, the maximum cell voltage of supercapacitors is limited. To obtain higher voltages, a series connection of supercapacitor cells is necessary to form a supercapacitor module. Caused by the statistical distribution of manufacturing tolerances of individual cell parameters, such as capacitance, internal resistance and self-discharge rate, the individual cell voltages will differ from each other. As described in the next section, this will affect performance and lifetime of the supercapacitors, which will be analyzed in detail in this paper.

6.1 AGING MECHANISM

Supercapacitors are capable of undergoing several hundreds of thousands of deep discharge and charge cycles, because no chemical reaction takes place at the electrodes. Hence, in contrast to electrochemical batteries, the life expectancy of supercapacitors in most industrial applications is not limited by cycling stress. Instead, the aging processes of supercapacitors are mostly driven by temperature and cell voltage, which have an influence on the calendar life of the devices.

At increased temperature, the aging processes are accelerated by the higher reactivity of the chemical components. Furthermore, at higher voltages more impurities undergo a redox reaction and the decomposition of the electrolyte is accelerated.[82] These effects lead to an increase of internal series resistance and self-discharge rate and to a decrease of the capacitance over time. Thus, the performance of the supercapacitor diminishes. If the capacitance of a supercapacitor falls below 80% of the initial value, or if the value of the internal resistance or the self-discharge rate increases by the factor two, it is defined as defective. Figure 1 illustrates the life expectancy as a function of cell voltage and cell temperature.

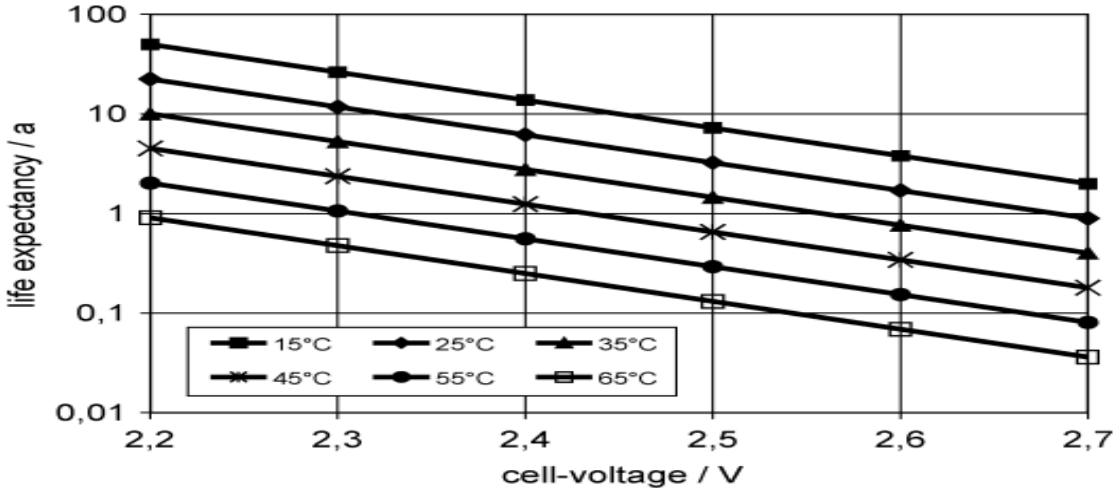

Figure 6.1: Life expectancy of a supercapacitor cell versus operating voltage and temperature. Top curve shows life expectancy at 15º C, and bottom curve is at 65º C.

In this paper, only the effect of cell voltage on life expectancy is analyzed. An analysis of the temperature influence would require an adequate thermal model of the entire supercapacitor system, which depends on the cooling and the packaging of the system. Both strongly depend on the specific application.

Hence, an average temperature of 25C is assumed for all simulations. It is important to know that an increase of the temperature of 10 C causes a reduction of the life expectancy by approximately a factor of two.

The cell voltage of supercapacitors depends on various factors, such as the application-specific current profile, the cell capacitance, the manufacturing tolerance of capacitance and self-discharge rate, the number of cells connected in series, and the voltage equalization electronics. Looking at real supercapacitor systems, the statistical distribution of the capacitance and the self-discharge rate lead to an unequal voltage distribution and, thus, to different life expectancies of the cells, which diminishes the reliability of the entire system.

6.1.1 LIFE EXPECTANCY

As mentioned in the previous section, cycling has a negligible effect on the aging process as opposed to operating voltage and temperature. Starting from Figure 1, it can be seen that life expectancy T_{exp} is a function of voltage and temperature. The relationship between life expectancy, voltage, and temperature can be described by an exponential function as given in (1)

$$T_{exp}(U,\vartheta)=c_1.e^{(\frac{U}{c2}+\frac{\vartheta}{c3})} \qquad (1)$$

Where U and ϑ are the cell voltage and the cell temperature, respectively. The constant parameters c_1-c_2 are derived from the relationship given in Figure 1 and have negative values. The average life expectancy T_{av} of a dynamic voltage profile can be calculated due to an accumulated wear of the supercapacitor, given by (2), where $u(t)$ is the dynamic voltage profile and t_0 and t_1 are the starting and end times, respectively

$$T_{av}(u(t),\vartheta) = \frac{t_1-t_0}{\int_{t_0}^{t_1}\frac{1}{T_{\exp(u(t),\vartheta)}}dt} \qquad (2)$$

6.1.2 CHARGE BALANCING CIRCUIT

Looking at real modules, series connections of supercapacitor cells lead to unequal voltage distributions because of the capacitance manufacturing tolerances and differences in self-discharge rates. For current in-production cells, the spread of capacitance and discharge rate is up to ±20% around the nominal values[83 84 85]. To guarantee an adequate life expectancy of the module, differences in cell voltages caused by the statistical distribution of the individual parameters have to be minimized by cell equalization circuits. Different equalization concepts are known from literature, with varying cost and packaging implications.[86] Figure 6.2 gives an overview.

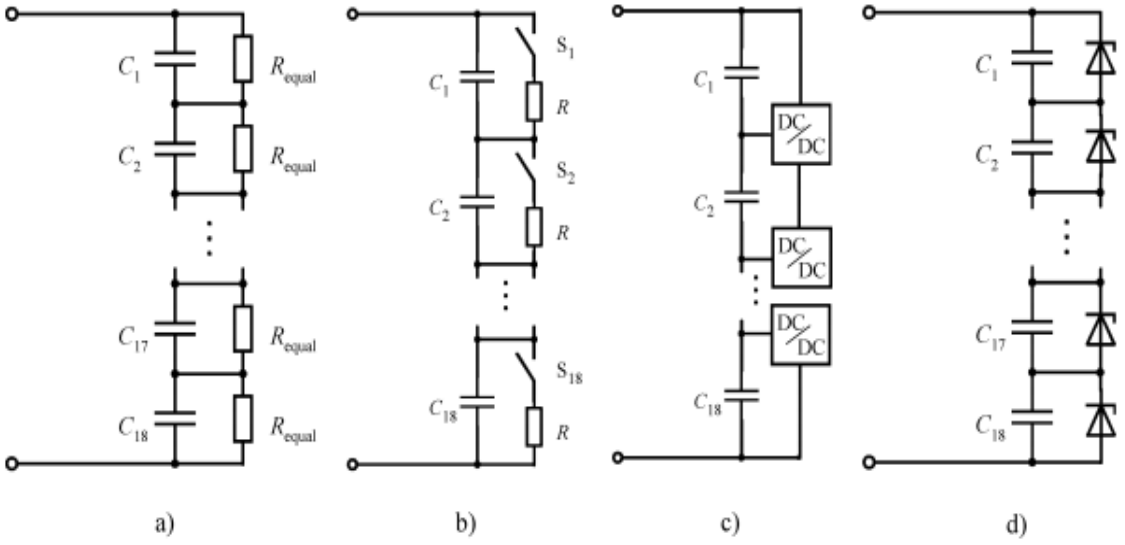

Figure 6.2: Cell equalization circuits. (a) Resistor. (b) Switched resistor. (c) DC/DC converter. (d) Zener diodes.

Passive Resistors

As simplest solution, a passive resistor across each capacitor cell is employed. This results in a higher effective “self-discharge” rate. The differences of the individual cell voltages become smaller when the module is at rest. The most important disadvantage of this solution is the high power loss which occurs in the external resistors. These losses reduce the efficiency of the module, depending on the value of the external resistor and the applied current profile.

Switched Resistors

Another concept utilizes actively switched resistors in parallel to each cell.[87] The switch is turned on when the cell voltage is higher than a pre-defined upper voltage level and is turned off when the cell voltage is below a lower voltage level. While the switch is on, the resistor operates as a bypass for the main current. This concept requires each cell voltage to be measured and this means additional costs, compared to the previous solution.

DC/DC Converters

A third concept consists of several dc/dc converters, each connected across two neighboring cells. This concept is called active charge equalization.[88] These converters actively equalize the cell voltages. Apart from the power losses of the converter, no additional losses appear. This results in a higher efficiency compared to the concepts mentioned above. Although the efficiency is high, this concept is not attractive, because the implementation of the hardware and its control is very costly. Hence, this equalization concept is not investigated further in this paper.

Zener Diodes

Another concept to equalize the cell voltage is the use of Zener diodes in parallel to the cells.[89] The cell voltage is held constant as soon as the Zener voltage is reached. The diode operates as a bypass for the main current. The most important disadvantages of this solution are the high power losses in the diode and a strong temperature dependency of the Zener voltage itself, which is not tolerable for most applications.

Chapter 7

FLEXIBLE SOLID-STATE SUPERCAPACITOR

7.1 FLEXIBLE SOLID-STATE CAPACITOR

The Use of microelectronic devices is increasing day by day. It needs portable power supplies. Possible candidates for micro energy storage devices are Li-ion batteries and supercapacitors. Among them, the flexible solid-state supercapacitors combined with exceptionally long cycle life, high power density, environmental friendliness, safety flexibility and stability, afford a very promising option for energy storage applications. The electrolyte and various electrode materials that are suitable for flexible solid-state supercapacitors are discussed in this chapter.

7.1.1 ELECTROLYTES

Electrolytes for solid-state SC can be classified into different types.

Aqueous Polymeric Gels

The first type is aqueous polymeric gels.[90] Polyvinyl alcohol (PVA)/ H_3PO_4 proton conducting polymer blend was made as a pioneer and the ionic conductivity could reach at 2.2×10^{-5} S/cm.[91] Since then many types of gel electrolytes have been explored to satisfy the specific condition, for instance, PVA/H_2SO_4,[92] PVA/KOH,[93] polyethyleneoxide (PEO)/$LiClO_4$,[94] poly(methylmethacrylate) (PMMA)/ /$LiClO_4$, polybenzimidazole/H_3PO_4,[95] PVA/Na_2SO_4-silica,[96] PVA/$NaNO_3$,[97] PVA/LiCl,[98] and so on. Generally, the neutral electrolytes like PVA/LiCl have a wider range of applications in pseudocapacitors, especially for metal oxides based SCs (ZnO,[99] V_2O_5, etc.).

Another example is Nafion, a typical perfluoroalkylsulfonate-based ionomer. Nafion can not only be used as membrane, but also as effective ionomer.[100] [101] [102] An all-solid-state flexible SC prepared through the assembly of Nafion-functionalized reduced graphene oxide (rGO) thin films and solvent-cast Nafion electrolyte membranes showed a 2-fold higher specific capacitance and rate capability compared to those of all-solid-state grapheme SCs.[103]

Non-Aqueous Polymeric Gels

The second type of electrolytes is non-aqueous polymeric gels.[104] They consist of either plasticized polymer complexes with electrolytic salts or polar polymer matrices swollen with organic electrolyte solutions, and have been many combinations of polymer–salt–liquid systems so far proposed as the gel electrolytes of SCs. As an example, a polymeric gel electrolyte composed of PEO-modified PMMA swollen with propylene carbonate (PC) that dissolves tetraethylammonium tetrafluoroborate ($TEABF_4$) is successfully applied in an all-solid-state EDLC system.[105] Because the organic solvents such as acetonitrile or PC can operate under much higher potential windows, the cell voltage can reach 2.7–3.7 V.[106] According to Eq. (14), the energy density of SC device will be greatly increased.

Inorganic Solid Materials

The third type is mainly inorganic solid materials. A $Li_{2.94}PO_{2.37}N_{0.75}$ (Lipon) electrolyte film can be applied between ruthenium oxide electrodes.[107] An all-solid-state thin film SC is fabricated with tungsten co-sputtered ruthenium oxide electrodes and Lipon electrolyte.[108] The effective reaction of the solid-state SC can be presented by RuO_2+xLi^+ (from the Lipon) + xe^- $\leftrightarrow Li_xRuO_2$.

The room-temperature charge–discharge behavior of the thin film SC is similar to that of a bulk-type SC. If the SC is fabricated on flexible substrate, an excellent device with flexibility and durability SC device will be realized. Other inorganic electrolytes such as phosphotungstic acid/$Al_2(SO_4)_3.18H_2O$,[109] and Li_2S-P_2S_5[110] have wide application in solid-state SC systems as well. In addition, the solid-state electrolytes for LIB can work as useful reference, which promote the research of solid-state electrolytes in SC systems.[111]

It is discovered that ionic conductivity of the electrolyte is improved when added mediators. For example, a quasi-solid-state SC is assembled by using PVA/KOH–KI as gel electrolyte and activated carbons electrodes.[112] The introduction of KI increases the ionic conductivity of electrolyte, and improves the pseudo-capacitance of the electrode, increasing by 74.28% compared to the PVA/KOH system at the same current density.

7.1.2 ELECTRODE MATERIALS

Carbon Materials

High surface area carbon materials mainly include activated carbon,[113] [114] porous carbon,[115] carbide-derived carbon,[116] onion-like carbon,[117] carbon aerogels,[118] carbon nanotubes (CNTs),[119] carbon shell,[120] graphene ,[121] and graphene quantum dots.[122] CNT, especially the single walled carbon nanotube (SWCNT), has intrinsically excellent properties as active materials such as high SSA, high conductivity, high flexibility, regular pore structures, and electrochemical stability. Woong et al. fabricated all-solid-state flexible SCs using CNTs, regular office papers, and ionic-liquid-based silica gel electrolyte.[123] Kaempgen et al. designed a kind of flexible electrodes made by coating CNTs on office papers by a drop-dry method .[124]

The maximum power and energy density of the SCs is 164 kW/kg and 41 Wh/kg, respectively. SWCNT network film printed on the flexible plastic substrate (polyethylene terephthalate, PET) is demonstrated as an easy fabrication SC that showed very high energy and power densities. The SWCNTs formed an entangled random network on the PET (Figure 7.1: (a)). The SWCNT networks and the gel electrolyte are sandwiched together constructing an SC device (Figure 7.1:(b)). CV and charge–discharge curves showed good electrochemical stability and capacitance in the SWCNT networks (Figure 7.1: (c),(d)).

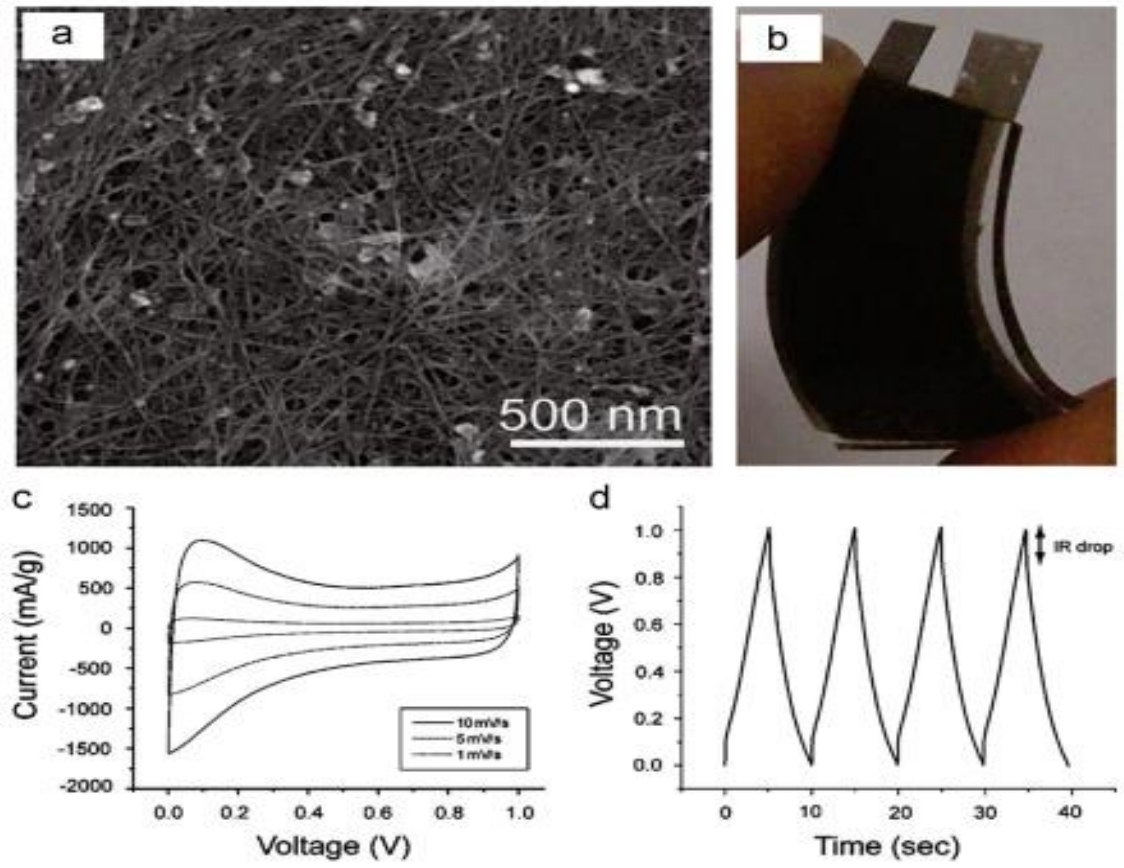

Figure 7.1: (a) Scanning electron microscopy (SEM) image of as-deposited SWCNT networks. (b) Thin film SC using sprayed SWCNT films on PET as electrodes and a PVA/H_3PO_4 based polymer electrolyte as electrolyte. (c) CV curves and (d) galvanostatic charge–discharge curve measured with a current density of 1 mA/cm^2 (30 mA/mg) of an SWCNT SC device.

Graphene-based materials are attractive because of their excellent mechanical and electrical properties as well as exceptionally high surface area.[125] [126] Recently, the intrinsic capacitance of single-layer graphene is reported to be 21μF/cm^2,[127] this value now sets the upper limit for EDLC capacitance for all carbon-based materials.

A direct laser reduces the graphite oxide (GO) to laser-scribed graphene (LSG) films, which are mechanically robust, show high electrical conductivity (1738 S/m) and high specific surface area (1520 m^2/g).[128] In order to evaluate the performance of the all-solid-state LSG-SC for flexible energy storage, a device placed under different bending conditions is shown in Figure 7.2(a). These SCs can be bent arbitrarily without degrading performance.

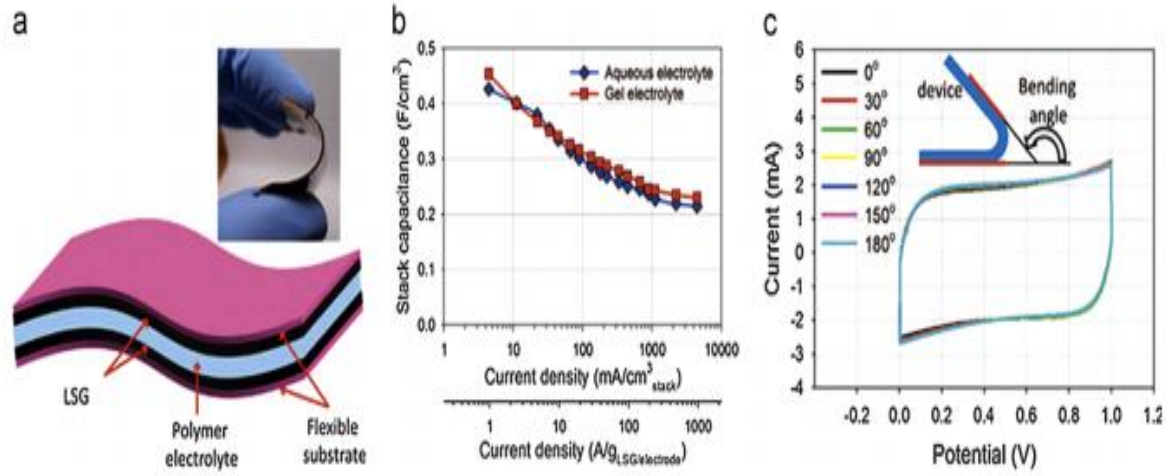

Figure 7.2: (a) A schematic diagram of the all-solid-state LSG-SC. Inset is a digital photograph showing the flexibility of the device. (b) A comparison between performances of LSG-SC using gelled versus aqueous electrolytes. (c) Bending the device has almost no effect on its performance, as seen in these CVs collected at a scan rate of 1000 mV/s.

Modification or composite of graphene and other capacitive materials may be a good approach into the rational designed fabrication of all-solid-state flexible SCs based on graphene materials. Graphene aerogels (GAs) represent a new class of ultra-light and porous carbon materials that are associated with high surface-area-to-volume ratios. A simplified prototype device of high-performance all-solid-state SC based on three dimensional nitrogen and boron co-doped monolithic graphene aerogels is achieved with using PVA/H_2SO_4 gel electrolyte.[129]

The fabricated device exhibited not only minimized thickness, but also showed high specific capacitance (≈62 F/g), good rate capability, enhanced energy density (≈8.65 Wh/kg) and power density (≈1.6 kW/kg). Three dimensional graphene exhibits exceptional electrical conductivity and mechanical robustness, making it an excellent material for flexible energy storage devices. Xu et al. reported with a 120μm thick graphene hydrogel thin film flexible SC exhibited excellent capacitive characteristics, including a high specific capacitance of 186 F/g, an unprecedented areal specific capacitance of 372 mF/cm^2, low leakage current (10.6μA), excellent cycling stability, and extraordinary mechanical flexibility.[130]

Porous graphene (PG) on carbon cloth via an electrophoretic deposition process is used as electrodes for flexible all-solid-state SCs.[131] The macroscopic porous morphology of carbon cloth is favorable for the ion diffusion and electron transport. The excellent mechanical stability and flexibility of PG on carbon cloth ensure the device with good flexibility. The resultant flexible SCs showed high specific capacitance, good cycling stability, and enhanced energy density and power density (1.64 Wh/kg and 0.67 kW/kg). Another type of carbon, exfoliated graphite (EG), is proposed as an electrode material for solid-state electrochemical capacitors.[132]

The EG-based capacitors assembled with a solid electrolyte show high areal capacitance in the range of 0.74–0.98 mF/cm^2

Metal/Metal Oxides Composite Electrode

The combination of graphene and conductive polymers, a rather unique method of preparing MnO_2-coated graphene fiber is carried out using the direct electrochemical deposition of MnO_2 onto a grapheme fiber network.[133] The 3D nanostructure of graphene that served as highly conductive backbones with high surface area is further enhanced with the deposition of nanoflowers (Figure 7.3). Therefore, the overall network possessed exceptionally large surface area that facilitated electrolyte ions with high accessibility. A flexible solid-state device is then fabricated by intertwining two MnO_2/G/GF electrodes separated by a PVA/H_2SO_4 polymer gel electrolyte.

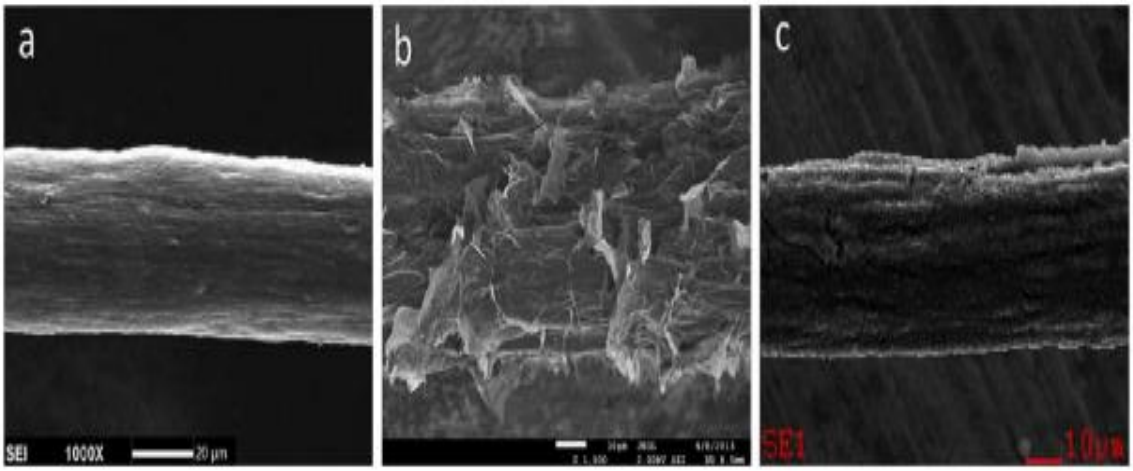

Figure 7.3: (a) SEM images of grapheme fiber (GF), (b) G/GF, and (c) MnO_2/G/GF with MnO_2 deposition time of 40 min.

Besides acting as the separator, the coating of the gel electrolyte provided a supporting structure to allow the rapid bending and twisting of the fabricated device without suffering an undesirable short circuit of the two electrodes. Moreover, when deformation is applied to the fiber capacitor, the lack of interference is shown by the nearly rectangular shape of the CV, without any distortion, with similar results obtained in the galvanostatic charge/discharge analysis (Figure 7.4: (a),(b)).

Remarkably, the fabricated device retained a stable capacitance of approximately 70−73μF after 1000 cycles of the straightening-bending-straightening process, as shown in both the CV profiles and charge/discharge curves (Figure 7.4: (c),(d)). On the basis of the surface area, the

device showed a specific capacitance of 9.1 to 9.6 mF cm^{-2}; however, an asymmetric device fabricated utilizing MnO_2/G/GF as the positive electrode and G/GF as the negative electrode doesn't not show a promising specific capacitance value in either an acidic (PVA/H_2SO_4) or neutral electrolyte (PVA/NaCl), with values of 1.6 and 0.1 mF cm^{-2}, respectively.

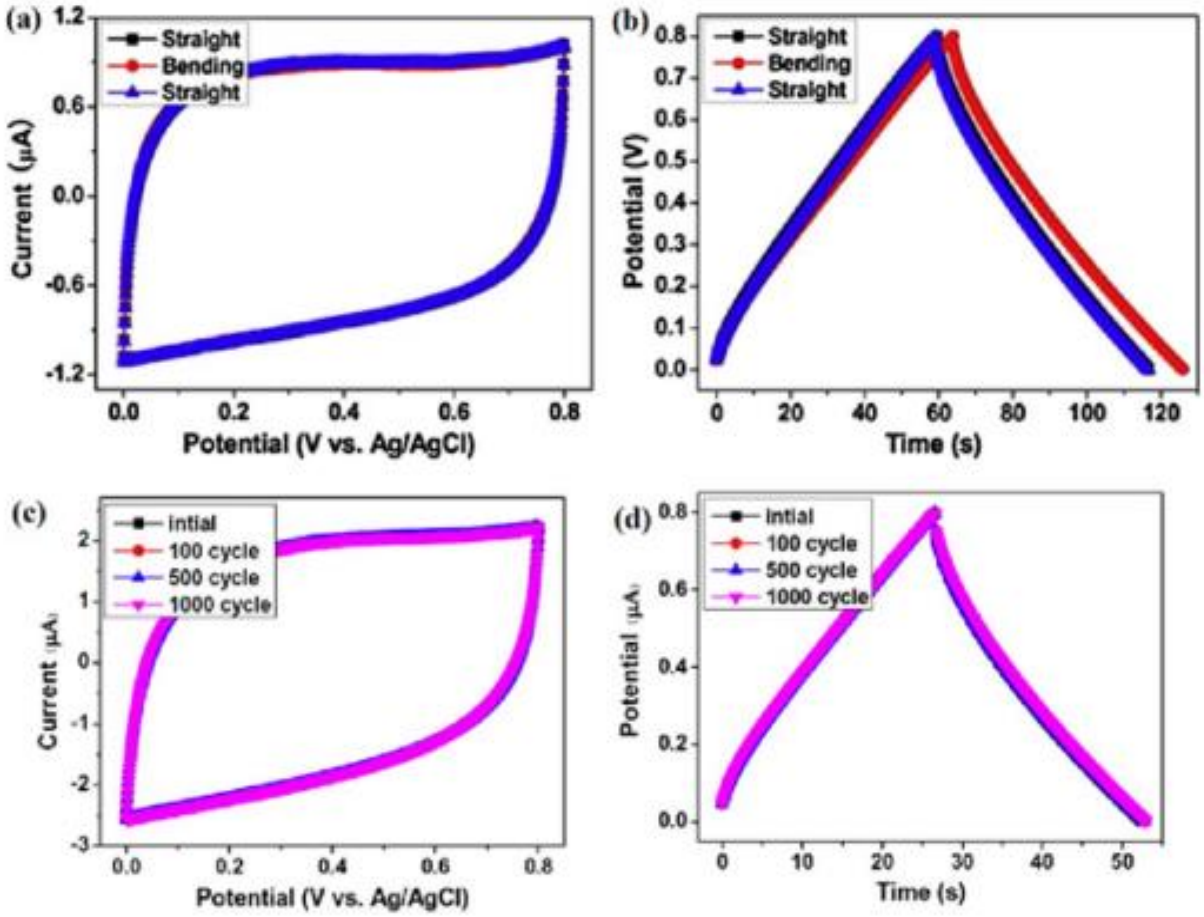

Figure 7.4: (a) CV at a scan rate of 10 mV$s^{-1}$and (b) charge/discharge curves of the fiber capacitor at a current of 1 mA, with an effective length of 0.5 cm under straight and bent conditions. (c) CV at a scan rate of 25 mVs^{-1} and (d) charge/discharge curves of 1.3 cm long MnO_2/G/GF fiber supercapacitor at 2 mA of applied current, with different straight/bending cycles.

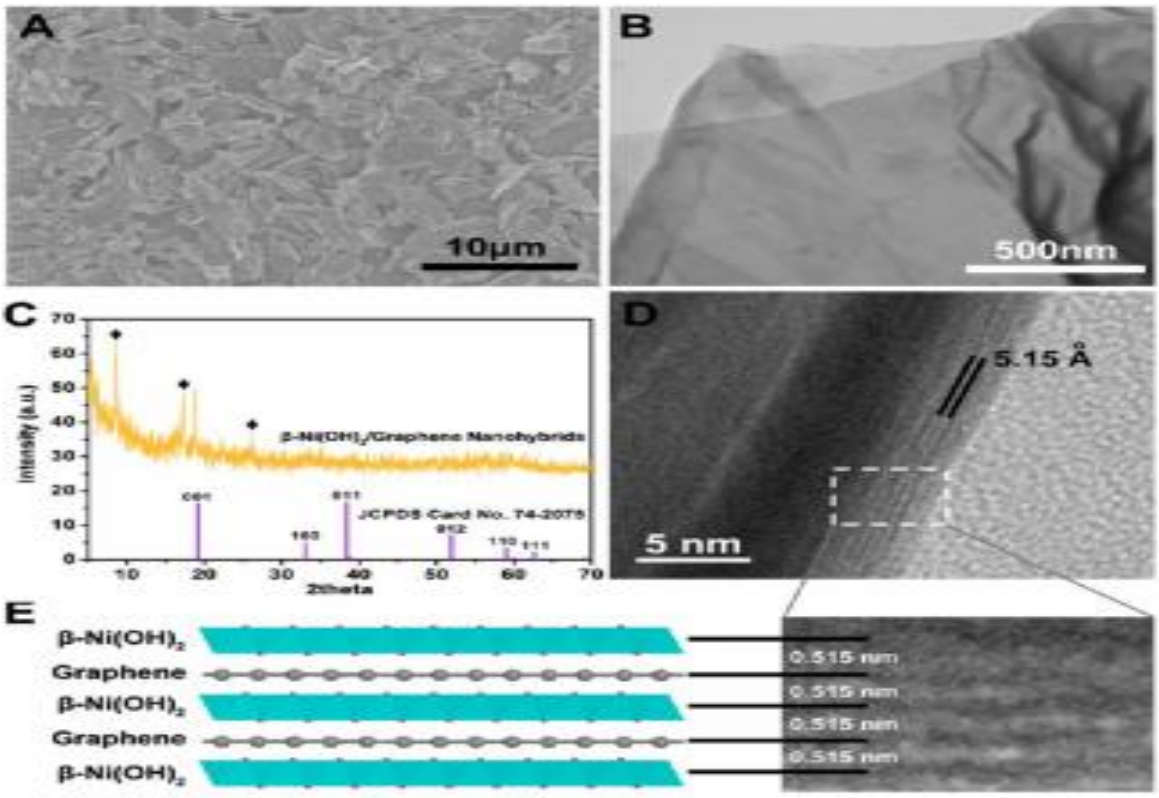

Figure 7.5: (A) Panoramic FE-SEM image of as-prepared b-$Ni(OH)_2$/ graphene nanohybrids. (B) TEM image of the as-prepared nanohybrids confirming the nanosheet morphology. (C) XRD pattern of the as-prepared b-$Ni(OH)_2$/graphene nanohybrids. (D) Cross-sectional HR-TEM image of the curled fringe of the nanohybrid sheet giving the interlayer spacing of 5.15 Å. (E) Enlarged view of the HR-TEM image and the structural model of the layer-by-layer nanohybrids.

Nanohybrid of β-$Ni(OH)_2$/ graphene is prepared via a solvothermal reaction, with a unique layer-by-layer characteristic structure obtained. The composite consists of nanosheet graphene morphology, with the scale of the sheets in the range of several micrometers (Figure 7.5(A),(B)). The unique structure is further confirmed by an XRD analysis, with a new series of peaks emerging with 2θ values of 8.61, 17.31, and 26.01°,which are equally spaced (0 0 L) reflections, indicating an ordered layer-by-layer stacking (Figure 7.5(C)).

In addition, the curled fringe of individual sheets showed parallel-aligned dark lines with a spacing of 5.15 Å (Figure 7.5:((D),(E)). An all solid-state flexible supercapacitor is fabricated by transferring the β-$Ni(OH)_2$/graphene film to a gold-coated PET substrate, followed by covering the surface of the working electrode with the PVA/KOH polymer electrolyte and then laying another identical electrode on the top. Very distinctive redox current peaks are recorded

on the CV curves over the potential of −0.6 to 0.6 V, regardless of the scan rates applied (see Figure 7.6: (a)), corresponding to the reversible pseudocapacitive reaction of $Ni(OH)_2$, as shown in eq 8.

$$Ni(OH)_2 + OH^- \rightleftharpoons NiOOH + H_2O + e^-$$

The fabricated device has a specific capacitance of up to 3304 μF $cm^{-2}2$ calculated from the discharge slope at a current density of 0.1 Am^{-2}. Increasing the current density by ten times resulted in a capacitance retention of 64.2% of its original value, 2120μF cm^{-2}. Furthermore, the measured galvanostatic charge/discharge curve for the bending configuration doesn't change obviously compared with the extending configuration, which showed a remarkable flexibility performance. The continuous bending/extending of the fabricated device does not degrade the overall electrochemical performance, even after 500 cycles (Figure 7.6: (b),(c)).

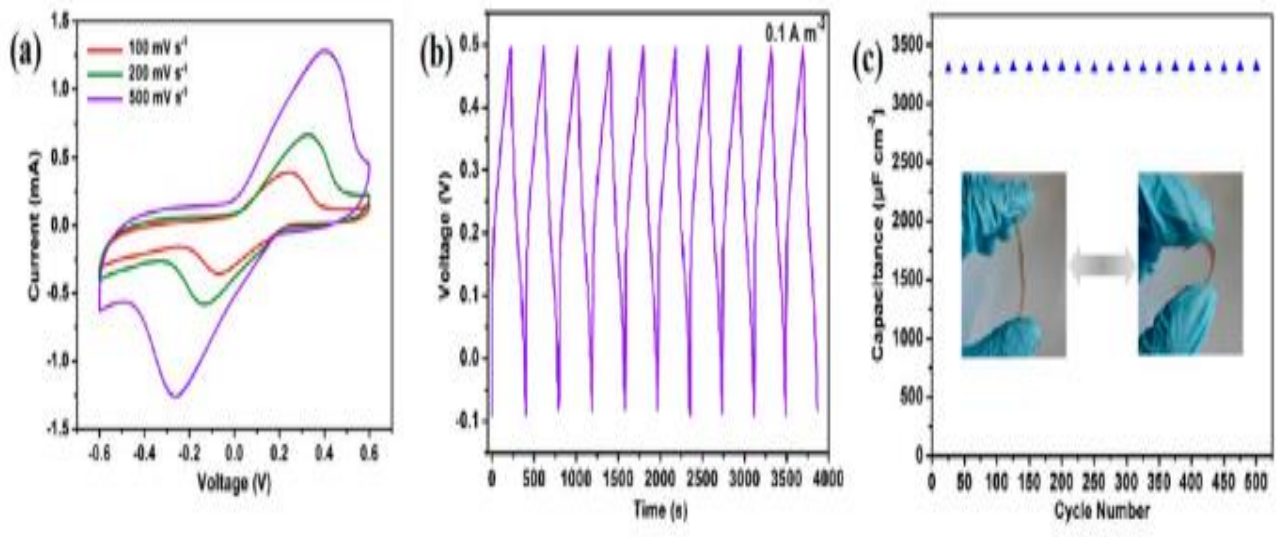

Figure 7.6: (a) CV curves of ASSTFS measured at different scan rates of 100, 200, and 500 mVs^{-1} (b) Galvanostatic charge/discharge curve of the ultra-flexible ASSTFS measured under bending configuration. (c) Cycling stability of the ultra-flexible ASSTFS measured after repeated bending/extending deformation.

While some active materials do not possess excellent conductivities for direct application as current collectors, a flexible substrate such as nickel foam has often been utilized both as a flexible framework and the current collector itself. For example, a graphene-based flexible electrode coated with MnO_2 is fabricated on a mechanically pressed nickel foam.[134] A uniform graphene layer is initially deposited on the nickel surface via the atmospheric pressure CVD method. A foam-like graphene structure (thickness <200μm) is then obtained after the removal of the nickel foam, which is further electro-deposited with MnO_2. A flexible supercapacitor is

fabricated using two graphene/MnO_2 composite electrodes with 0.4 mg/cm^2 each, separated by a polymer separator (Figure 7.7: (a)). The as-prepared device is lightweight (<10 mg), thin (~0.8 mm), and has high mechanical flexibility. It shows a rectangular CV curve, even at a high scan rate of 1000 mVs^{-1}. Furthermore, the CV curve at 10 mVs^{-1} is retained even upon bending the flexible device, which significantly demonstrated the flexible properties of the prepared electrodes (see Figure 7.7: (b)). The device possessed a low series resistance at 6.4 ohm (Figure 7.7: (c)), with energy and power densities of 6.8 Wh $Kg^{-1}$and 62 W $Kg^{-1}$for a 1 V potential. Only a minor drop in specific capacitance was detected after 500 charge/discharge cycles, with the Coulombic efficiency remained at 93%. Interestingly, the supercapacitor was able to retain 92% of its initial capacitance even, after 200 times of bending cycles at a constant bending angle of 90°(Figure 7.7d).

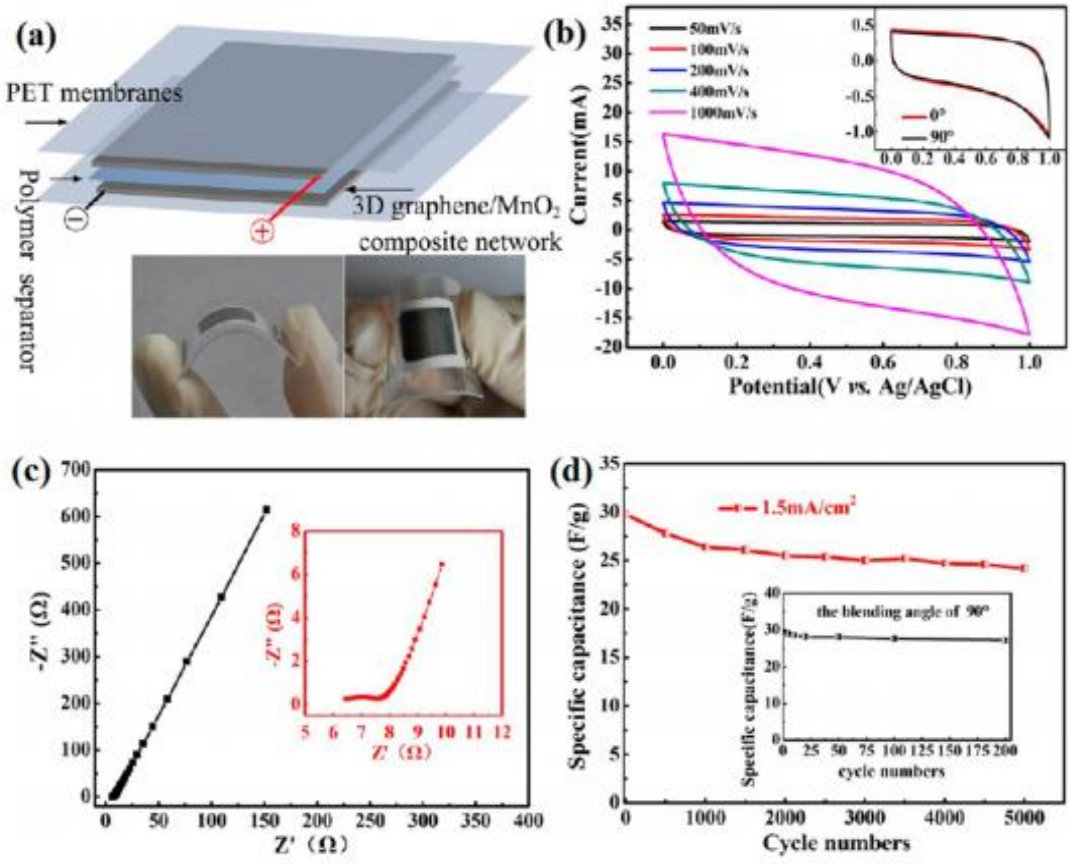

Figure 7.7: (a) Schematic of structure of the flexible supercapacitors. The two digital photographs show the flexible supercapacitors when bent. (b) CVs of the flexible supercapacitors at various scan rates. Inset shows the CVs of the flexible supercapacitors with bending angles of 0 and 90°at a fixed scan rate of 10 mVs^{-1}. (c) Nyquist plot of the flexible supercapacitor. (d) Cycling performance of the flexible supercapacitors. Inset shows the cycling performance of the flexible supercapacitors for bending cycles with a bending angle of 90°.

Another attempt at fabricating an MnO_2-rGO nanocomposite on a flexible carbon fiber paper (CNP) was reported in the literature.[135] rGO nanosheets were prepared using a commonly

applied chemical reduction method, whereby MnO_2 nanoparticles were produced via ethylene-glycol-assisted synthesis, followed by hydrolysis and condensation reactions.[136] The rGO and MnO_2 produced were premixed in an ethylene glycol solution, stirred, and coated on the CNP using a simple spraycoating technique. A flexible supercapacitor was fabricated by having the MnO_2-rGO/CFP act as symmetrical electrodes, sandwiching $NaNO_3$/PVA, which acted as the polymer gel electrolyte and separator itself; however, the electrochemical performance of the fabricated device was not determined. As shown in the TEM images, the MnO_2-rGO composite was composed of tiny MnO_2 nanoparticles sitting on an rGO surface (Figure 7.8: (a)) with high porosity among the adjacent MnO_2-rGO nanosheets, which were coated on CFP, as depicted in Figure 7.8: (b).

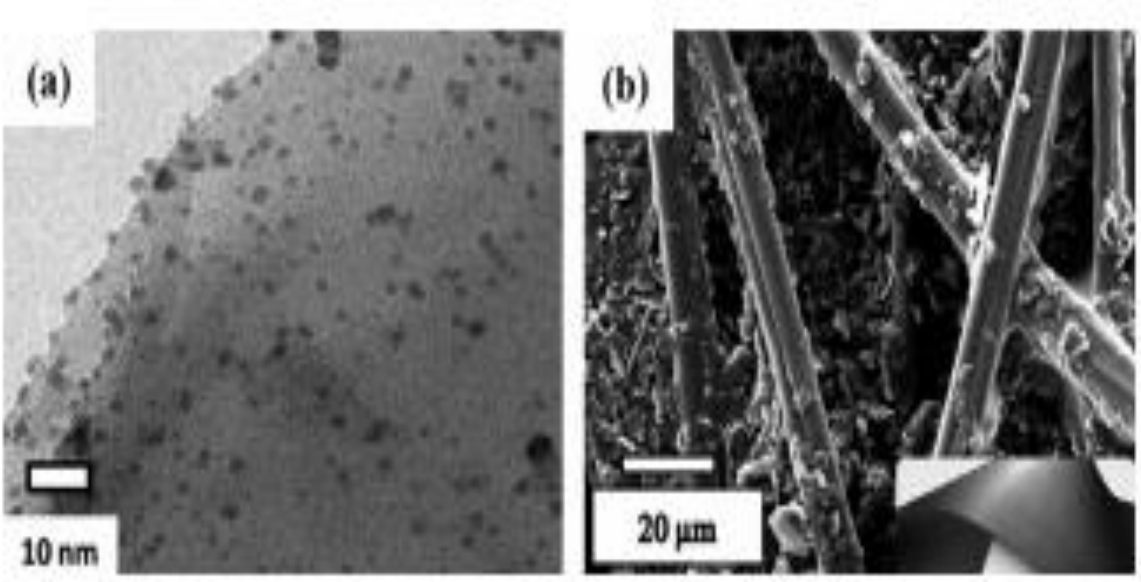

Figure 7.8: TEM images of (a) MnO_2-rGO nanocomposite and (b) low magnification SEM image of MnO_2-rGO coated on CFP.

The electrochemical performance of the electrode material was tested in 0.5 M Na_2SO_4 electrolyte at a potential of 0 to 1 V versus an Ag/AgCl electrode, and the MnO_2-rGO electrode showed a box-shaped CV curve at a scan rate of 10 mVs^{-1}, indicating excellent capacitive behavior supported by a very high specific capacitance of 393 F g−1based on the discharge curve at a current density of 0.1 Ag^{-1}. The excellent capacitance performance was attributed to the combination of large surface area provided by the MnO_2 particles, along with the high conductivity of the rGO nanosheets.[137] The high conductivity of the MnO_2-rGO electrode was further confirmed by a low polarization resistance ($\sim 2\Omega cm^{-2}$) as evaluated via an EIS measurement. The performance of the solid-state as-fabricated supercapacitor was demonstrated by its ability to spin up a 3 V motor; however, no flexibility demonstration was conducted to fully describe its bent capability.

7.1.3 SYNTHESIS APPROACH FOR ELECTRODE MATERIALS

Electro-Polymerization/Electrodeposition

The electrodeposition technique is one of the most common techniques for the preparation of supercapacitor electrode materials. This facile and straightforward synthesis technique provides precise control of the thickness of the resulting films as well as the rate of the polymerization, which could be easily controlled by the current density applied. Therefore, this technique involves only mild processing conditions at room temperature without toxic or excess chemicals being used throughout the process. This method is usually utilized in the synthesis of common conductive polymers, including PANI, PPy, PEDOT, and polyacetylene; however, these conductive polymers have the same limitation of poor mechanical strength, which results in low and limited cycle stability.[138 139]

Numerous modifications to the synthesis method and prepared materials have been reported to overcome this limitation including the introduction of EDLC based materials such as activated carbons, CNTs, and graphene, which have been reported to improve the specific capacitance and overall cycle stability performance. For instance, the fabrication of PANI nanowire with the addition of SWCNT resulted in a significant increase in the capacitive behavior of the modified electrode.[140] Recently, the modification trend focused on the utilization of graphene to enhance the conductivity of conductive polymers. Graphene is a one-layer-thick carbon planar sheet arranged in a hexagonal manner, which offers numerous advantages such as a superb conductivity, large area, and high capacity.[141]

In Situ Polymerization

In situ polymerization often refers to a common chemical polymerization technique that has been widely reported. In general, the polymerization technique involves a reaction in an aqueous solution, whereby the monomers usually disperse into an aqueous solution with the aid of a sonication process. A specific oxidizing agent is added to initiate the polymerization process within the solution, and the sample is obtained via a direct filtration technique. Previously, this specific method was reported to yield irregular granular aggregates with only small portions of nanofibers; however, with certain modifications, it was recently reported that nanostructures such as nanoparticles, nanorods, and nanofibers were obtained with improved solution process ability, along with better physical and chemical properties than their bulk counterparts.[142] In addition, improvements and modifications of this conventional method have also been reported elsewhere.[143 144]

Direct Coating

Direct coating is one of the most common techniques utilized in the fabrication of supercapacitor electrodes. Because the active materials are usually applied directly to the surface of the substrate itself, this method heavily relies on the physical adhesion of the electrode materials on the substrate. Often, additive or binder such as carbon black and polyvinylidinefluoride (PVDF) was used as an to provide maximum adhesion, while maintaining the electrical conductivity at the electrode material/substrate interface.[145] This was prepared in a slurry form and physically coated directly onto the substrate surface.

Chemical Vapor Deposition (CVD)

CVD is commonly applied when the porosity of the final product is very crucial. In the graphene synthesis approach, CVD is often described as being able to produce a defect-free graphene structure that possesses a highly conductive network for charge transfer, with the absence of inter sheet junction resistance in the continuous network;[146] however, this method usually requires a template or growth substrate to provide a surface for the attachment of the newly deposited graphene layers. As described by its name, the process is carried out under a vapor phase, whereby the starting material of graphene is initially prepared in vapor form, flowed, and subjected to a very high temperature (800−1000°C), along with the targeted substrate. The sample will therefore grow on the substrate with a very fine and even morphology.

Vacuum Filtration Technique

This fast yet efficient technique utilizes the simplest concept of vacuum filtration to obtain a nanocomposite from physical combination of different materials. In general, a mixture of graphene and other active materials is premixed, followed by a simple vacuum filtration process. The active materials undergo layer-by-layer stacking at the interface between the nanocomposite and the filter membrane by means of excessive water filtration toward the membrane itself.[147] After drying, the nanocomposite is ready to be detached from the filter membrane as a free-standing film. Therefore, the composition of the nanocomposite could be altered by simply adjusting the concentration or weight percentage of each component during the mixture preparation

Chapter 8

APPLICATION OF SUPERCAPACITOR

8.1 APPLICATIONS

Today small size supercapacitors as for example gold caps from Tokin are widely used as maintenance-free power sources for IC memories and microcomputers.[148] Among newly proposed applications for large size supercapacitors are load leveling in electric and hybrid vehicles as well as in the traction domain, the starting of engines, applications in the telecommunication and power quality and reliability requirements for uninterruptable power supply (UPS) installations. In general supercapacitors may be adapted to the following two application domains.

The first one corresponds to the high power applications, where the batteries have no representative access. The EDLCs, thanks to their high power capability, will allow new opportunities for power electronics. All applications where short time power peaks are required can be provided by these capacitors. Typical examples where a big current is required during a short time are the fast energy management in hybrid vehicles or the starting of heavy diesel engines.

The second one corresponds to the low power applications, where the batteries could be more suitable but are at the origin of maintenance problems or of insufficient lifetime performance. The supercapacitors, even if they are much bigger, bring enough advantages to substitute the batteries. In this field, the UPS as well as security installations are the most representative examples.

The ECDL capacitors may be used wherever high power delivery or electrical storage is required. The following examples give an overview over typical supercapacitor applications

8.1.1 MOBILE DEVICES

Some recent mobile phones have high quality xenon flash inbuilt into the phone to enable good photo quality when light is scarce. Xenon flash has traditionally been used on cameras, and consumes much power in an instant. Should the mobile phone have to cater to the power requirement, it would have added unnecessary bulk and weight to the battery, failing which would result in severely shortened battery life.

Some mobile manufacturers have incorporated a supercapacitor into the mobile phone to ease the temporary high power demand. In this application, the supercapacitor performs peak load shaving, as observed in Figure 8.1. It is shown that with peak load shaving, the battery current is suppressed at a maximum of 0.2A even though the camera flash current may be as high as 4A. Although the battery supplies the entire energy requirement, it does not see high power demand. The supercapacitor voltage experiences a significant fall as a result of supplying energy to the flash. As a result, the battery does not have to be large to cater to temporal high power demands.

Figure 8.1: Mobile phone with supercapacitor built-in

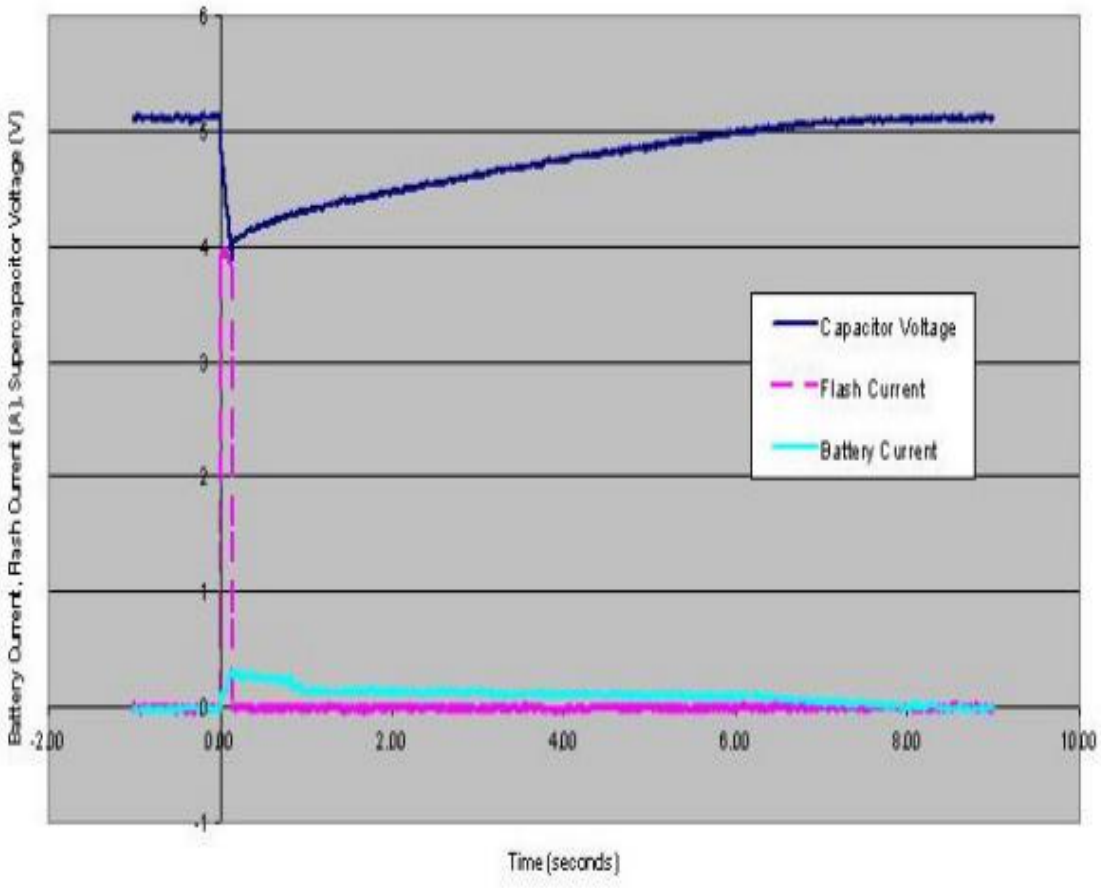

Figure 8.2: Supercapacitor peak load shaving in mobile phone camera flash

It has also been proven that using supercapacitor as a peak load shaving device can result in much better performance for camera flashes.[149] Therefore, using supercapacitor in mobile phones not only improve battery life but also camera performance. To achieve the peak load shaving operation as observed in Figure 8, it is necessary to incorporate a SMPS.

8.1.2 STARTER

Today the energy that is required to crank a small or big engine is stored in either Pb or NiCd batteries. Because of their high internal resistance, which limits the initial peak current, they have to be oversized. The fast battery discharging and the cold environmental temperature affect heavily their properties. The supercapacitors have a better power behavior and a better environmental acceptance.

8.1.3 MICRO GRID

The micro-grid is labeled as a possible next-generation energy network. It comprises of electrical power generation units as well as electrical energy storage components. Popular electrical power generator includes photovoltaic cell, wind turbine, fuel cell and micro turbine while commonly used electrical energy storage units would be the supercapacitor and battery. As the micro-grids can be inter connected to the power grid, it is able to supply or demand power from the power grid. At times, this configuration is known as the smart grid. The micro-grid has the capability of reducing carbon emission through green energy harnessing as well as having the potential of providing self-sustainable energy. Thus, it is regarded as a contender for the next generation energy network.[150]

Whilst electrical power can be generated by a combination of any generators, the electrical energy storage units can also comprise of a combination of any batteries or supercapacitors. The Battery Supercapacitor Hybrid Storage (BSHS) is a combination of battery and supercapacitor used in the micro-grid. Due to the higher energy density of the battery, it takes on the role of the main energy storage device while the supercapacitor performs the role of peak load shaving through a SMPS. The BSHS combination is greatly enhanced to handle temporal high power requirements during operation, such as a sudden spike in input power from the electrical power generators.[151]

8.1.4 UPS

The Uninterruptable Power Supplies (UPS) may find some economical interests by using the ECDL capacitors, thanks to the suppression of an inverter and to the suppression of the maintenance. The energy supply during a limited time, at a voltage much higher than that of batteries, is easier to perform with these capacitors.

8.1.5 TOY APPLICATIONS

Another domain are toy applications, where the total running time is typically not longer than 10 hours.[152] A supercapacitor designed for ten years or several 100'000 cycles is not optimized for such application, lower performance is thoroughly sufficient. For short terms the largest markets are for devices with <12 V and only around 2004 the market for devices with > 48 V will have grown to the same size and will give opportunities for the supercapacitor market

8.1.6 DATA STORAGE DEVICE

Supercapacitors opened up a new era of cache protection functionality. Data centers traditionally rely on UPS to cater power to data storage devices whilst the mains power is offline. However, UPS capacity is not only limited but also unable to sustain long periods of operation relying on the batteries alone. To overcome this issue, enterprise Redundant Array of Independent Disks (RAID) controllers contain a Lithium Ion battery which is aimed to sustain the operation of data storage devices for a period of up to 3 days.

Whilst this is a good solution, it presented several disadvantages. The first disadvantage is that the system will lose precious data after the battery ran out of charge. Additional disadvantage include periodic change of battery even though the battery may not have been utilized during the period. These incur additional costs and hassle in the long run.

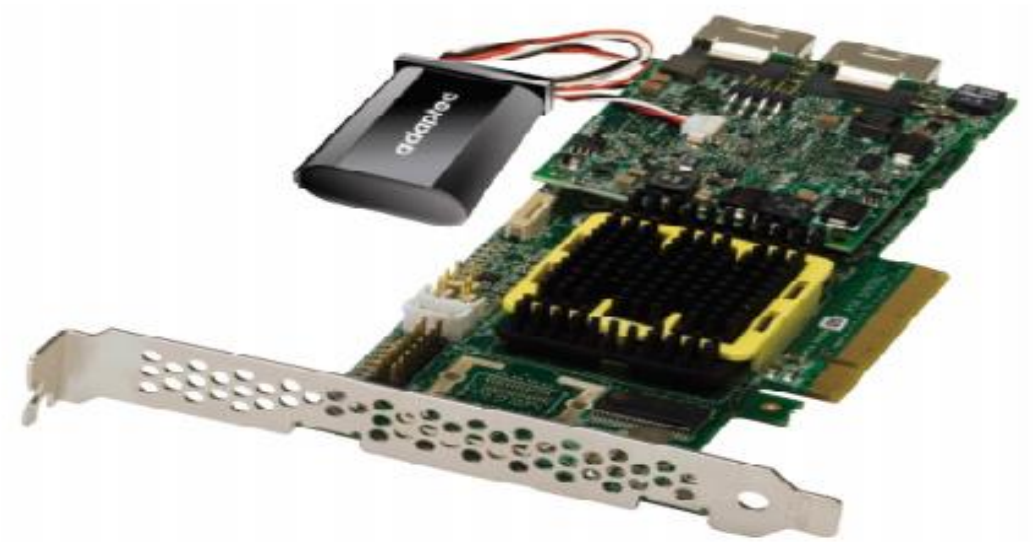

Figure 8.3: Adaptec 5Z RAID controller with supercapacitor

In recent years, major RAID controller companies have been seen ditching the Lithium Ion batteries for supercapacitors, mainly due to the maintenance-free nature of supercapacitor. Not only is it environmentally friendly, supercapacitors also eliminate the need to replace the Li-Ion battery periodically.[153] [154] [155] [156] Adaptec is amongst the earliest to implement the supercapacitor backup system, and calls it Zero-Maintenance Cache Protection (ZMCP).

Under this system, the supercapacitor energy storage kick in the moment mains power is lost to maintain data storage device operation. The data on cache and other volatile memory would be written to the embedded non-volatile flash memory for permanent storage. These operations

are accomplished in matters of seconds, during which they are being sustained by the supercapacitor.

When the mains power came back on again, the system would recover the cache and memory through the embedded flash memory, and resume operation.[157] The novelty of this system is that the data storage devices can resume original operations even though untouched for years. The system was touted Zero-Maintenance due to the fact that supercapacitors have virtually unlimited charge cycles and suffer little degeneration compared to chemical batteries.

8.1.7 HYBRID VEHICLE

Here supercapacitor is coupled with battery. Supercapacitor is used in series with a power battery to provide power requirement in transient state. An energy battery is placed in parallel to give power in steady state.

Fig 8.4: Hybrid vehicle

The objective of this project consists to associate an energy battery (with high capacity) in parallel of a supercapacitor module associated with a power battery (with low capacity) in series. The goal of this association is to reduce the starting current and the current when the vehicle accelerates into the energy battery (with high capacity), in order to guarantee the best lifecycle for the energy battery (with high capacity).

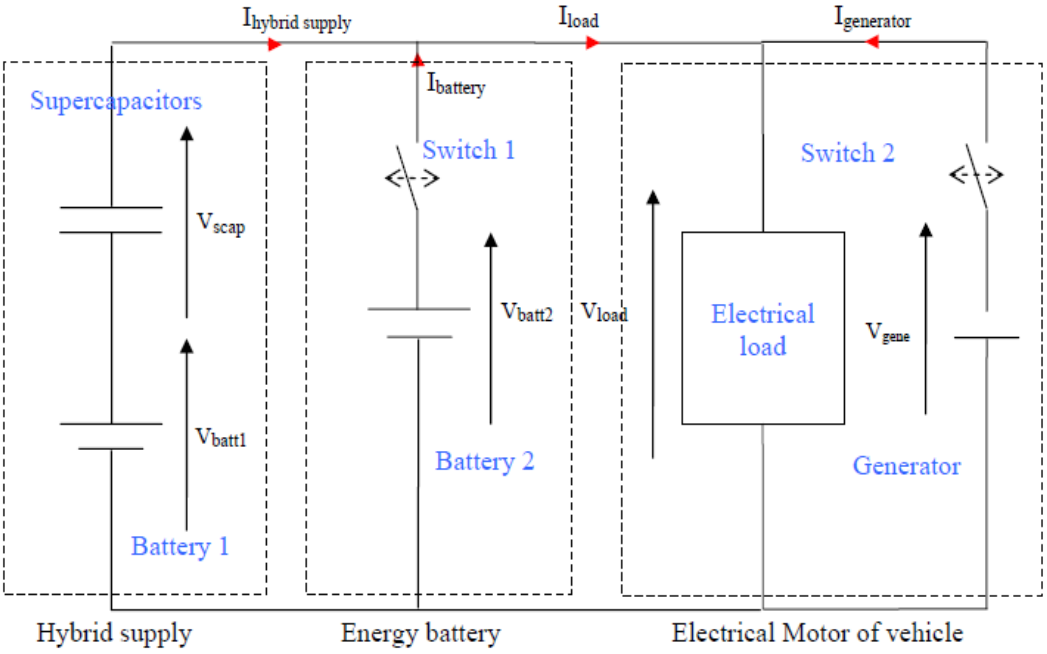

Figure 8.5: Experimental setup principle

Battery 1 will be selected with a capacity lower than that of battery 2 and the same than that of the supercapacitor module, this in order to guarantee better held in temperature (in particular in cold weather) and the best held with the variations of capacity according to ageing.
Battery 2 will be an energy battery with a strong capacity dimensioned either to provide the points of power, but dimensioned to supply the electric installation (headlight, air-conditioning, motor in steady operation). This new dimensioning will make possible to reduce the capacity of the battery, and so the price like the volume. However this battery must have a resistance higher than the resistance of the hybrid supply.
The supercapacitor module will be dimensioned to provide the high demand of power. Moreover supercapacitors will be able to limit the depth of discharge of the battery, and to inform us of his state of charge more or less precisely, according to the battery used (depend on the self-discharge, internal resistance, ageing). The supercapacitors will ensure the part of energy buffer at the time of braking phases, energy stored may be retransmitted quickly to the electrical load, or slowly to battery 2 if this one is not entirely charged. Finally the supercapacitors will be able to ensure the part of energy source, if the energy battery is failing.

The first results presented in figure 4 are obtained with the following configuration: Supercapacitor module (12V) is connected in series with a 12V battery. The used load is a motor-ventilator group for vehicle application. These results show that when the electrical motor starts supercapacitor module provides the requirement power in transient state. Hence, the battery current peak is very low compared with that of supercapacitors. In steady state, the

battery current rises and the supercapacitors current decreases. So, battery voltage and supercapacitors voltage are the same in the beginning. The battery current depends on the supercapcitors state of charge. It's clear that this association allows to reduce the battery peak power in transient regime. Consequently, this makes it possible to increase the lifetime of the battery and to improve the energy performances of the system.

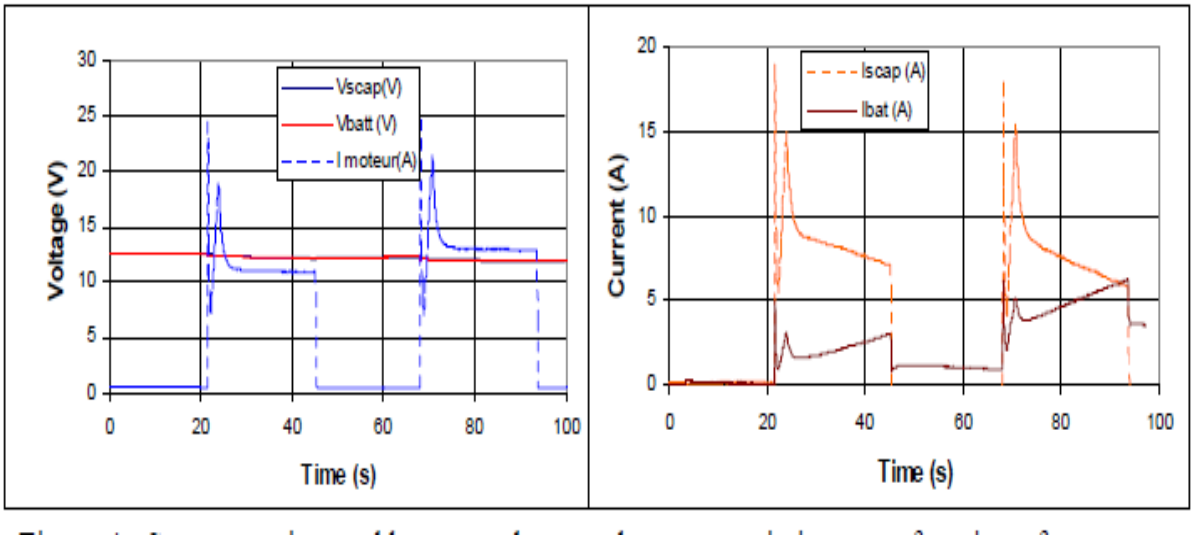

Figure 8.6: Supercapacitor and battery voltage and current variations as a function of time, the used load is a motor ventilator

The hybrid power source with batteries and supercapacitor for vehicle applications presented in this paper can be used to start the internal combustion engine, for stop & go application and for micro hybrid vehicle.

8.1.8 ELECTRIC LOCOMOTIVE

In modern time supercapacitors are used in electric locomotive.
CHINA: CSR Zhuzhou Electric Locomotive has unveiled a prototype light metro trainset which uses supercapacitor energy storage to operate without an external power supply.
Developed in conjunction with Chinese Academy of Engineering, the trainset has underfloor power pick-ups which are used to charge the roof-mounted supercapacitor unit from a fixed supply while the train is stood at a station. Charging takes 30 sec and can power the train for 2 km. Energy regenerated during braking is recovered for reuse.
The two-car articulated trainset which was rolled out on August 10 is designed for a maximum speed of 80 km/h, with an intended operating speed of 70 km/h. It is 2 650 mm wide, has a capacity of 320 passengers and is suitable for a minimum curve radius of 80 m.

The supercapacitor has a greater power density than lithium-ion batteries, and wireless operation is seen as a cheaper and less visually intrusive alternative to conventional electrification.
Commercial production is envisaged by 2014, with the manufacturer believing the technology could be viable for use in more than 100 smaller and medium-sized Chinese cities, as well as for the export market.

Fig 8.7: CSR Zhuzhou Electric Locomotive

8.1.9 AIRCRAFT DRISTRIBUTED POWER SYSTEM

A supercapacitor and a DC-DC power converter is used to improve the regulation of the bus voltage of an aircraft. A PWM boost DC-DC power converter is used to transfer the energy

from the capacitor to the DC bus. A PWM buck DC-DC power converter is used to transfer the energy from the DC bus to the super capacitor. Experimental results indicate that a super capacitor and a DC-DC power converter can be used to improve the regulation of the DC bus voltage of distributed power system.

Fig 8.8: Air Craft

Chapter 8

Conclusion

In this study, emphasis was given on the electrodes, as they are the ones that differentiate a supercapacitor from a normal one. Electrodes made of CNT, was proposed, which would maximize the efficiency of supercapacitor. Research work is still continuing throughout the world and it's only a matter of time that new improved electrode is made. Another focus point of research is, how to further expand the life-cycle of supercapacitor with minimum amount of expenditure. Various phenomena of application was introduced above, which is trending worldwide. From mobile to big power station, supercapacitor is being used. Still more research needs to be done one the electrolyte of the supercapacitor also, which can open the doors to new possibilities.

References

[1] Dillon, Edward C., et al. "Large surface area activated charcoal and the inhibition of aspirin absorption." *Annals of emergency medicine* 18.5 (1989): 547-552.

[2] Alemán, J. V., et al. "Definitions of terms relating to the structure and processing of sols, gels, networks, and inorganic-organic hybrid materials (IUPAC Recommendations 2007)." *Pure and Applied Chemistry* 79.10 (2007): 1801-1829.

[3] Taher, Abul. "Scientists hail 'frozen smoke'as material that will change world." *News Article (London: Times Online). Retrieved* (2007): 08-22.

[4] Aegerter, Michel A., Nicholas Leventis, and Matthias M. Koebel, eds. *Aerogels handbook*. Springer Science & Business Media, 2011.

[5] Kistler, Samuel Stephens. "Coherent Expanded Aerogels and Jellies." *Nature* 127 (1931): 741.

[6] Kistler, S. S. "Coherent expanded-aerogels." *The Journal of Physical Chemistry* 36.1 (1932): 52-64.

[7] Pekala, R. W. "Organic aerogels from the polycondensation of resorcinol with formaldehyde." *Journal of Materials Science* 24.9 (1989): 3221-3227.

[8] Conway, Brian E. *Electrochemical supercapacitors: scientific fundamentals and technological applications*. Springer Science & Business Media, 2013.

[9] Halper, M. S., and J. C. Ellenbogen. "Supercapacitors: A Brief Overview, March 2006." (2014).

[10] Frackowiak, Elzbieta, and Francois Beguin. "Carbon materials for the electrochemical storage of energy in capacitors." *Carbon* 39.6 (2001): 937-950.

[11] Garthwaite, Josie. "How ultracapacitors work (and why they fall short)." *Retrieved from gigaom. com: http://gigaom. com/2011/07/12/how--ultracapacitors--work--and--why--they--fall--short* (2011).

[12] Brezesinski, Torsten, et al. "Ordered mesoporous [alpha]-MoO3 with iso-oriented nanocrystalline walls for thin-film pseudocapacitors." *Nature materials* 9.2 (2010): 146-151.

[13] Kim, Il-Hwan, et al. "Synthesis and electrochemical characterization of vanadium oxide on carbon nanotube film substrate for pseudocapacitor applications." *Journal of the electrochemical society* 153.6 (2006): A989-A996.

[14] Jayalakshmi, M., and K. Balasubramanian. "Simple capacitors to supercapacitors-an overview." *Int. J. Electrochem. Sci* 3.11 (2008): 1196-1217.

[15] Simon, Patrice, and Yury Gogotsi. "Materials for electrochemical capacitors." *Nature materials* 7.11 (2008): 845-854.

[16] Volfkovich, Yu M., et al. *Studies of supercapacitor carbon electrodes with high pseudocapacitance*. INTECH Open Access Publisher, 2012.

[17] Li, Xin, and Bingqing Wei. "Facile synthesis and super capacitive behavior of SWNT/MnO 2 hybrid films." *Nano Energy* 1.3 (2012): 479-487.

[18] Gualous, Hamid, et al. "Lithium Ion capacitor characterization and modelling." *ESSCAP*. 2008.

[19] Schindall, Joel. "CHARGE OF THE ULTRACAPACITORS: Energy storage may be in for a radical change, as nanotechnology-enhanced capacitors begin to catch up to batteries." *IEEE SPECTRUM* 44.11 (2007): 38-42.

[20] Naoi, Katsuhiko, et al. "New generation “nanohybrid supercapacitor”." *Accounts of chemical research* 46.5 (2012): 1075-1083.

[21] Volfkovich, Yu M., et al. *Studies of supercapacitor carbon electrodes with high pseudocapacitance*. INTECH Open Access Publisher, 2012.

[22] Niu, Chunming, et al. "High power electrochemical capacitors based on carbon nanotube electrodes." *Applied Physics Letters* 70.11 (1997): 1480-1482.

[23] Barisci, Joseph N., Gordon G. Wallace, and Ray H. Baughman. "Electrochemical Characterization of Single-Walled Carbon Nanotube Electrodes." *Journal of the electrochemical society* 147.12 (2000): 4580-4583.

[24] Shiraishi, Soshi, et al. "Electric double layer capacitance of highly pure single-walled carbon nanotubes (HiPco™ Buckytubes™) in propylene carbonate electrolytes." *Electrochemistry Communications* 4.7 (2002): 593-598.

[25] Zhang, H., G. P. Cao, and Y. S. Yang. "Using a cut–paste method to prepare a carbon nanotube fur electrode." *Nanotechnology* 18.19 (2007): 195607.

[26] Frackowiak, E., et al. "Supercapacitor electrodes from multiwalled carbon nanotubes." *Applied Physics Letters* 77.15 (2000): 2421-2423.

[27] Ahn, Hyo-Jin, et al. "Electrochemical capacitors fabricated with carbon nanotubes grown within the pores of anodized aluminum oxide templates." *Electrochemistry communications* 8.4 (2006): 513-516.

[28] Li, Chensha, et al. "Oxidation of multiwalled carbon nanotubes by air: benefits for electric double layer capacitors." *Powder technology* 142.2 (2004): 175-179.

[29] Moon, Jeong-Mi, et al. "High-yield purification process of singlewalled carbon nanotubes." *The Journal of physical chemistry B* 105.24 (2001): 5677-5681.

[30] An, Kay Hyeok, et al. "Electrochemical properties of high-power supercapacitors using single-walled carbon nanotube electrodes." *Advanced functional materials* 11.5 (2001): 387-392.

[31] Frackowiak, E., et al. "Supercapacitor electrodes from multiwalled carbon nanotubes." *Applied Physics Letters* 77.15 (2000): 2421-2423.

[32] Frackowiak, E., et al. "Enhanced capacitance of carbon nanotubes through chemical activation." *Chemical Physics Letters* 361.1 (2002): 35-41.

[33] Liu, Chen G., et al. "Single-walled carbon nanotubes modified by electrochemical treatment for application in electrochemical capacitors." *Journal of Power Sources* 160.1 (2006): 758-761.

[34] Kim, Yong-Tae, et al. "Drastic change of electric double layer capacitance by surface functionalization of carbon nanotubes." *Applied physics letters* 87.23 (2005): 234106.

[35] Lee, Ji Yeong, et al. "Fabrication of supercapacitor electrodes using fluorinated single-walled carbon nanotubes." *The Journal of Physical Chemistry B* 107.34 (2003): 8812-8815.

[36] Pan, H., Y. P. Feng, and J. Y. Lin. "Ab initio study of F-and Cl-functionalized single wall carbon nanotubes." *Journal of Physics: Condensed Matter* 18.22 (2006): 5175.

[37] Pan, H., Y. P. Feng, and J. Y. Lin. "Ab initio study of F-and Cl-functionalized single wall carbon nanotubes." *Journal of Physics: Condensed Matter* 18.22 (2006): 5175.

[38] Zhou, Chongfu, et al. "Functionalized single wall carbon nanotubes treated with pyrrole for electrochemical supercapacitor membranes." *Chemistry of materials* 17.8 (2005): 1997-2002.

[39] Frackowiak, E., et al. "Enhanced capacitance of carbon nanotubes through chemical activation." *Chemical Physics Letters* 361.1 (2002): 35-41.

[40] Liu, Chen G., et al. "Single-walled carbon nanotubes modified by electrochemical treatment for application in electrochemical capacitors." *Journal of Power Sources* 160.1 (2006): 758-761.

[41] Lee, Ji Yeong, et al. "Fabrication of supercapacitor electrodes using fluorinated single-walled carbon nanotubes." *The Journal of Physical Chemistry B* 107.34 (2003): 8812-8815.

[42] Yoon, Beom-Jin, et al. "Electrical properties of electrical double layer capacitors with integrated carbon nanotube electrodes." *Chemical Physics Letters* 388.1 (2004): 170-174.

[43] Futaba, Don N., et al. "Shape-engineerable and highly densely packed single-walled carbon nanotubes and their application as super-capacitor electrodes." *Nature materials* 5.12 (2006): 987-994.

[44] Kim, Il-Hwan, Jae-Hong Kim, and Kwang-Bum Kim. "Electrochemical characterization of electrochemically prepared ruthenium oxide/carbon nanotube electrode for supercapacitor application." *Electrochemical and Solid-State Letters* 8.7 (2005): A369-A372.

[45] Fang, Wei-Chuan, et al. "Ultrafast charging-discharging capacitive property of RuO2 nanoparticles on carbon nanotubes using nitrogen incorporation." *Journal of The Electrochemical Society* 155.1 (2008): K15-K18.

[46] Ramachandran, Kartik, et al. "Intercalation chemistry of cobalt and nickel dioxides: a facile route to new compounds containing organocations." *Materials research bulletin* 31.7 (1996): 767-772.

[47] Shan, Yan, and Lian Gao. "Formation and characterization of multi-walled carbon nanotubes/Co 3 O 4 nanocomposites for supercapacitors." *Materials chemistry and physics* 103.2 (2007): 206-210.

[48] Subramanian, V., Hongwei Zhu, and Bingqing Wei. "Synthesis and electrochemical characterizations of amorphous manganese oxide and single walled carbon nanotube composites as supercapacitor electrode materials." *Electrochemistry Communications* 8.5 (2006): 827-832.

[49] Ma, Sang-Bok, et al. "Electrochemical properties of manganese oxide coated onto carbon nanotubes for energy-storage applications." *Journal of Power Sources* 178.1 (2008): 483-489.

[50] Xie, Xiaofeng, and Lian Gao. "Characterization of a manganese dioxide/carbon nanotube composite fabricated using an in situ coating method." *Carbon* 45.12 (2007): 2365-2373.

[51] Fan, Zhen, et al. "Preparation and capacitive properties of cobalt–nickel oxides/carbon nanotube composites." *Electrochimica Acta* 52.9 (2007): 2959-2965.

[52] Jayalakshmi, M., et al. "Hydrothermal synthesis of SnO 2–V 2 O 5 mixed oxide and electrochemical screening of carbon nano-tubes (CNT), V 2 O 5, V 2 O 5–CNT, and SnO 2–V 2 O 5–CNT electrodes for supercapacitor applications." *Journal of Power Sources* 166.2 (2007): 578-583.

[53] Wang, Guixin, et al. "LiNi 0.8 Co 0.2 O 2/MWCNT composite electrodes for supercapacitors." *Materials Chemistry and Physics* 105.2 (2007): 169-174.

[54] Lota, Grzegorz, et al. "High performance supercapacitor from chromium oxide-nanotubes based electrodes." *Chemical physics letters* 434.1 (2007): 73-77.

[55] Khomenko, V., E. Frackowiak, and F. Beguin. "Determination of the specific capacitance of conducting polymer/nanotubes composite electrodes using different cell configurations." *Electrochimica Acta* 50.12 (2005): 2499-2506.

[56] Hughes, Mark, et al. "Electrochemical capacitance of a nanoporous composite of carbon nanotubes and polypyrrole." *Chemistry of Materials*14.4 (2002): 1610-1613.

[57] An, Kay Hyeok, et al. "High-capacitance supercapacitor using a nanocomposite electrode of single-walled carbon nanotube and polypyrrole." *Journal of the Electrochemical Society* 149.8 (2002): A1058-A1062.

[58] Gupta, Vinay, and Norio Miura. "Polyaniline/single-wall carbon nanotube (PANI/SWCNT) composites for high performance supercapacitors." *Electrochimica Acta* 52.4 (2006): 1721-1726.

[59] Dong, Bin, et al. "Preparation and electrochemical characterization of polyaniline/multi-walled carbon nanotubes composites for supercapacitor." *Materials Science and Engineering: B* 143.1 (2007): 7-13.

[60] Mi, Hongyu, et al. "Microwave-assisted synthesis and electrochemical capacitance of polyaniline/multi-wall carbon nanotubes composite." *Electrochemistry communications* 9.12 (2007): 2859-2862.

[61] Béguin, Francois, et al. "A Self-Supporting Electrode for Supercapacitors Prepared by One-Step Pyrolysis of Carbon Nanotube/Polyacrylonitrile Blends." *Advanced Materials* 17.19 (2005): 2380-2384.

[62] Barisci, Joseph N., Gordon G. Wallace, and Ray H. Baughman. "Electrochemical studies of single-wall carbon nanotubes in aqueous solutions." *Journal of Electroanalytical Chemistry* 488.2 (2000): 92-98.

[63] Källquist, Ida. "Lithium titanium oxide materials for hybrid supercapacitor applications." (2016).

[64] Frackowiak, E., et al. "Nanotubular materials for supercapacitors." *Journal of Power Sources* 97 (2001): 822-825.

[65] Shiraishi, Soshi, et al. "Electric double layer capacitance of highly pure single-walled carbon nanotubes (HiPco™ Buckytubes™) in propylene carbonate electrolytes." *Electrochemistry Communications* 4.7 (2002): 593-598.

[66] Liu, Chen G., et al. "Single-walled carbon nanotubes modified by electrochemical treatment for application in electrochemical capacitors." *Journal of Power Sources* 160.1 (2006): 758-761.

[67] Du, Chunsheng, and Ning Pan. "Supercapacitors using carbon nanotubes films by electrophoretic deposition." *Journal of Power Sources* 160.2 (2006): 1487-1494.

[68] S. Iijima, Helical microtubules of graphitic carbon, Nature (London), 1991, 354, 56-58.

[69] Iijima, Sumio, and Toshinari Ichihashi. "Single-shell carbon nanotubes of 1-nm diameter." (1993): 603-605.

[70] Bethune, D. S., et al. "Cobalt-catalysed growth of carbon nanotubes with single-atomic-layer walls." (1993): 605-607.

[71] B. E. Conway, *Electrochemical Supercapacitors-Scientific Fundamentals and Technological Applications* _Kluwer/Academic/Plenum, New York, 1999

[72] Frackowiak, E., et al. "Supercapacitor electrodes from multiwalled carbon nanotubes." *Applied Physics Letters* 77.15 (2000): 2421-2423.

[73] Niu, Chunming, et al. "High power electrochemical capacitors based on carbon nanotube electrodes." *Applied Physics Letters* 70.11 (1997): 1480-1482.

[74] Wang, Yong-gang, Le Yu, and Yong-yao Xia. "Electrochemical Capacitance Performance of Hybrid Supercapacitors Based on Ni (OH) 2∕Carbon Nanotube Composites and Activated Carbon." *Journal of the Electrochemical Society* 153.4 (2006): A743-A748.

[75] Kim, Jong-Huy, Ashok K. Sharma, and Yong-Sung Lee. "Synthesis of polypyrrole and carbon nano-fiber composite for the electrode of electrochemical capacitors." *Materials Letters* 60.13 (2006): 1697-1701.

[76] Kötz, R., and M. Carlen. "Principles and applications of electrochemical capacitors." *Electrochimica acta* 45.15 (2000): 2483-2498.

[77] Jang, Jong H., et al. "Electrophoretic deposition (EPD) of hydrous ruthenium oxides with PTFE and their supercapacitor performances." *Electrochimica acta* 52.4 (2006): 1733-1741.

[78] Wang, Jie, et al. "Capacitance properties of single wall carbon nanotube/polypyrrole composite films." *Composites Science and Technology*67.14 (2007): 2981-2985.

[79] Park, Jong Hyeok, et al. "Improved asymmetric electrochemical capacitor using Zn-Co co-doped Ni (OH) 2 positive electrode material." *Applied Physics A* 82.4 (2006): 593-597.

[80] Fang, Hai-Tao, et al. "Purification of single-wall carbon nanotubes by electrochemical oxidation." *Chemistry of Materials* 16.26 (2004): 5744-5750.

[81] Wang, Jiajun, et al. "Electrochemical durability investigation of single-walled and multi-walled carbon nanotubes under potentiostatic conditions." *Journal of Power Sources* 176.1 (2008): 128-131.

[82] Hermann, V., A. Schneuwly, and R. Gallay. "High performance double-layer capacitor for power electronic applications." *proc. PCIM*. 2001.

[83] (2002, Aug.) NESSCAP Products Datasheets. [Online] Available: www.nesscap.com

[84] (2002, Aug.) Boostcap double-layer capacitors, product profile. Montena. [Online] Available: www.montena.com

[85] (2002, Aug.) UltraCap double layer capacitors, a new energy storage device for peak power applications, product profile. EPCOS. [Online] Available: www.epcos.com

[86] Härri, V. V., et al. "All-purpose circuitry concept" SAM", Applications and networking for supercapacitors." *Proceedings 2nd Boostcap-Meeting*. Vol. 29. No. 01. 2001.

[87] (2002, Aug.) UltraCap double layer capacitors, a new energy storage device for peak power applications, product profile. EPCOS. [Online] Available: www.epcos.com

[88] Barrade, Philippe, Serge Pittet, and Alfer Rufer. "Energy storage system using a series connection of supercapacitors, with an active device for equalizing the voltages." *IPEC 2000: International Power Electronics Conference*. No. LEI-CONF-2005-044. 2000.

[89] Härri, V. V., et al. "All-purpose circuitry concept" SAM", Applications and networking for supercapacitors." *Proceedings 2nd Boostcap-Meeting*. Vol. 29. No. 01. 2001.

[90] NAOI, Katsuhiko, and Masayuki MORITA. "Advanced polymers as active materials and electrolytes for electrochemical capacitors and hybrid capacitor systems." *The Electrochemical Society Interface* 17.1 (2008): 44-48.

[91] Petty-Weeks, S., J. J. Zupancic, and J. R. Swedo. "Proton conducting interpenetrating polymer networks." *Solid State Ionics* 31.2 (1988): 117-125.

[92] Wu, Zhong-Shuai, et al. "Three-Dimensional Nitrogen and Boron Co-doped Graphene for High-Performance All-Solid-State Supercapacitors." *Advanced Materials* 24.37 (2012): 5130-5135.
[93] C.-C. Yang, S.-T. Hsu, W.-C. Chien, J. Power Sources 152
(2005) 303.

[94] Liu, Xingjiang, and Tetsuya Osaka. "All-Solid-State Electric Double-Layer Capacitor with Isotropic High-Density Graphite Electrode and Polyethylene Oxide/LiClO4 Polymer Electrolyte." *Journal of the Electrochemical Society*143.12 (1996): 3982-3986.

[95] Rathod, Dhanraj, et al. "Design of an “all solid-state” supercapacitor based on phosphoric acid doped polybenzimidazole (PBI) electrolyte." *Journal of applied electrochemistry* 39.7 (2009): 1097-1103.

[96] Kang, Yu Jin, Haegeun Chung, and Woong Kim. "1.8-V flexible supercapacitors with asymmetric configuration based on manganese oxide, carbon nanotubes, and a gel electrolyte." *Synthetic Metals* 166 (2013): 40-44.

[97] Sawangphruk, Montree, et al. "High-performance supercapacitor of manganese oxide/reduced graphene oxide nanocomposite coated on flexible carbon fiber paper." *Carbon* 60 (2013): 109-116.

[98] Wang, Gongming, et al. "LiCl/PVA gel electrolyte stabilizes vanadium oxide nanowire electrodes for pseudocapacitors." *ACS nano* 6.11 (2012): 10296-10302.

[99] Yang, Peihua, et al. "Hydrogenated ZnO core–shell nanocables for flexible supercapacitors and self-powered systems." *ACS nano* 7.3 (2013): 2617-2626.

[100] Lufrano, Francesco, and Pietro Staiti. "Conductivity and capacitance properties of a supercapacitor based on Nafion electrolyte in a nonaqueous system." *Electrochemical and solid-state letters* 7.11 (2004): A447-A450.

[101] Lufrano, Francesco, and Pietro Staiti. "Performance improvement of Nafion based solid state electrochemical supercapacitor." *Electrochimica acta*49.16 (2004): 2683-2689.

[102] Rikukawa, M., and K. Sanui. "Proton-conducting polymer electrolyte membranes based on hydrocarbon polymers." *progress in polymer science*25.10 (2000): 1463-1502.

[103] Choi, Bong Gill, et al. "Facilitated ion transport in all-solid-state flexible supercapacitors." *ACS nano* 5.9 (2011): 7205-7213.

[104] NAOI, Katsuhiko, and Masayuki MORITA. "Advanced polymers as active materials and electrolytes for electrochemical capacitors and hybrid capacitor systems." *The Electrochemical Society Interface* 17.1 (2008): 44-48.

[105] Matsuda, Yoshiharu, et al. "New Electric Double-Layer Capacitors Using Polymer Solid Electrolytes Containing Tetraalkylammonium Salts." *Journal of The Electrochemical Society* 140.7 (1993): L109-L110.

[106] MacFarlane, Douglas R., et al. "Energy applications of ionic liquids." *Energy & Environmental Science* 7.1 (2014): 232-250.

[107] Yoon, Y. S., et al. "Solid-state thin-film supercapacitor with ruthenium oxide and solid electrolyte thin films." *Journal of power sources* 101.1 (2001): 126-129.

[108] Kim, Han-Ki, et al. "All solid-state rechargeable thin-film microsupercapacitor fabricated with tungsten cosputtered ruthenium oxide electrodes." *Journal of Vacuum Science & Technology B* 21.3 (2003): 949-952.

[109] Wang, Y. G., and X. G. Zhang. "All solid-state supercapacitor with phosphotungstic acid as the proton-conducting electrolyte." *Solid State Ionics* 166.1 (2004): 61-67.

[110] Francisco, Brian E., et al. "Nanostructured all-solid-state supercapacitor based on Li2S-P2S5 glass-ceramic electrolyte." *Applied Physics Letters*100.10 (2012): 103902.

[111] Oudenhoven, Jos FM, Loïc Baggetto, and Peter HL Notten. "All-Solid-State Lithium-Ion Microbatteries: A Review of Various Three-Dimensional Concepts." *Advanced Energy Materials* 1.1 (2011): 10-33.

[112] Yu, Haijun, et al. "Improvement of the performance for quasi-solid-state supercapacitor by using PVA–KOH–KI polymer gel electrolyte." *Electrochimica Acta* 56.20 (2011): 6881-6886.

[113] Wei, Lu, Naoki Nitta, and Gleb Yushin. "Lithographically patterned thin activated carbon films as a new technology platform for on-chip devices." *ACS nano* 7.8 (2013): 6498-6506.

[114] Wang, Gongming, et al. "Solid-State Supercapacitor Based on Activated Carbon Cloths Exhibits Excellent Rate Capability." *Advanced Materials*26.17 (2014): 2676-2682.

[115] Wang, Da-Wei, et al. "3D aperiodic hierarchical porous graphitic carbon material for high-rate electrochemical capacitive energy storage." *Angewandte Chemie* 120.2 (2008): 379-382.

[116] Chmiola, John, et al. "Anomalous increase in carbon capacitance at pore sizes less than 1 nanometer." *Science* 313.5794 (2006): 1760-1763.

[117] Pech, David, et al. "Ultrahigh-power micrometre-sized supercapacitors based on onion-like carbon." *Nature nanotechnology* 5.9 (2010): 651-654.

[118] Wu, Xi-Lin, et al. "Biomass-derived sponge-like carbonaceous hydrogels and aerogels for supercapacitors." *ACS nano* 7.4 (2013): 3589-3597.

[119] Portet, C., G. Yushin, and Y. Gogotsi. "Electrochemical performance of carbon onions, nanodiamonds, carbon black and multiwalled nanotubes in electrical double layer capacitors." *Carbon* 45.13 (2007): 2511-2518.

[120] Zheng, Huimin, et al. "TiO 2@ C core–shell nanowires for high-performance and flexible solid-state supercapacitors." *Journal of Materials Chemistry C*1.2 (2013): 225-229.

[121] Wu, Zhong-Shuai, et al. "Three-dimensional graphene-based macro-and mesoporous frameworks for high-performance electrochemical capacitive energy storage." *Journal of the American Chemical Society* 134.48 (2012): 19532-19535.

[122] Liu, Wen-Wen, et al. "Superior Micro-Supercapacitors Based on Graphene Quantum Dots." *Advanced Functional Materials* 23.33 (2013): 4111-4122.

[123] Kang, Yu Jin, et al. "All-solid-state flexible supercapacitors based on papers coated with carbon nanotubes and ionic-liquid-based gel electrolytes." *Nanotechnology* 23.6 (2012): 065401.

[124] Kaempgen, Martti, et al. "Printable thin film supercapacitors using single-walled carbon nanotubes." *Nano letters* 9.5 (2009): 1872-1876.

[125] Zhu, Yanwu, et al. "Carbon-based supercapacitors produced by activation of graphene." *Science* 332.6037 (2011): 1537-1541.

[126] Yang, Xiaowei, et al. "Liquid-mediated dense integration of graphene materials for compact capacitive energy storage." *Science* 341.6145 (2013): 534-537.

[127] Xia, Jilin, et al. "Measurement of the quantum capacitance of graphene." *Nature nanotechnology* 4.8 (2009): 505-509.

[128] El-Kady, Maher F., et al. "Laser scribing of high-performance and flexible graphene-based electrochemical capacitors." *Science* 335.6074 (2012): 1326-1330.

[129] Wu, Zhong-Shuai, et al. "Three-Dimensional Nitrogen and Boron Co-doped Graphene for High-Performance All-Solid-State Supercapacitors." *Advanced Materials* 24.37 (2012): 5130-5135.

[130] Xu, Yuxi, et al. "Flexible solid-state supercapacitors based on three-dimensional graphene hydrogel films." *ACS nano* 7.5 (2013): 4042-4049.

[131] Wang, Shuangyin, et al. "Highly porous graphene on carbon cloth as advanced electrodes for flexible all-solid-state supercapacitors." *Nano Energy* 2.4 (2013): 530-536.

[132] Mitra, Sagar, and S. Sampath. "Electrochemical capacitors based on exfoliated graphite electrodes." *Electrochemical and solid-state letters* 7.9 (2004): A264-A268.

[133] Chen, Qing, et al. "MnO 2-modified hierarchical graphene fiber electrochemical supercapacitor." *Journal of Power Sources* 247 (2014): 32-39.

[134] He, Yongmin, et al. "Freestanding three-dimensional graphene/MnO2 composite networks as ultralight and flexible supercapacitor electrodes." *ACS nano* 7.1 (2012): 174-182.

[135] Sawangphruk, Montree, et al. "High-performance supercapacitor of manganese oxide/reduced graphene oxide nanocomposite coated on flexible carbon fiber paper." *Carbon* 60 (2013): 109-116.

[136] Sawangphruk, Montree, and Jumras Limtrakul. "Effects of pore diameters on the pseudocapacitive property of three-dimensionally ordered macroporous manganese oxide electrodes." *Materials Letters* 68 (2012): 230-233.

[137] Gómez-Navarro, Cristina, et al. "Electronic transport properties of individual chemically reduced graphene oxide sheets." *Nano letters* 7.11 (2007): 3499-3503.

[138] Zhang, Qingqing, et al. "Electropolymerization of graphene oxide/polyaniline composite for high-performance supercapacitor." *Electrochimica Acta* 90 (2013): 95-100.

[139] Chang, Hao-Hsiang, et al. "Electrochemically synthesized graphene/polypyrrole composites and their use in supercapacitor." *Carbon*50.6 (2012): 2331-2336.

[140] Ge, Jun, Guanghui Cheng, and Liwei Chen. "Transparent and flexible electrodes and supercapacitors using polyaniline/single-walled carbon nanotube composite thin films." *Nanoscale* 3.8 (2011): 3084-3088.

[141] Lim, Yee Seng, et al. "Polypyrrole/graphene composite films synthesized via potentiostatic deposition." *Journal of Applied Polymer Science* 128.1 (2013): 224-229.

[142] Li, Yan, et al. "Synthesis and electrochemical performance of sandwich-like polyaniline/graphene composite nanosheets." *European Polymer Journal*48.8 (2012): 1406-1412.

[143] Zhou, Shuiping, et al. "Graphene-wrapped polyaniline nanofibers as electrode materials for organic supercapacitors." *Carbon* 52 (2013): 440-450.

[144] Dong, Xiaochen, et al. "Supercapacitor electrode based on three-dimensional graphene–polyaniline hybrid." *Materials Chemistry and Physics* 134.2 (2012): 576-580.

[145] Park, Sukeun, and Seok Kim. "Effect of carbon blacks filler addition on electrochemical behaviors of Co 3 O 4/graphene nanosheets as a supercapacitor electrodes." *Electrochimica Acta* 89 (2013): 516-522.

[146] Dong, Xiaochen, et al. "Hybrid structure of zinc oxide nanorods and three dimensional graphene foam for supercapacitor and electrochemical sensor applications." *RSC Advances* 2.10 (2012): 4364-4369.

[147] Wang, Yaming, et al. "Graphene/carbon black hybrid film for flexible and high rate performance supercapacitor." *Journal of Power Sources* 271 (2014): 269-277.

[148] Haas, Otto, and Elton J. Cairns. ". Electrochemical energy storage." *Annual Reports Section" C"(Physical Chemistry)* 95 (1999): 163-198.

[149] "Super Snap on Camera Phones", Cap-XX

[150] Wu Bingbing, Yin Zhongdong, Xiao Xiangning, "Super-capacitors Energy Storage System Applied in the Microgrid", ICIEA, 15-17 June2010

[151] Peng Li, Bruno Francois, Philippe Degobert, Benoit Robyns, "Power Control Strategy of a Photovoltaic Power Plant for Microgrid Applications", Proceedings of ISES World Congress 2007, 4, pp 1611-1616.

[152] J. Nickerson, Fullpower Technologies, 9th Seminar ECDL Deerfield Beach FL, 1999

[153] "RAID controller using capacitor energy source to flush volatile cache data to nonvolatile memory during main power outage", US Patent 73

[154] "Adaptec's new controller bids goodbye to Li-ion batteries", http://cleantech.com/news/4628/adaptec-new-controller-bids-goodb

[155] "Cap-XX Supercapacitors provide power backupfor Solid State Drives", White Paper, Cap-XX

[156] "ATTO Adds Supercapacitor for Cache Protection", http://www.ibmsubnet.com/newsletters/stor/2010/080910stor1.html

[157] US Patent No. 7809886, "RAID controller using capacitor energy source to flush volatile cache data to non-volatile memory during main power outage "